

การวิเคราะห์ความอ่อนไหวการเกิดไฟฟ้าในประตศภูฏาน
โดยอาศัยเทคโนโลยีภูมิสารสนเทศ



นายชำมตรูบ โตร์จี้

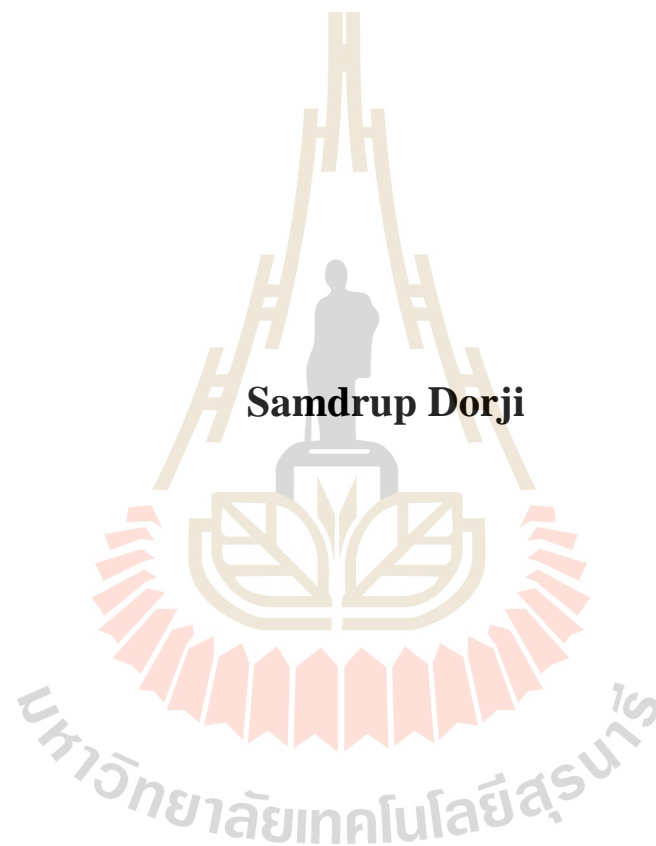
วิทยานิพนธ์นี้เป็นส่วนหนึ่งของการศึกษาตามหลักสูตรปริญญาวิทยาศาสตรมหาบัณทิต

สาขาวิชาภูมิสารสนเทศ

มหาวิทยาลัยเทคโนโลยีสุรนารี

ปีการศึกษา 2559

**WILDFIRE SUSCEPTIBILITY ANALYSIS IN BHUTAN
USING GEOINFORMATICS TECHNOLOGY**



A Thesis Submitted in Partial Fulfillment of the Requirements for the

Degree of Master of Science in Geoinformatics

Suranaree University of Technology

Academic Year 2016

**OPTIMAL BURNED AREA AND FIRE DETECTION
ALGORITHMS USING MODIS AND LANDSAT DATA:
CASE STUDY OF UPPER NORTHERN REGION, THAILAND**

Suranaree University of Technology has approved this thesis submitted in partial fulfillment of the requirements for the Degree of Doctor of Philosophy.

Thesis Examining Committee

S. Dasananda
(Assoc. Prof. Dr. Songkot Dasananda)

Chairperson

Suwit Ong
(Assoc. Prof. Dr. Suwit Ongsomwang)

Member (Thesis Advisor)

Vivarad Phonekeo
(Dr. Vivarad Phonekeo)

Member

Sunya Sarapirome
(Asst. Prof. Dr. Sunya Sarapirome)

Member

Sura Pattanakit
(Assoc. Prof. Dr. Sura Pattanakit)

Member

Sukit Limpijumnong
(Prof. Dr. Sukit Limpijumnong)

Vice Rector for Academic Affairs
and Innovation

Santi Maensiri
(Prof. Dr. Santi Maensiri)

Dean of Institute of Science

SAMDRUP DORJI: การวิเคราะห์ความอ่อนไหวการเกิดไฟป่าในประเทศภูฏาน โดยอาศัยเทคโนโลยีภูมิสารสนเทศ (WILDFIRE SUSCEPTIBILITY ANALYSIS IN BHUTAN USING GEOINFORMATICS TECHNOLOGY) อาจารย์ที่ปรึกษา: รองศาสตราจารย์ ดร. สุวิทย์ อ่องสมหวัง, 162 หน้า.

การบูรณาการเทคโนโลยีภูมิสารสนเทศกับแบบจำลองเชิงพื้นที่ที่เหมาะสมได้ถูกนำมาใช้งานอย่างแพร่หลายในการศึกษาไฟป่าเพื่อใช้พัฒนาและเพิ่มประสิทธิภาพของระบบการจัดการไฟป่าในภูมิภาคต่างๆ ของโลก การประยุกต์ใช้การรับรู้จากระยะไกลและระบบสารสนเทศภูมิศาสตร์ร่วมกับแบบจำลองเชิงพื้นที่ที่เหมาะสมได้มีบทบาทสำคัญในการจำแนกและการทำแผนที่ไฟป่า ไฟป่าเป็นสาเหตุสำคัญอย่างหนึ่งที่ส่งผลทำให้ป่าของประเทศภูฏานเสื่อมสภาพ จึงนับว่าเป็นภัยคุกคามอย่างร้ายแรงต่อความพยายามการอนุรักษ์ทรัพยากรป่าของประเทศ ดังนั้น การวิเคราะห์ความอ่อนไหวของการเกิดไฟป่าจึงเป็นองค์ประกอบสำคัญของระบบการจัดการไฟป่าสำหรับประเทศภูฏาน เป้าหมายสูงสุดของการศึกษาคือ การประยุกต์ใช้นวัตกรรมของเทคโนโลยีภูมิสารสนเทศร่วมกับแบบจำลองการถดถอยโลจิสติกและแบบจำลองอัตราส่วนความถี่เพื่อสร้างแผนที่ความอ่อนไหวการเกิดไฟป่า ในการศึกษาครั้งนี้ ได้ทำการรวบรวมและเตรียมข้อมูลปัจจัยที่มีอิทธิพลต่อการเกิดไฟป่า การวิเคราะห์ และสร้างแผนที่ความน่าจะเป็นของการเกิดไฟป่าจากแบบจำลองที่แตกต่างกันสองรูปแบบ โดยอาศัยเครื่องมือของการรับรู้จากระยะไกลและระบบสารสนเทศภูมิศาสตร์ จากนั้น ทำการเปรียบเทียบประสิทธิภาพของแบบจำลองทั้งสองโดยอาศัยการประเมินความถูกต้องและความสมเหตุสมผลด้วยวิธีการ ROC เพื่อคัดเลือกแบบจำลองที่เหมาะสม

จากการแปลตีความผลลัพธ์ที่ได้รับจากแบบจำลองทั้งสอง พบว่า ตัวแปรอิสระที่มีนัยสำคัญต่อการเกิดไฟป่าในพื้นที่ศึกษา ได้แก่ อุณหภูมิพื้นผิวดิน ระยะห่างจากถนน ระดับความสูง ความหนาแน่นของประชากร ดัชนีพืชพรรณ EVI ระยะห่างจากที่ดินการเกษตร ความชื้นสัมพัทธ์ และทิศด้านลาด อัตราการคาดการณ์และอัตราความสำเร็จของแบบจำลองการถดถอยโลจิสติกเท่ากับ 88.3% และ 88.1% ตามลำดับ ในขณะที่ อัตราการคาดการณ์และอัตราความสำเร็จของแบบจำลองอัตราส่วนความถี่เท่ากับ 85.3% และ 85.5% ตามลำดับ จากผลลัพธ์ที่ได้รับแสดงให้เห็นว่า แบบจำลองทั้งสองสามารถคาดการณ์การเกิดไฟป่าได้ดี

โดยที่แบบจำลองการถดถอยโลจิสติกมีประสิทธิภาพสูงกว่าแบบจำลองอัตราส่วนความถี่เล็กน้อย ดังนั้น ในการศึกษาครั้งนี้จึงเลือกใช้แบบจำลองการถดถอยโลจิสติกเป็นแบบจำลองที่เหมาะสมสำหรับการจัดทำแผนที่ความอ่อนไหวของการเกิดไฟป่า ซึ่งแบ่งระดับระดับความอ่อนไหวออกเป็น 5 เขต ประกอบด้วย ต่ำมาก ต่ำ ปานกลาง สูง และสูงมาก เขตความอ่อนไหวของการเกิดไฟป่าสูงและสูงมากครอบคลุมพื้นที่ประมาณร้อยละ 30 ของพื้นที่ศึกษาทั้งหมด และประกอบด้วยจุดความร้อนส่วนใหญ่ (ร้อยละ 72) ของจุดความร้อนทั้งหมด พื้นที่ส่วนใหญ่เกิดขึ้นใกล้กับถนนที่ตั้งอยู่ในระดับความสูงต่ำที่สัมพันธ์กับอุณหภูมิพื้นผิวดินที่สูงและมีพืชพรรณเด่น ได้แก่ ไม้พุ่มและทุ่งหญ้า ทุ่งหญ้าแห้งผสมกลุ่มไม้ตระกูลสน

ผลลัพธ์ที่ได้รับจากการศึกษาแสดงให้เห็นว่า การบูรณาการเทคโนโลยีภูมิสารสนเทศกับแบบจำลองการถดถอยโลจิสติกและแบบจำลองอัตราส่วนความถี่เชิงพื้นที่ในระบบสารสนเทศภูมิศาสตร์เป็นองค์ประกอบสำคัญที่ใช้สร้างแผนที่การเกิดไฟป่า ซึ่งสามารถระบุถึงปัจจัยที่มีอิทธิพลสำคัญต่อการเกิดไฟป่าและความน่าจะเป็นของการเกิดไฟป่าได้อย่างมีประสิทธิภาพ รวมทั้งการพัฒนาแผนที่ความอ่อนไหวของการเกิดไฟป่า ผลลัพธ์ที่ได้รับจากการศึกษาได้ให้สารสนเทศที่มีคุณค่าซึ่งสามารถนำไปใช้เป็นแนวทางและสนับสนุนระบบการจัดการไฟป่าของประเทศภูฏานให้มีประสิทธิภาพ ซึ่งจะช่วยสนับสนุนการคุ้มครองและส่งเสริมทรัพยากรป่าไม้ที่มีความอุดมสมบูรณ์และความหลากหลายทางชีวภาพในที่สุด

มหาวิทยาลัยเทคโนโลยีสุรนารี

สาขาวิชาการรับรู้จากระยะไกล
ปีการศึกษา 2559

ลายมือชื่อนักศึกษา _____

ลายมือชื่ออาจารย์ที่ปรึกษา _____




SAMDRUP DORJI: WILDFIRE SUSCEPTIBILITY ANALYSIS IN
BHUTAN USING GEOINFORMATICS TECHNOLOGY. THESIS
ADVISOR: ASSOC. PROF. SUWIT ONGSOMWANG, Dr. rer. Nat.
162 PP.

WILDFIRE SUSCEPTIBILITY ANALYSIS/ LR MODEL/ FR MODEL/ THIMPU
AND PARO/ BHUTAN

The integration of geoinformatics technology with suitable geospatial models have been widely employed in many wildfire studies to enhance the wildfire management system in different parts of the world. Particularly, remote sensing and GIS with appropriate geospatial models have played a vital role in identifying and mapping wildfires. Wildfire is perceived as one of the most noticeable causes of forest degradation in Bhutan with serious threat to the national conservation efforts. Thus, wildfire susceptibility mapping is seen as an indispensable component of wildfire management system for Bhutan. The ultimate objective of the study is to apply the innovative approach of geoinformatics technology with the integration of GIS based logistic regression (LR) and frequency ratio (FR) models to establish a wildfire susceptibility map. Herein, the study collected and prepared various wildfire influential factors, analyzed and established probability maps from two different models using remote sensing and GIS tools. The efficiency of two models are evaluated and compared to determine an optimal model based on the accuracy assessment and validation using relative operating characteristic (ROC) method.

The interpretations of the results revealed that the most significant predictor variables that played a major role in determining the wildfire occurrence in the study area are land surface temperature, proximity to roads, elevation, population density, enhance vegetation index, distance to agriculture land, relative humidity and aspect. The prediction and success rates of LR model was 88.3% and 88.1%, while for FR model was 85.3% and 85.5%, respectively. The results indicated that both models are good predictors of wildfire with LR model performing slightly better than FR model. Thus, LR model was chosen as optimum model to establish wildfire susceptibility map and it was classified into five susceptibility zones: very low, low, moderate, high and very high. The high and very high susceptibility zones covered 30% of the total study area and contained majority (72%) of the total hotspot. These zones are closer to the roads at lower elevations associated with high land surface temperature where the vegetation is dominant with shrubs and meadows, dry grasslands mixed with scattered conifers and blue pines.

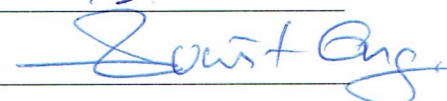
In conclusion, the results from the study demonstrates that the integration of geoinformatics technology with GIS-based LR and FR models are inevitable component of wildfire mapping that can effectively determine the most significant influential factors of wildfire and its probability that can eventually develop the wildfire susceptibility map. The findings may provide valuable information that can effectively guide in wildfire management system of Bhutan, ultimately assisting the preservation and promotion of rich forest resources and biodiversity.

School of Remote Sensing

Academic Year 2016

Student's Signature _____

Advisor's Signature _____



ACKNOWLEDGEMENTS

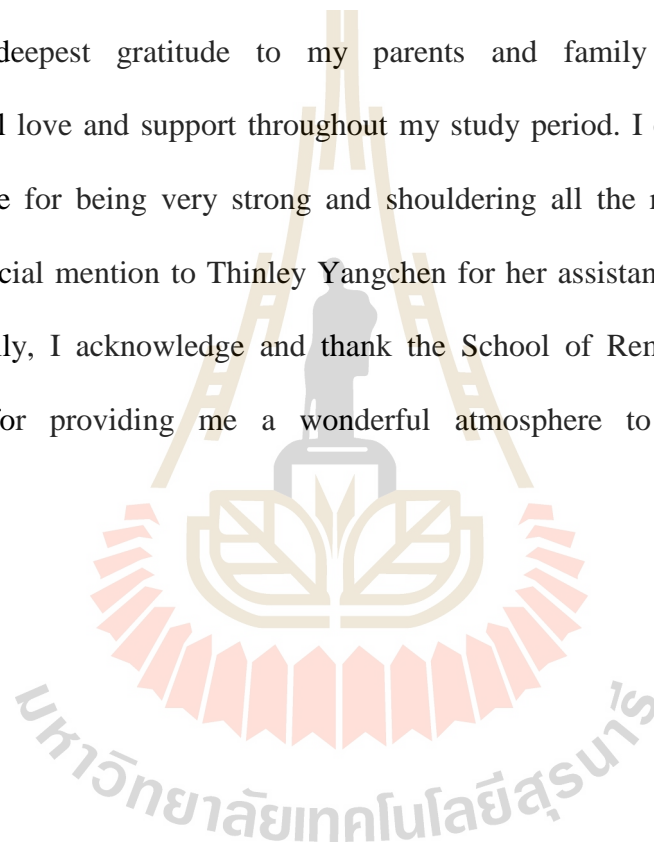
Firstly, I am grateful to the Thailand International Cooperation Agency (TICA) and the Royal Civil Service Commission (RCSC) of Bhutan for awarding me a scholarship to pursue this M. Sc. course in Geoinformatics at the School of Remote Sensing, Institute of Science, Suranaree University of Technology. It was a wonderful opportunity for me to upgrade my carrier in the field of geoinformatics. The successful completion of this thesis would not have been possible without the inspiration and support of many wonderful individuals. I wish to offer my heartfelt thanks to all of them. To my advisor Assoc. Prof. Dr. Suwit Ongsomwang, it has been an honor for me to be his advisee, I would like to express my sincere gratitude for his continuous support, for his patience, motivation, immense knowledge and guidance rendered throughout different phases of this research. Besides my advisor, I would like to extent my profound gratitude to my thesis committee members: Assoc. Prof. Songkot Dasananda (Chairperson), Asst. Prof. Dr. Sunya Sarapirome, Dr. Pantip Piyatadsananon and Asst. Professor Dr. Kobsak Wanthongchai (External Committee), for their invaluable ideas, insightful comments, opinions and suggestions that improved my research from various perspectives. I thank my fellow labmates of School of Remote Sensing for their friendship, guidance and assistance rendered, and for the times we worked and enjoyed together during my study.

I am very grateful to different agencies: Department of Hydro-Met Services (DHMS), National Land Commission (NLCS), and National Statistical Bureau (NSB) for sharing their resources and required data for my research. Without their support

my thesis would not have been successful. In particular, I thank the honorable Secretary of NLCS, Dasho Pema Chewang and Director Tenzin Namgay for their unwavering encouragement and inspiring words of advice. I am also indebted to Ms. Panitee Srisawang at TICA office in Bangkok and the staffs of Center for International Affairs (CIA) office at Suranaree University of Technology for their unfailing support and guidance throughout my study period.

My deepest gratitude to my parents and family members for their unconditional love and support throughout my study period. I owe special thanks to my dear wife for being very strong and shouldering all the responsibilities in my absence. Special mention to Thinley Yangchen for her assistance and support to my family. Finally, I acknowledge and thank the School of Remote Sensing and the University for providing me a wonderful atmosphere to pursue my studies successfully.

Samdrup Dorji



CONTENTS

	Page
ABSTRACT IN THAI.....	I
ABSTRACT IN ENGLISH	III
ACKNOWLEDGEMENTS.....	V
CONTENTS.....	VII
LIST OF TABLES	XI
LIST OF FIGURES	XII
LIST OF ABBREVIATIONS.....	XIV
CHAPTER	
I INTRODUCTION.....	1
1.1 Background and significance of the study	1
1.2 Research objectives	7
1.3 Scope of the study	8
1.4 Limitation of the study	8
1.5 Study area	10
1.6 Benefit of the study	11
II BASIC CONCEPTS AND LITERATURE REVIEWS.....	12
2.1 Definitions and basic concepts of wildfire.	12
2.2 Basic characteristics of wildfire	14
2.2.1 Fire triangle.....	14

CONTENTS (Continued)

2.2.2	Types of fire.....	15
2.2.3	Fire behaviour triangle.....	17
2.3	Logistic regression (LR) model.....	19
2.4.	Frequency ratio (FR) model.....	23
2.5	Influential factors of wildfire.....	26
2.5.1	Environmental factors.....	27
2.5.2	Meteorological factors.....	32
2.5.3	Anthropogenic factors.....	34
2.6	Causes of wildfire in Bhutan.....	35
2.7	MODIS hotspot.....	36
2.7.1	MODIS hotspot detection and its characteristics.....	37
2.7.2	MODIS fire detection algorithm.....	40
2.7.3	Caveats of the hotspot.....	44
2.7.4	Statistics of MODIS hotspot in Bhutan (2002-2016).....	44
2.8	Literature review.....	46
III RESEARCH METHODOLOGY.....		57
3.1	Data collection and preparation.....	59
3.1.1	Dependent variable (MODIS hotspot/active fire data).....	59
3.1.2	Independent variables (Wildfire influential factors).....	63
3.1.3	Resampling and cell size of raster dataset.....	69
3.1.4	Standardization of raster dataset.....	70
3.1.5	Sampling of dependent variable.....	71
3.1.6	Input data preparation for LR and FR model.....	72

CONTENTS (Continued)

3.1.7	Multicollinearity analysis.....	73
3.2	Wildfire susceptibility analysis using LR and FR models	75
3.2.1	Wildfire susceptibility analysis using LR model	75
(a)	Goodness of fit of LR model (Likelihood ratio test)	77
(b)	Wald statistics (Statistical tests for individual predictors)	79
(c)	Odds Ratio (OR).....	80
3.2.2	Wildfire susceptibility analysis using FR model	81
3.3	Accuracy assessment and validation of gained probability maps	83
IV	RESULTS AND DISCUSSIONS	85
4.1	Input variables for LR model	85
4.2	Multicollinearity Analysis.....	89
4.3	Wildfire susceptibility analysis using LR model	90
4.3.1	Impact of influential factors on wildfire occurrence (LR).....	94
4.3.2	Wildfire probability map generation.....	104
4.4	Wildfire susceptibility analysis using FR model.....	108
4.4.1	Impact of influential factors on wildfire occurrence (FR)	113
4.4.2	Computation of prediction rates (PR) from FR analysis.....	117
4.4.3	Wildfire susceptibility index (WSI) map generation	120
4.5	Comparative assessment of probability map of LR and FR models	121
4.6	Accuracy assessment and validation of LR and FR models	124
4.7	Wildfire susceptibility mapping	126

CONTENTS (Continued)

V	CONCLUSIONS AND RECOMMENDATIONS.....	131
5.1	Conclusions	131
5.1.1	Logistic regression model.....	131
5.1.2	Frequency ratio model	133
5.1.3	Accuracy assessment and validation.....	134
5.1.4	Wildfire susceptibility mapping.....	135
5.2	Recommendations	136
	REFERENCES	138
	APPENDICES	150
	APPENDIX A ATTRIBUTE FIELDS FOR MODIS HOTSPOT DATA DISTRIBUTED BY FIRMS.....	151
	APPENDIX B ALOS DEM USED FOR DERIVING TOPOGRAPHIC VARIABLES	153
	APPENDIX C METEOROLOGICAL STATIONS USED TO INTERPOLATE WEATHER VARIABLES.....	155
	APPENDIX D POPULATION DATA AND SUB-DISTRICT BOUNDARY MAP OF THIMPHU AND PARO FOR INTERPOLATION OF POPULATION DENSITY	157
	APPENDIX E EXAMPLE OF INPUT ASCII FILES IMPORTED TO SPSS FOR LR ANALYSIS.....	160
	CURRICULUM VITAE.....	162

LIST OF TABLES

Table	Page
2.1	Specification of MODIS sensor and its characteristics..... 37
2.2	MODIS spectral characteristics..... 38
2.3	MODIS channels used in fire detection algorithm..... 42
2.4	Statistics of MODIS Hotspot in Bhutan (2002-2016)..... 45
3.1	Basic remote sensing and GIS input data for wildfire susceptibility analysis 62
3.2	Selected influential factors for wildfire susceptibility analysis 66
3.3	Characteristics of input variables for LR and FR analysis..... 67
4.1	Input variables used for LR analysis 86
4.2	Results of multicollinearity diagnostic test of independent variables..... 89
4.3	Model statistics and classification summary of LR analysis 92
4.4	Variables in the equation retained by LR analysis (LR result) 94
4.5	Frequency ratio of each class of independent factors (FR result)..... 110
4.6	Prediction rates of wildfire influential factors119
4.7	Percentage of hotspots and the area coverage of each susceptibility zones.. 128

LIST OF FIGURES

Figure	Page
1.1	Number of fire incidences and area damaged (2008-2014)..... 4
1.2	Map and location of the study area 10
2.1	Fire triangle..... 14
2.2	Types of wildfire..... 16
2.3	Fire behavior triangle 17
2.4	Sigmoid (Logistic) function/S-shaped curve 22
2.5	Fire pixel detection using MODIS 39
2.6	Graphical representation of hotspot in Bhutan (2002-2016). 45
2.7	Distribution of MODIS hotspot in Bhutan (2002-2016)..... 46
3.1	Flow chart of research methodology for wildfire susceptibility mapping 58
3.2	MODIS Hotspot data from 2002-2016 in the study area 61
3.3	Monthly distribution of MODIS hotspot in the study area 61
3.4	Basic input maps for wildfire susceptibility analysis 62
3.5	Example of resampling technique..... 69
3.6	Characteristics of ROC curve 84
4.1	Dependent variable (Hotspot map) used in the LR analysis..... 86
4.2	Independent variable (predictor maps) used in the LR analysis 87
4.3	Model structure for LR analysis in ArcGIS 10.3 software 106
4.4	Wildfire probability map from LR model..... 107

LIST OF FIGURES (Continued)

Figure	Page
4.5 Input factor maps FR analysis.....	108
4.6 Graphical representation of prediction rate of each factors	119
4.7 Module structure for FR analysis in ArcGIS 10.3	120
4.8 Wildfire susceptibility index (WSI) from FR model	121
4.9 Comparative view of wildfire probability maps of LR and FR models	122
4.10 Comparison of predictive power of each factors from LR and FR models ..	123
4.11 Success rate curves of LR and FR models.....	125
4.12 Prediction rate curves of LR and FR models	125
4.13 Comparison of success and prediction rate curves of LR and FR model	126
4.14 Histogram statistics report for wildfire probability map of LR model	127
4.15 Final wildfire susceptibility map of the study area.....	128

LIST OF ABBREVIATIONS

ADRC	=	Asian Disaster Reduction Center
ASTER	=	Advanced Spaceborne Thermal Emission and Reflection
ATSR	=	Along Track Scanning Radiometer
AUC	=	Area Under Curve
AVHRR	=	Advanced Very High Resolution Radiometer
DEM	=	Digital Elevation Model
DoFPS	=	Department of Forest and Park Services
ECIU	=	Energy and Climate Intelligence Unit
EOS	=	Earth Observing System
ERDAS	=	Earth Resources Data Analysis System
ESRI	=	Environmental Systems Research Institute
EVI	=	Enhanced Vegetation Index
FAO	=	Food and Agriculture Organization
FIRMS	=	Fire Information and Resource Management System
FR	=	Frequency Ratio Model
GIS	=	Geographical Information System
GLOF	=	Glacial Lake Outburst Flood
GNH	=	Gross National Happiness
GOES	=	Geostationary Operational Environmental Satellite

LIST OF ABBREVIATIONS (Continued)

GPS	=	Global Positioning System
IFFN	=	International Forest Fire News
ISDR	=	International Strategy for Disaster Reduction
LANCE	=	The Land, Atmosphere Near real-time Capability for EOS
LL ₀	=	Log-Likelihood of the model with intercept only
LL _m	=	Log-Likelihood of the model
LR	=	Logistic Regression Model
LST	=	Land Surface Temperature
LULC	=	Land Use and Land Cover
MoAF	=	Ministry of Agriculture and Forest
MODIS	=	Moderate Resolution Imaging Spectroradiometer
NASA	=	National Aeronautics and Space Administration
NCRP	=	National Cadastral Resurvey Program
NDEC	=	National Disaster Education Coalition
NDVI	=	Normalized Difference Vegetation Index
NIR	=	Near Infra-Red
NLCS	=	National Land Commission Secretariat
NOAA	=	National Oceanic and Atmospheric Administration
NSB	=	National Statistical Bureau
OLS	=	Ordinary Least Square
OR	=	Odds Ratio

LIST OF ABBREVIATIONS (Continued)

PHCB	=	Population and Housing Census
PPC	=	Policy and Planning Commission
PR	=	Prediction Rate
RGoB	=	Royal Government of Bhutan
RNR	=	Renewal Natural Resources
ROC	=	Relative Operating Characteristic
SE	=	Standard Error
Sig.	=	Significance
SPSS	=	Statistical Package for the Social Sciences
TOL	=	Tolerance
TWI	=	Topographic Wetness Index
UN	=	United Nations
VIIRS	=	Visible Infrared Imaging Radiometer Suite
VIF	=	Variance Inflation Factor
WSI	=	Wildfire Susceptibility Index

CHAPTER I

INTRODUCTION

1.1 Background and significance of the study

Wildfire presents a substantial threat to the precious forest resources and numerous studies have indicated an increasing trend in wildfire occurrences around the world (Williamson et al. 2015, Hushaw 2016 and Johann et al. 2004). As a result, in recent years the topic on wildfire has gained new attention among many researchers globally. Wildfire influences vegetation dynamics and land use change at global scale and its issues have become more extreme with rise in global temperatures. Wildfires which play an important role in global warming and climate change have major impact on ecosystems and environment by releasing large amounts of aerosols and greenhouse gases (CO₂ and CO) into the atmosphere. It is estimated that wildfire contributes about 30% to the total amount of tropospheric ozone, global CO and CO₂ (Levine, 1991). Thus, wildfire is considered as a continuous contributor to the earth's deforestation, desertification and ecology damage. Meanwhile, wildfires are expected to increase with global warming and variations in the climatic parameters (Stocks et al., 1998).

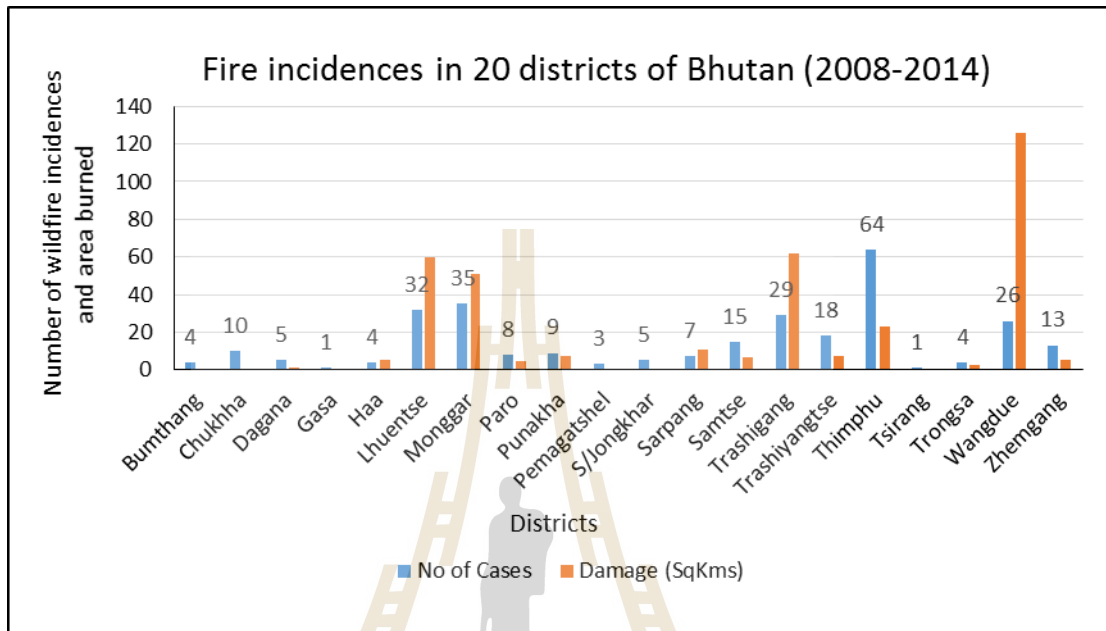
In Bhutan, among many natural disasters such as earthquake, Glacial Lake Outburst Flood (GLOF), flash flood, and windstorm, wildfire is one of the most common threat that poses frequent potential hazard with physical, biological,

ecological and environmental consequences. It is one of the most prominent causes of forest degradation in the country (Tshering, 2006) and perceived as a biggest threat to our national conservation efforts. About 80.9% of Bhutan's land is under pristine forest area, out of which 70.46% is covered by trees (Drukpa, 2015). This has contributed to the country's position of being the first carbon negative country in the world according to the 2015 UN Climate Summit held in Paris. Based on the Carbon Comparator Tool developed by the Energy and Climate Intelligence Unit (ECIU), Bhutan's forest cover observes three times more CO₂ than its people produce, making a significant contribution to the world that is threatened by climate change. Today, at the age of globalization, Bhutan still remains one of the few countries in the World with rich natural and pristine forest cover still intact, providing homes to diverse flora and fauna including many critical and endangered faunal species. As a result, Bhutan is also considered as one of the 10th Global Biodiversity hotspot in the World (RGoB, 1999). This was possible, because of the exemplary and wise leadership of our beloved kings, and due to a strong and effective laws for the preservation and protection of environment regulated by the government. For instance, the constitution of the Kingdom of Bhutan mandates to maintain 60% of the country under forest cover for all times to come. In addition, the conservation of environment is one of the four main pillars of Gross National Happiness (GNH) where a sustainable use of natural resources has given the highest priority. Bhutan's forest also plays a vital role in maintaining the sustainability of hydropower industry, sustains rural livelihoods and food subsistence. It is one of the largest renewable natural resource and wealth of the country that plays an integral role in the development of Bhutan. Hence, the future economy of the people and the country depends on the protection, conservation and

scientific management of forest resources (RGoB, 1969). As a result, the preservation and protection of forest resources is given top priority and every year there is a mass plantation and reforestation program being initiated at various capacities ranging from community to national level.

However, wildfire provides a consistent threat and every year thousands of acres of forest and its biodiversity are lost to wildfire despite of stringent legislation and public awareness programs on wildfire. This has affected the country, socially, economically and environmentally. It destroys the habitats and the intricate relationships of flora and fauna leading to loss of ecosystems and biodiversity, consequently threatening the endangered plant and animal species. It is estimated that on an average more than 10,000 acres of forest cover is lost due to wildfire every year (Kuensel, 2016) reducing the quality of forest features like soil fertility, biodiversity and ecosystem. The rugged topographic conditions with high ground fuel loads and erratic wind conditions during dry winter season increases the risk of wildfire incidents. According to Department of Forest and Park Services (DoFPS), the rate of wildfire had rapidly increased in 2015. Within last five years (2010-2015), a country recorded 216 wildfire incidences that burned almost 950,351.76 acres of forest cover. The number of wildfire incidence and areas damaged reported between 2008 and 2014 (Yeshey, 2015) is displayed in Figure 1.1. In this period, a total of 72 wildfire incidences was observed and 6,766.734 acres were reported damage. The record shows that Thimphu, has the highest cumulative frequency of 64 wildfire incidences (Figure 1.1). The graph indicates that, the damaged area by the wildfire does not necessarily depend on the number of fire incidences or otherwise it is not proportional with the frequency of fire incidences. This is an indication that the wildfire frequency

and its burning characteristics are influenced by many influential factors, which is addressed in the current study.



Source Country Report ADRC (2015).

Figure 1.1 Number of fire incidences and area damaged (2008-2014).

In addition, wildfire also causes decline of air quality due to pollution, soil degradation, economic loss, destruction of watersheds and even impacts the health and well-being of humans. According to Janbaz, Gholizadeh and Dashliburun (2012), the organic matter, which is needed to maintain an optimum level of humus in the soil, is destroyed during ground fire affecting the physical and chemical characteristics of soil, which in turn affects the growth rate of the ground floras and soil organisms due to intense heat released by fire. This causes release and leaching of soil chemicals resulting in the loss of soil nutrient and damaging the soil stability. In turn this leads to soil erosion, increasing surface run off and silt in rivers. It is reported

that the heavier silt load in rivers damages the turbine blades which in turn affects power production of hydropower projects, the backbone and main source of national revenue for Bhutan. So, loss of forest cover due to wildfire will directly affect the sustainability of hydropower industry. Thus, there is high national concern on forest protection, conservation and its management. Wildfire issues have been extensively discussed and deliberated in various sessions of National Assembly since 1960s (Dorji, 2006). In general, wildfire management constitutes an important part of overall national forest policy in any country.

To establish an effective management system, most of the developed countries use prediction systems that involve a large number of monitoring tools, including advanced weather forecast algorithms. However, a developing country like ours cannot afford the use of such technologies due to weakness of technical and human resources constraints. Therefore, an alternative approach, such as identification of key factors to control wildfires and the use of susceptibility maps can serve as preventive approach in wildfire management system.

Nowadays, geoinformatics technology particularly remote sensing, GIS, and GPS provides comprehensive information that can be effectively used in all aspects of wildfire management including wildfire susceptibility mapping, and it has proved to be a valuable tool. The improved remote sensing and computational capabilities enable the rapid processing of large image datasets in near-real time. Meanwhile GIS technology has become more common and important in managing natural resource management including land use planning, natural hazard/disaster assessment, wildlife habitat analysis, riparian zone monitoring, and timber management (Chang, 2014). As a result, remote sensing and GIS has become common tools for wildfire monitoring at

local, regional and global levels. The availability of remotely sensed fire data and the powerful capability of GIS technology in storing and processing spatial data, and GIS approach has made it possible to combine several wildfire variables to establish wildfire hazard areas and susceptibility maps (Chuvieco and Congalton, 1989). Overall, remote sensing and GIS plays a vital role in mapping wildfire prone areas, monitoring fuel load and risk modelling for wildfire mitigation and they are widely used in wildfire detection, predicting spread/direction of wildfire, early warning and coordinating fire-fighting efforts for preparedness and response. In addition, remote sensing and GIS are used as a damage assessment tool useful for mapping the extent of burn, understanding biological responses due to wildfire severity and quantifying extent and pattern of burned areas for wildfire recovery.

However, this novel approach of geoinformatics technology is rarely applied either due to the lack of afford to use these technologies or due to technical constraints and lack of spatial data. Tshering (2006) also highlighted that, wildfire prediction service is virtually non-existent in Bhutan indicating that wildfire prediction research is never done before. Thus, wildfire probability mapping and prediction research in Bhutan using geospatial technology is still at developing stage and the human resource capacity needs to be strengthened. The previous research efforts and information on the wildfire in Bhutan are mainly confined to development of wildfire management strategy and policies, prevention, suppression and mitigation programs, which is not adequate in the absence of proper wildfire susceptibility map. Hence, for Bhutan, identification of effective factors to control wildfire and the use of wildfire susceptibility map can serve as a preventive or protective approach to improve wildfire management. Since there is a lack of advanced methods to monitor

the early detection of wildfire in Bhutan, identifying influential factors and mapping wildfire susceptibility is very important.

Therefore, the ultimate aim of this study is to employ this innovative approach of geoinformatics technology by integrating with GIS based LR and FR models in wildfire susceptibility analysis and examine the impact of environmental, climatic and human variables on wildfire occurrence. The results obtained from the current study will be useful in the effective wildfire management system for Bhutan.

1.2 Research objectives

The primary objective of the study is to apply geoinformatics technology, particularly remote sensing and GIS by integrating with geospatial models in wildfire susceptibility mapping in Thimphu and Paro districts of Bhutan. The specific objectives include:

- (1) To apply remote sensing and GIS technology with the integration of geospatial models (LR and FR) and determine the impact of three key influential factors (environmental, climatic and anthropogenic) of wildfire occurrence;
- (2) To formulate wildfire probability models (LR and FR) and generate probability maps based on identified significant influential factors;
- (3) To examine an optimal geospatial model (FR or LR) based on accuracy assessment and validation using ROC method and establish a reliable wildfire susceptibility zonation map.

1.3 Scope of the study

This research focuses on wildfire susceptibility analysis using geoinformatics technology with reliable geospatial models (LR and FR) in Thimphu and Paro districts of Bhutan by considering the three key influential factors of wildfire (environmental, climatic and anthropogenic) variables.

(1) MODIS wildfire hotspot data (dependent variable) of NASA's EOS of MODIS Terra and Aqua satellites for 15 years (2002-2016) period are obtained from NASA FIRMS (<http://earthdata.nasa.gov>) via E-mail.

(2) Selected wildfire influential factors (independent variables): elevation, slope, aspect, curvature, topographic wetness index, enhanced vegetation index, land surface temperature, rainfall, relative humidity, land use, distance to road, distance to river, distance to settlements, distance to agricultural land and population density are prepared using various remote sensing and GIS tools, particularly ESRI ArcGIS and ERDAS software. Multicollinearity is tested using variance inflation factor (VIF) and tolerance (TOL).

(3) The accuracy assessment and validation of the two models is performed using the ROC method based on the independent validation dataset and the selected optimum model is employed to establish the final wildfire susceptibility map.

1.4 Limitation of the study

The accuracy and the reliability of final results will ultimately depend on quality of input data and the performance of the geospatial models used. Thus, following possible limitations and constraints are felt as necessary to address in this current research.

(1) Although, LR and FR models have several advantages over other available models used in susceptibility analysis, it is important to mention that these models are abstract and simplified representations of reality. They require precise location of hotspot and large amounts of data to produce reliable results since it is based on the assumption that future wildfires will occur under the same conditions as past wildfires. For the present study, the spatial location of wildfire in was not available, so the availability of wildfire hotspot (2002-2016) rely on MODIS downloadable data from NASA FIRMS. Though, MODIS fire detection algorithms are fully automated to produce daily fire information for the entire globe, there are few limitations being reported which may sometimes produce considerable commission and omission errors (Li et al., 2001). Moreover, MODIS hotspot cannot determine the burned area.

(2) Variables such as wind speed/direction, sunshine, unemployment rate etc. could not be included due to lack of data. It must also be mentioned that the results of the models are constraint by the quality of available input GIS data.

(3) While LR and FR models utilizes a rich database, the data layers themselves may not be perfect. For example, the rainfall and relative humidity data is based on only few weather stations, which are not uniformly distributed over the entire study area. Also, few missing records are observed and manually recorded data are subject to human errors. This may have compromised the accuracy during interpolation process in GIS environment.

1.5 Study area

The study area covers Thimphu and Paro districts in western Bhutan (Figure 1.2). The two districts combined has recorded one of the highest fire incidences according to the ADRC statistics of 2015. The study area is characterized by fragile mountain ecosystem with rugged topographic terrains combined with high fuel loads and erratic wind conditions, becoming more prone to wildfire especially during the dry winter season.

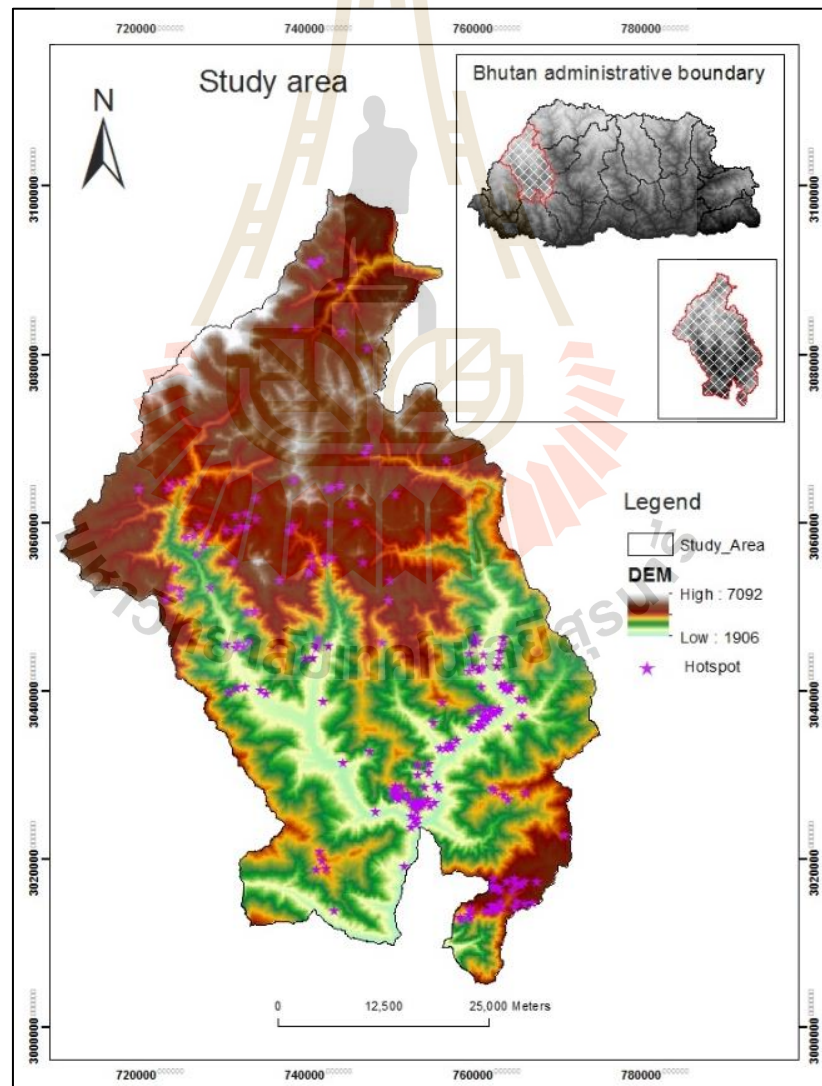


Figure 1.2 Study area.

It is bounded by geographic coordinates of longitude $89^{\circ} 07' 20''$ to $89^{\circ} 45' 56''$ E and latitude $27^{\circ} 8' 41''$ to $28^{\circ} 0' 3''$ N, covering a total area of $3,084 \text{ km}^2$ approximately. The altitude of the area varies from 1,906 meters to 7,107 meters above the MSL. The average annual mean temperature in Thimphu and Paro varies between 7°C to 15°C approximately during the winter. Most of the developments and settlements are located in the low valleys surrounded by mountains.

1.6 Benefits of the study

Since wildfire is very difficult to predict, the wildfire susceptibility map deduced from the present study would help to minimize the impact and consequences from wildfire and eventually serve as an additional tool in the effective wildfire management system, particularly, wildfire susceptibility zones in the study area. The specific benefits of the current study are presented below:

- (1) Determine the degree of significance of each influential factors on wildfire occurrence based on model statistics and regression coefficients of LR model.
- (2) Examine the spatial relationships between distribution of hotspot and its related factor to deduce the level of correlation between hotspot locations and each influential factors based on frequency ratio of each class of factor from FR model.
- (3) Establish a wildfire probability maps from LR and FR models and their performance was determined based on accuracy assessment and validation using ROC method.
- (4) Determine the optimum geospatial model (LR) for wildfire susceptibility zonation mapping with five levels of susceptibility (VL, L, M, H, and VH).

CHAPTER II

BASIC CONCEPTS AND LITERATURE REVIEWS

This chapter contains the basic concepts and theories related to the research: The major contents include: (1) definitions and basic concepts of wildfire, (2) basic characteristics of wildfire, (3) logistic regression model, (4) frequency ratio model, (5) influential factors of wildfire, (6) causes of wildfire in Bhutan, (7) MODIS hotspot, its specification, characteristics and basic concepts on fire detection algorithm and Statistics of MODIS hotspot in Bhutan and (8) relevant literature reviews on previous wildfire researches based on the application of geospatial models (LR and FR) and remote sensing and GIS technology.

2.1 Definitions and basic concepts of wildfire

The term “**wildfire**” is used for any uncontrolled fire, that destroys forests and many other types of vegetation including animal species or it is an unplanned fire burning in natural areas such as forests, shrub lands and grasslands (Stein et al., 2013). In some parts of the World wildfire is caused by lightning and from few other natural causes however, nowadays most wildfire is caused by humans, either accidentally, as a result of carelessness, or arson. Depending on the type of vegetation or material being burnt, wildfire is known by different names such as forest fire, bush fire, grass fire, vegetation fire, peat fire or wildland fire, but all describes the same phenomenon.

To understand wildfire terminology, various technical terms associated with wildfires like “risk”, “hazard”, “vulnerability” “severity” etc., are addressed here. Fire vulnerability is defined as the degree of loss to biotic and abiotic elements of the environment to a given magnitude of fire hazard. It is expressed in a scale between “0” (no damage) to “1” (total damage.) (Castillo and Avendano, 2004). It is also defined as a set of conditions and processes resulting from physical, social, economic and environmental factors, which increase susceptibility of community to the impact of hazards (ISDR, 2002). Wildfire hazard is defined as a physical event of certain magnitude in a given area and at a given time, which has the potential to disrupt the functionality of a society, its economy and its environment (Boonchut, 2005). Wildfire risk is expected losses due to wildfire hazard to various elements at risk over specific time. Thus, it is measured in terms of expected loss such as economic loss, number of lives loss and extent of physical damage. Mathematically wildfire risk expressed as:

$$\text{Wildfire Risk} = \text{Hazard} * \text{Susceptibility} * \text{Amount} \quad (2.1)$$

$$\text{Wild fire Risk} = \text{Hazard} * \text{Susceptibility} * \text{Capacity} \quad (2.2)$$

Where “Amount” is the quantity of elements at risk, e.g. number of peoples, number of trees, number of animals etc. and “Capacity” is the skills and operational resources to cope up with the fire risk factors so that the damage can be reduced. Wildfire severity refers to the magnitude of significant negative impact on wildland systems (Simard, 1991), while susceptibility map gives an estimation of the probability that an event occurs in a specific area without considering an absolute temporal scale.

2.2 Basic characteristics of wildfire

The basic characteristic of wildfire which includes fire triangle, type of fire and fire behavior triangle are summarized in this section based on Bennett et al. (2010).

2.2.1 Fire triangle.

The fire triangle is a simple way of understanding the factors of fire (Figure 2.1). It is used as a model for conveying the components of a fire. The three sides of fire triangle illustrate the three elements of fire: heat, fuel and oxygen. These elements must be combined in the right proportions for a fire to occur and sustain: enough oxygen to sustain combustion; enough heat to raise the material to its ignition temperature and a fuel/combustible material. If one of the three elements are removed, the fire is extinguished.

(a) Heat

Heat is the most essential part of fire elements. A fire cannot ignite unless it has a certain amount of heat, and it cannot grow without heat either. One of the first things firefighters do to extinguish a fire is to apply a cooling agent, usually water or a chemical fire retardant used in fire extinguishers.



Source: <http://firefoxfiresolutions.com>.

Figure 2.1 Fire triangle.

(b) Fuel

A fire needs a fuel source in order to burn. The fuel source can be anything that is flammable, such as wood, paper, fabric, or chemicals. Once the fuel element of the fire triangle is removed, the fire will go out. If a fire is allowed to burn without any attempt to extinguish it, it will extinguish on its own when it has consumed all of the fuel.

(c) Oxygen

Oxygen is another essential component of fire. A fire needs oxygen to start and continue. That is why small fires are often extinguished by smothering with a non-flammable blanket, sand or dirt. A decrease in the concentration of oxygen retards the combustion process.

2.2.2 Types of fire

Basically, fire can be categorized into three types: surface fire, ground fire and crown fire (Bennett et al., 2010) as shown in Figure 2.2. The relative proportion of each type can provide clues to the overall severity of a particular wildfire.

(a) Surface fire

A surface fire is the most common type that burns surface litter and loose debris of the forest floor and small vegetation, moving slowly and damaging trees. It produce flaming fronts that consume needles, moss, lichen, herbaceous vegetation, shrubs, small trees, and saplings (Figure 2.2a). It can ignite large woody debris and decomposing duff, and burn long after surface flames have moved past.

(b) Ground fire

A ground fire usually burns the organic matter like duff, musk or peat present beneath the surface litter of the forest floor. It not easy to detect as it spreads in and do not produce visible flames (Figure 2.2b). In times of drought conditions the fire may penetrate several feet below the surface and travel entirely underground often smoldering for days or weeks, without flames producing little smoke.

(c) Crown Fire

Crown fire is usually intense and is strongly influenced by wind, topography, and tree (crown) density. It moves from top to top of trees/shrubs and becomes active when enough heat is released to preheat and combust fuel above the surface, spreading from one tree crown to the next though the canopy (Figure 2.2c).



(a) Surface fire

(b) Ground fire

(c) Crown fire

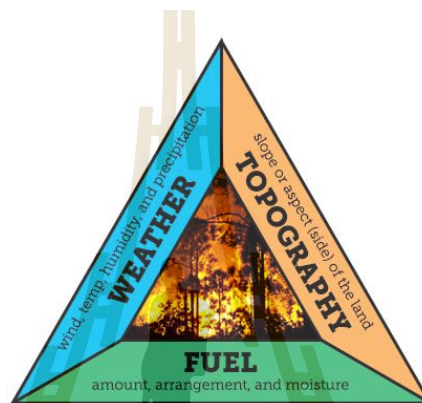
Source: Bennett et al. (2010)

Figure 2.2 Types of wildfire.

In actual fire situations, all three types of fire may occur simultaneously and in all possible combinations depending on the type of fuel available and influential factors. A surface fire may spread into the crown and develop a crown fire, while a crown fire may drop to the ground and become a surface fire. Similarly, a surface fire may develop into a persistent ground fire that is difficult to detect.

2.2.3 Fire behavior triangle

Another significant characteristic of fire is its behavior, once a fire is ignited its rate of spread and its intensity will depend on the three elements that make up the fire behavior triangle: topography, weather and fuel (Figure 2.3). A change in any one factor during the fire alters its behavior and fire type. Details on the influence of topography, weather, and fuels on fire behavior can be summarized as follows:



Source: <https://learn.weatherstem.com>

Figure 2.3 Fire behavior triangle.

(a) Topography

Topography is the most stable variable in the fire behavior triangle. Slope, aspect, elevation, and topographic features influence fire spread. Fire tends to spread faster up a slope than down one. As heat rises in front of the fire, it more effectively preheats and dries upslope fuels, making for more rapid combustion. Aspect affects how much solar radiation a site receives and it dictates the vegetation types. Elevation affects fire behavior by influencing the amount and timing of precipitation, as well as exposure to prevailing wind. It also affects the seasonal drying of fuel. In lower elevations, fuels tend to dry out faster because of higher temperatures and lower precipitation.

(b) Weather

Weather influences how fast and to what degree fuels dry out during the fire season. It is the most variable factor in the fire behavior triangle. Long periods of low relative humidity and high winds can quickly dry fuels. Extended drought periods leave fuels with very low moisture content, resulting in increased fire activity and intensity. Fire is wind-driven which pushes the fire rapidly in one direction. In contrast, a change in weather from hot and dry to cooler, moister conditions can reduce fire intensity and rate of spread.

(c) Fuel

Fuel consists of dead woody material (needles, fallen branches, dried herbaceous vegetation, snags, and logs) or live trees and other vegetation like shrubs. The size, moisture and chemical content of fuel also influence combustion and fire behavior. Fuel is categorized into four classes:

(1) Ground fuel consists of duff (decomposed needles and other organic material), buried (rotten) roots and logs, and accumulations of decomposing bark at the base of trees;

(2) Surface fuel consists of litter or undecomposed needles; moss; lichens; rotten and sound logs; woody debris and slash piles; stumps; low vegetation like grass, herbs, and small shrubs;

(3) Ladder fuel contains large shrubs; small and medium-size trees; low-growing branches on medium to large trees that allow a surface fire to move up into the overstory tree crowns and

(4) Crown fuel consists of lichen, tree needles, and small branches that compose the forest canopy; and snags.

2.3 Logistic regression model

Logistic regression (LR) model which is sometimes known as logistic model or logit model is a special case of multiple linear regression used to predict the presence or absence of outcome variable based on the set of predictor variables. It is suitable to models where the dependent variable is dichotomous or binary in nature. It is used to analyze the relationship between multiple independent variables and a categorical dependent variable and estimates the probability of occurrence of an event by fitting data to a logistic curve. There are different multivariate statistical approaches like multiple linear regression, discriminant analysis, logistic regression, etc. The nature of the dependent variables guide the selection of the most appropriate model. If the dependent variable is continuous in nature, then multiple linear regression can be used. When the dependent variable is dichotomous or binary in nature, both discriminant analysis and LR are suitable. Natural data are usually discrete (can be categorical) or continuous. Both linear discriminant analysis and logistic regression are appropriate for the development of linear classification models, nevertheless, the two methods differ in their basic idea and it is reported that LR is better than discriminant analysis when the independent variables are categorical, continuous or a combination of both (Atkinson and Massari, 1998).

The other type of LR is multinomial LR which is used when the dependent variable is not dichotomous and is comprised of more than two categories. LR generates the model statistics and coefficients of a formula useful to predict a logit transformation of the probability that the dependent variable is 1 (occurrence of an event). It does not define susceptibility directly but the constant and the coefficients of the predictor

variables retained by the LR model can be used to draw inference and calculate the probability of occurrence of dependent variable.

The main advantages of LR model are that, it gives the freedom to use both categorical and continuous predictor variables together in a regression analysis, whereby an independent variables can be non-linear, continuous, categorical or a combination of both continuous and categorical (Menard 1995; Schicker and Moon, 2012). LR is applicable to a broader range of research situations compared to discriminant analysis. It is relatively robust, flexible and easily used, and it lends itself to a meaningful interpretation. LR model can be validated by receiver operating characteristic (ROC) curve where by the accuracy of the model can be obtained. It does not require the variables to be normally distributed or it makes no assumptions on the distribution of the explanatory data, whereas, linear discriminant analysis has been developed for normally distributed explanatory variables, which is not always met in case of data on natural phenomena like geology, land use or land cover, etc. The LR does not assume a linear relationship between the independent variable, so with other forms of regression, multicollinearity among the predictors can lead to biased estimates and inflated standard errors (SPSS, 2003). It is also robust when the data are auto-correlated, which occurs frequently, when derived as GIS raster coverage (Ohlmacher and Davis, 2003).

For linear regression, where the output is a linear combination of input feature(s), and it is expressed as:

$$Y = \beta_0 + \beta_1 X + \epsilon \quad (2.3)$$

In LR, the same equation is used, but some modification is made to Y (response variable). Herein, probabilities are calculated that always lie between 0 and 1.

Therefore, the response value must be positive and it should be lower than 1. To meet this two criteria, two known conditions are applied i.e., exponential of any value is always a positive number and, any number divided by number + 1 will always be lower than 1. Implementing these two findings:

$$P(Y = 1|X) = \frac{e^{(\beta_0 + \beta_1 X)}}{e^{(\beta_0 + \beta_1 X)} + 1} \quad (2.4)$$

This is the logistic function where the probability value will always lie between 0 and 1. Now, to determine the link function, $P(Y=1|X)$ represents probability that $Y = 1$ given some value for predictor variable x . Y can take only two values, 1 or 0. To simplify calculation, $P(Y=1|X)$ be expressed as $P(Y)$.

$$\Rightarrow P(Y) = \frac{e^{(\beta_0 + \beta_1 X)}}{e^{(\beta_0 + \beta_1 X)} + 1} \quad (2.5)$$

$$\Rightarrow P \cdot (e^{(\beta_0 + \beta_1 X)} + 1) = e^{\beta_0 + \beta_1 X} \quad (2.6)$$

$$\Rightarrow P = e^{(\beta_0 + \beta_1 X)} (1 - P) \quad (2.7)$$

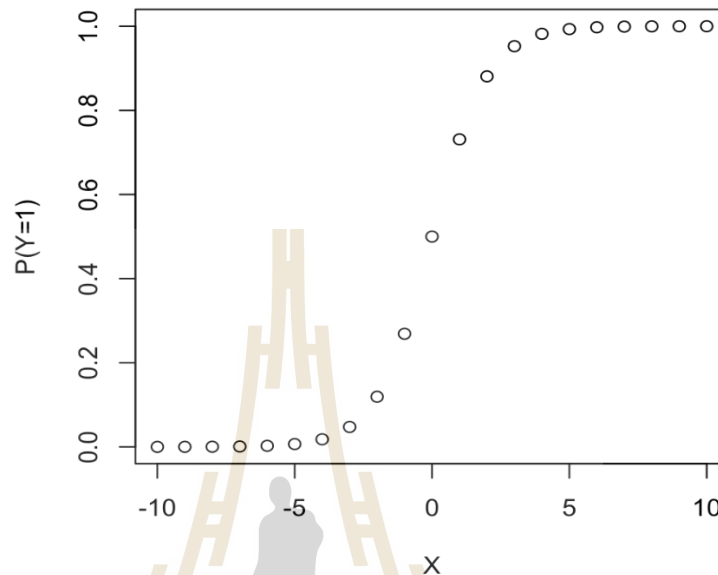
$$\Rightarrow \left(\frac{P}{1-P} \right) = e^{(\beta_0 + \beta_1 X)} \quad (2.8)$$

$$\Rightarrow \text{Logit}(Y) = \ln \left(\frac{P}{1-P} \right) = \beta_0 + \beta_1 X \quad (2.9)$$

The right side of equation 2.9 depicts the linear combination of independent variables. The left side is known as the log-odds or odds ratio or logit function and it is the link function for LR. This link function (or logit function) follows a sigmoid (Figure

2.4) function which limits its range of probabilities between 0 and 1 for any value of x .

This function outputs the probability that $y=1$.



Source: Source: <http://practical-guide-logistic-regression-analysis-r>.

Figure 2.4 Sigmoid (Logistic) function/S-shaped curve.

Equation 2.9 is interpreted as, a unit increase in variable X results in multiplying the odds ratio by e to power β . In other words, the regression coefficients explain the change in \log (odds) in the response for a unit change in predictor. In multiple regression, the ordinary least square (OLS) method is used to determine the best coefficients to attain good model fit. In the LR, maximum likelihood method is used to determine the best coefficients and eventually a good model fit. Maximum likelihood tries to find the value of coefficients such that the predicted probabilities are as close to the observed probabilities as possible. In other words, for a binary classification (1/0), maximum likelihood will try to find values of coefficients such that the resultant probabilities are closest to either 1 or 0.

By solving Equation 2.9 for P for “n” independent variables, the final probability equation is derived as shown below:

$$\text{Logit}(y) = \log \frac{P}{(1-P)} = \frac{e^{(\beta_0 + \beta_1 x_1 + \beta_2 x_2 + \beta_3 x_3 + \dots + \beta_n x_n)}}{1 + e^{(\beta_0 + \beta_1 x_1 + \beta_2 x_2 + \beta_3 x_3 + \dots + \beta_n x_n)}} \quad (2.10)$$

$$P = \frac{1}{1 + e^{-(\beta_0 + \beta_i x_i)}} \approx \frac{1}{1 + e^{-z}} ; \quad 0 < P < 1 \quad (2.11)$$

In this study, the basic requirement is to map the areas of wildfire susceptibility based on the prevailing wildfire scenario with its influential factors. The main aim of the LR is to find the best-fitting model to describe the relationship between the dependent variable and a set of independent variables. The coefficient of the predictor variables generated by the LR model describes the significance of each variable, the positive and negative influences, and the probability of the presence of wildfire hotspot. Using the coefficients of the LR as weights, the probability map of the wildfire can be obtained using the Equation 2.11.

2.4 Frequency Ratio model

Frequency ratio (FR) model is a simple geospatial assessment tool for computing the probabilistic relationship between dependent and independent variables, including multi-classified maps (Oh, Kim, Choi, and Lee, 2011). It is defined as the ratio of occurrence probability to non-occurrence probability for specific attributes (Lee and Talib, 2005). For wildfire, the FR is based on the observed relationships between distribution of hotspot and each hotspot-related factor, to reveal the level of correlation

between hotspot locations and the influential factors in the study area (Pradhan, Suliman, and Awang, 2007).

The FR model is very popular and have been widely used for the wildfire susceptibility and in many other risk analysis including landslide and flood susceptibility analysis (Lee and Pradhan, 2007; Oh et al., 2011) and it has shown high accuracy. Yilmaz (2009) emphasized that the procedure for preparing susceptibility map must be simple and have a higher accuracy. Thus, the FR model has several advantages of simplicity; more importantly, inputs, output, and calculation process are readily understood. In addition, large amount of data can be processed in the GIS environment quickly and easily, whereas in statistical package it is hard to process the large amount of data.

The calculation steps for an FR for a class of the wildfire-affecting factor is expressed as (Lee and Pradhan, 2007 and Lee and Talib, 2005):

$$FR = \frac{\text{Hotspot Ratio}}{\text{Area Ratio}} = \frac{(A/B)}{(C/D)} = \frac{P}{K} \quad (2.12)$$

Where, A is the number of hotspot pixels in each class of factor; B is the total number of hotspot pixels in the entire study area; P represents % of hotspot pixels for entire study area; C is the number of pixels (hotspot and non-hotspot) in each class of factor; D is the total number of pixels (hotspot and non-hotspot) in all/whole class (i.e. the entire study area); K represents the % of pixels (hotspot and non_hotspot) in each class for the factor.

The next step is to assign these computed FR values of each class of factors using the reclassify option of spatial analyst tool in Arc GIS. Finally, all the factor maps,

with assigned FR values, are added to produce wildfire susceptibility index (WSI) map using the equation below.

$$WSI = FR_1 + FR_2 + FR_3 + \dots \dots \dots FR_n \quad (2.13)$$

Where, WSI represents wildfire susceptibility index, $FR_1+FR_2+FR_3+\dots+FR_n$ represents frequency ratio factor maps of wildfire influential factors. WSI value represents the relative susceptibility to forest fire occurrence, where higher values are associated with high susceptibility and lower values will represent low susceptibility

In wildfire susceptibility analysis, FR model provides how each class of influential factor affects fire occurrence, while the LR model gives a clear information about the degree of influence each factors have on fire occurrence. Though LR and FR models take different approaches to identify susceptibility area, comparison of their results provides more insight on the complicated interaction between fire events and the environmental conditions in the study area.

2.5 Influential factors of wildfire

The complex relationship between fire, environment, climate, and vegetation are the most interesting and challenging aspects in understanding how fire is changing on the landscape in response to climatic change. Occurrence of wildfire does not depend on any single factor instead its behavior, intensity and its rate of spread depend on various integrated factors. Although, the spread of a wildfire in a particular area depends on many factors, most importantly it is influenced by local weather, vegetation, and topography. Of these three factors, the topographic features remain static while

vegetation changes over time. Weather is the most dynamic factor which affects wildfire. Its unpredictable nature makes modelling wildfire a difficult task. Therefore, to obtain a reliable wildfire susceptibility map, a detailed study of fire influential factors, fire events and fire prone areas must be well understood and analyzed carefully in advance.

According to the relevant literatures (Brown and Davis, 1973; Chuvieco and Congalton, 1989; Preisler et al., 2004 and San-Miguel-Ayanz, Ravail, Kelha, Ollero, 2005), environmental factors including fuel characteristics, climatic characteristics, topographic characteristics and fire history are mentioned to have major impacts over the creation, propagation and intensity of wildfires, and reported as the critical factors in any fire hazard rating system. In another research, Vasconcelos, Pereira and Zeigler (1995) stated that vegetation, topography, climatology and fire history are considerable components of hazard to assess forest fire risk. Pradhan et al., (2007) emphasized that NDVI, soil, slope, aspect, and land use are the effective factors to assess fire risk hazard. Also, Janbaz et al., (2012) used topography, vegetation, slope, aspect, NDVI and climatic factors to develop forest fire risk mapping in Iran. Furthermore, Ghomi et al. (2013) stated that vegetation cover, distance from settlements and slope are important factors for forest fire hazard mapping. Hence, understanding the spatial distribution and significant predictors of fire occurrence is crucial for wildfire management system.

Based on extensive literature reviews, the significant influential factors of wildfire can be classified under three broad categories: environmental, meteorological, and anthropogenic factors as summarized in the following sections.

2.5.1 Environmental factors

Environmental factors consist of topography which includes slope, aspect, elevation, curvature etc., and fuel characteristics, such as vegetation type, amount, and leaf dryness or fuel moisture content etc. Topographic variables characterize the landscape features and they are strongly recommended to be included when modeling fire occurrence. The fuel characteristics is another significant factor which changes the fire behavior. The amount of fuel and its moisture content have significant influence on the rate of combustion and fire behavior.

(a) Slope

Slope represents the gradient of the land, and is generally expressed in terms of percentage (%) or degrees. It measures the rate of change of elevation at a surface location. Among all the topographic factors slope is considered to be the most critical. Depending upon slope angle and wind speed, slope can be more important than wind in determining the rate of fire spread. Terrain with high or steep slopes can accelerate the spread of fires because of more efficient connective preheating. As the warm air rises preheating the uphill fuels, fires advance uphill faster than they travel downhill (Rawat, 2003). It is claimed that a fire burning up to a slope of +20% to +39% will spread twice as fast as a fire on level terrain (Brown and Davis, 1973).

(b) Aspect

Aspect refers to the direction of slope, which in turn determines the intensity and direction of sunlight received by that face. It determines how much sunlight is received. Aspect measures are often classified into four principle directions and or eight principle directions. South aspects receive more sun light and have higher

temperatures with robust winds, low humidity, and low fuel moistures in the North Hemisphere. Generally slope facing north is cooler than the south facing slope because south and west aspect receives more sunlight than the north and east aspect. Hence, vegetation is typically drier and less dense on south-facing aspects than north-facing ones which hold more moisture and stay green longer and support more vegetation (Prasad et al., 2008). Thus, drier fuels with less moisture content are more exposed to ignition. In addition, earlier in the day, east aspects get more ultraviolet and direct sunlight than west aspect. Consequently, east aspects dry faster (Adab et al., 2013).

(c) Elevation

Elevation is the height at any point on the surface of the Earth above the mean sea level. Places at higher elevation are much cooler than the places at lower elevation. Hence, elevation is a crucial topographic variable that is associated with temperature, moisture, and wind which plays an important role in fire spreading (Jaiswal et al., 2002). It has also been observed that fire behavior trends are less severe at higher altitude because of higher rainfall (Chuvieco and Congalton, 1989). Furthermore, Brown and Davis (1973) reported that high elevation has greater rainfall and a colder and wetter climate, resulting in a fire season that is shorter with fire incidences that are less severe.

(d) Curvature

Curvature is the rate of change of slope gradient or aspect in a particular direction (Wilson and Gallant, 2000). It determines whether a land surface is upwardly convex or concave. It measures the difference between profile curvature and plan curvature in which, profile curvature is estimated along the direction of maximum slope and plan curvature is estimated across the direction of maximum slope (Chang,

2014). The curvature value can be evaluated by calculating the reciprocal value of the radius of curvature of that particular direction. Negative curvature represents concave surface, zero curvature represents flat and positive curvature is known as convex surface.

(e) Topographic Wetness Index (TWI)

Wildfire is influenced by hydrogeological conditions as well, therefore, TWI is here selected to represent hydrogeological conditions in the analysis. Topography firstly controls the spatial variation of hydrological conditions and slope stabilities. It affects the spatial distribution of soil moisture, and groundwater flow often follows surface topography. (Moore, Grayson, and Ladson, 1991). TWI, also known as compound topographic index (CTI) was developed by Beven and Kirkby (1979) within the runoff model to represent a steady state of wetness index. It is commonly used to quantify topographic control on hydrological processes. The index is function of both the slope and upstream contributing area per unit width orthogonal to the flow direction. TWI will be higher in flat areas where the flow accumulation is higher. It is reported that the index is highly related with several soil attributes such as horizon depth, silt percentage, organic matter content, and phosphorous, hence the use of this variable will also suffice the soil type variable which is often used as relevant factor in fire prediction. TWI is defined based on equation 2.14 (Moore et al., 1991):

$$TWI = \left(\frac{\alpha}{\tan \beta} \right) \quad (2.14)$$

Where α is the cumulative up slope area draining through a point (per unit contour length) and $\tan \beta$ is the slope angle at the point. TWI reflects the tendency of water to accumulate at any point in the catchment and the tendency of gravitational forces to move that water down slope (Pourtaghi, Pourghasemi, and Rossi, 2014). In other words,

TWI identifies and locates area where water or ponds or any wet area in a landscape, and measures the potential wetness in any portion of the landscape. It is a combination of catchment area/flow accumulation and slope. Low slope and high catchment area will have high potential to collect water, thus it will have high TWI value.

(f) EVI (Enhanced vegetation index)

The main factor affecting the spread of a forest fire is the type and characteristics of the vegetation because they represent the total fuel available for the fire. Vegetation indices play an important role in monitoring variations in vegetation. NDVI is the most used common factor for assessing the live fuel moisture content (Chuvieco et al., 2003). NDVI is computed based on equation 2.15:

$$NDVI = \frac{(NIR-RED)}{(NIR+RED)} \quad (2.15)$$

The enhanced vegetation index (EVI) was developed as an alternative vegetation index to address some of the limitations of the NDVI. The EVI is specifically developed to:

- i. Be more sensitive to changes in areas having high biomass (a serious shortcoming of NDVI).
- ii. Reduce the influence of atmospheric conditions on vegetation index values, and
- iii. Correct for canopy background signals.

EVI tends to be more sensitive to plant canopy differences like leaf area index (LAI), canopy structure, and plant phenology and stress than does NDVI which generally responds just to the amount of chlorophyll present. With the launch of

the MODIS sensors, NASA adopted EVI as a standard MODIS product that is distributed by the USGS and it is calculated as:

$$EVI = \frac{(NIR-RED)}{(NIR+C1*RED-C2*BLUE+L)} * G \quad (2.16)$$

Where, RED = Reflectance in MODIS red channel; NIR = Reflectance in MODIS NIR channel; BLUE = Reflectance in MODIS blue channel; C1 = Atmospheric resistance red correction coefficient (C1 = 6); C2 = Atmospheric resistance red correction coefficient (C2 = 7.5); L = Canopy background brightness correction factor (L = 1) and G = Gain factor (G = 2.5)

The output of EVI is a single image layer with values typically from 0.0 to 1.0. Each band in the image is a 16-day composite image (that is the “best representation” of the vegetation index in a 16-day period). The NDVI and EVI are specifically intended to map vegetation but their values are also influence by the presence of clouds and snow cover. Both clouds and snow have low NIR and high visible reflectance, thus when snow or clouds are present for much or all of the 16 days used to create each composite, the NDVI and EVI will be negative. Therefore, regions that experience much cloud cover over the winter months may have negative vegetation indices even though they would normally have high amounts of vegetation biomass. Areas that are snow-covered over much of the year will also have negative NDVI and EVI values.

(g) Land use

The human relationship to fire is complex, and it varies substantially across the globe (Pyne, 2001). Since the beginning of history, humans have used fire as a mechanism for creating areas suitable for agriculture and settlement resulting in the change of landscape. Land use changes also influence fire occurrence frequency and fuel loads altering fire regimes leading to altered fire patterns in many parts of the World. Hence, land use change has become a key driver of fire in many systems across multiple scales. For example, Carmoa et al., (2011) found that fire proneness was higher in shrub lands and steep slopes. It was observed that, there was a slope effect on the fire proneness of all land cover types.

2.5.2 Meteorological factors

Meteorological factors such as annual rainfall, temperature, relative humidity and wind effect have significant influence and play important role in the occurrence of wildfire. In most of the fire prediction research studies, the weather variables are taken into consideration as an important factor and it is reported to have significant influence in the occurrence of fire.

(a) Temperature

Temperature strongly affects the moisture content in forest fuels. High temperature helps dry fuels quickly and fuels exposed to direct solar radiation become much warmer than the surrounding air, as a result moistures move from warmer fuel to the air even if the relative humidity of the air is high (Rawat, 2003). Areas with high crown density keeps the ground cooler as it is less exposed to direct sunlight, whereas open areas are more prone to fire and often get burned due to higher air temperature as a result of exposure to direct sunlight (Brown and Davis, 1973).

Land surface temperature (LST) is one of the critical biophysical and/or climatic variables, that plays an important role in understanding various environmental phenomena, such as surface wetness conditions, evapotranspiration, urban heat island, vegetation health, forest fire danger conditions etc. (Wan et al., 2004). Nowadays, several LST acquiring satellites are operational, such as MODIS, Advanced Spaceborne Thermal Emission and Reflection (ASTER), Landsat-7 ETM+, Landsat-8 TIRS, Geostationary Operational Environmental Satellite (GOES), NOAA Advanced Very High Resolution Radiometer (AVHRR), Indian National Satellite System (INSAT), Geostationary Meteorological Satellite (GMS), and Meteorology Satellite (Meteosat), etc. In the current study MODIS LST is used as the proxy for temperature.

(b) Precipitation

Rainfall is another significant factor which has an effect on both fuel and soil moisture. Drought associated with the El Nino turns moist forests into drier habitats and increases the flammability of forest vegetation, thus increasing the number, frequency, size, intensity and duration of fires (FAO, 2001). In general, rainfall increases moisture content in the fuel and surrounding environment and reduces the ignition of fires. However, rains during the growing season can spark a plant growth in barren lands and then if dry conditions follow, the risk of setting for fire increases with lots of dry fuel.

(c) Relative humidity

Relative humidity is expressed as the ratio of the amount of moisture in the air compared to the amount that the air can hold at the same temperature and pressure if it were saturated. A relative humidity of 95 percent indicates that the air is nearly saturated with almost all of the water vapor it can hold. The air is much drier

when the relative humidity is 30 percent, as compared to 100 percent. Moisture is exchanged between the air and nearby objects, including dead and live fuels. For example, at low relative humidity the moisture moves out of fuels to the air, and thus, drying occurs. At high relative humidity the dead fuels retain most moisture, i.e., less moisture moves out of the fuel into the air. When a fuel has more moisture, it is harder to ignite and burn. The relative humidity of the air changes faster than an entire fuel particle can exchange moisture with the air (<http://learningcenter.firewise.org>).

2.5.3 Anthropogenic factors

The probability of wildfire occurrence is also determined by the nearby habitation and the access humans have to the forest, because humans, animals and vehicular movement, and activities on roads provide suitable opportunities for accidental/man-made fires. Therefore, forests located near roads and habitats are more prone to fires. Hence the extent of human interference with the forest can help in assessing the potential risk areas from man-induced fires. Forest near by the agricultural fields are also very prone to fires due to burning of agricultural debris. However two major effects can be considered from proximity data (Chuvieco and Congalton, 1989). First, they can serve as fire breaks or pathways for suppression of the fire reducing the fire hazard. On the other hand, they are potential routes for hiking or camping areas that may increase fire hazard because of the more intense human activities. Hence, proximity variables including socio-economic factors play a vital role in wildfire occurrence. Generally, the influence of population density can be either positive or negative on wildfire occurrence depending on awareness, income, occupation, literacy rate, and unemployment etc.

2.6 Causes of wildfire in Bhutan

Identifying the causes and driving factors of wildfire ignition is the primary step towards effective wildfire management system. In general most of the wildfire worldwide are related to human activities while natural causes only play a minor role.

In Bhutan, it is reported that almost all the wildfires are caused by anthropogenic activities, either accidentally or deliberately (Mckinnell, 2000). Although, few cases remain with no concrete evidence, the common causes of wildfires include: burning of debris agricultural/waste; electrical defaults; making fires near or inside the forest; children playing with flammable materials; deliberate lighting of forest fire to clear land to graze cattle; smokers disposing of burning matches or cigarettes butts; picnickers, unattended camp fire/warming fire by hikers; cattle herders, both migratory and sedentary; road side workers, lemon grass harvester and deliberate acts of arson, either to scare away damaging wild animals. Other reasons for the increase in wildfire could be associated rapid urbanization and economic growth of the country. In addition, mining activities also present a constant threat of sparking off forest fire. Unlike in western countries, natural causes like lightning are very rare and does not account for any wildfire. The assumed reason is that, most of the lightning strikes are associated with heavy rains and thus eliminates the chance of fire incidences, however, the wildfire from natural causes is not ruled out. Tshering (2006) mentioned that there exists high degree of uncertainty regarding the causes of wildfire in Bhutan referring to the suggestions of many fire experts who worked on fire projects in Bhutan. The survey conducted also showed that only 36% of the respondents were confident in expressing the familiarity with the causes of wildfire in Bhutan, indicating that there are many unknown causes.

2.7 MODIS hotspot

Several remote sensing satellite sensors have been used to extract hotspot for long term and large scale fire monitoring. However, each of the instruments has reported unique advantages and limitations. The design of the MODIS sensor took into account these limitations, by improving the number and sensitivity of thermal channels and it is widely used sensor for active fire detection nowadays.

MODIS on board of Terra and Aqua of NASA's Earth Observation System (EOS) was the first satellite image to provide thermal sensors specifically designed for fire monitoring. MODIS fire hotspots at a global scale provides highly relevant information on fire events. It has a great potential for monitoring fire dynamics, the data is delivered free and nearly real time information can be obtained from a maximum of four satellite overpasses each day with a data record that spans more than a decade. The MODIS instruments provide global coverage of the Earth's surface in high radiometric sensitivity (12 bit). Data collected from the MODIS instruments span over 36 spectral bands, ranging from the visible (0.4 μm) to the long wave infrared (14.4 μm). The MODIS design combines high resolution data from the visible and near infrared channels (250-500 m) with the moderate resolution of its infrared channels (1 km). MODIS Terra spacecraft was launched in December 1999 and the Aqua spacecraft in May 2002. The orbit of the Terra satellite goes from north to south across the equator in the morning with a 10:30 am and 10:30 pm equatorial overpass and Aqua passes south to north over the equator in the afternoon with a 1:30 pm and 1:30 am equatorial overpass resulting in global coverage every 1 to 2 days. However, for most parts of the Earth's equator, there are 4 overpasses in a twenty-four-hour period (NASA FIRMS,

2012). Details of MODIS specification are summarized in Table 2.1 and its spectral characteristics in Table 2.2.

Table 2.1 Specification of MODIS sensor and its characteristics.

Structure	Specification
Orbit:	705 km, Terra (10:30 and 22:30) and Aqua (13:30 and 01:30), sun-synchronous, near-polar, circular
Scan Rate:	20.3 rpm, cross track
Swath Dimensions:	2,330 km (cross track) by 10 km (along track at nadir)
Telescope:	17.78 cm diam. off-axis, a focal (collimated), with intermediate field stop
Size:	1.0 x 1.6 x 1.0 m
Weight:	228.7 kg
Power:	162.5 W (single orbit average)
Data Rate:	10.6 Mbps (peak daytime); 6.1 Mbps (orbital average)
Quantization:	12 bits
Spatial Resolution:	250 m (bands 1-2) 500 m (bands 3-7) 1,000 m (bands 8-36)
Design Life:	6 years

Source: <http://modis.gsfc.nasa.gov/about/specifications.php>.

2.7.1 MODIS Hotspot detection and its characteristics

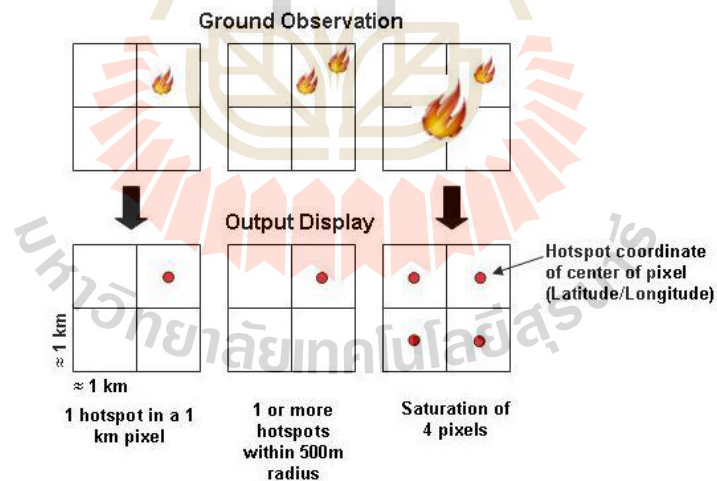
The MODIS Rapid Response Team produces the MODIS fire location data that identify and characterize actively burning fires (e.g. wildfires, agricultural fires, etc.) and other thermal anomalies (e.g. volcanoes, etc.) at the time of satellite overpass. Fires that do not emit sufficient heat under relatively cloud-free conditions at overpass time are unlikely to go detected. The fire detection algorithms are fully automated and produce daily fire information for the entire globe.

Table 2.2 MODIS spectral characteristics.

Primary Use	Band	Bandwidth	Spectral Radiance (W/m ² - μ m-sr)
Land/Cloud/Aerosols Boundaries	1	620 - 670 nm	21.8
	2	841 - 876 nm	24.7
Land/Cloud/Aerosols Properties	3	459 - 479 nm	35.3
	4	545 - 565 nm	29.0
	5	1230 - 1250 nm	5.4
	6	1628 - 1652 nm	7.3
	7	2105 - 2155 nm	1.0
Ocean Color/ Phytoplankton/ Biogeochemistry	8	405 - 420 nm	44.9
	9	438 - 448 nm	41.9
	10	483 - 493 nm	32.1
	11	526 - 536 nm	27.9
	12	546 - 556 nm	21.0
	13	662 - 672 nm	9.5
	14	673 - 683 nm	8.7
	15	743 - 753 nm	10.2
Atmospheric Water Vapor	16	862 - 877 nm	6.2
	17	890 - 920 nm	10.0
	18	931 - 941 nm	3.6
	19	915 - 965 nm	15.0
Surface/Cloud Temperature	20	3.660 - 3.840 μ m	0.45 (300K)
	21	3.929 - 3.989 μ m	2.38 (335K)
	22	3.929 - 3.989 μ m	0.67 (300K)
	23	4.020 - 4.080 μ m	0.79 (300K)
Atmospheric Temperature	24	4.433 - 4.498 μ m	0.17 (250K)
Atmospheric Temperature	25	4.482 - 4.549 μ m	0.59 (275K)
Cirrus Clouds	26	1.360 - 1.390 μ m	6.00
Water Vapor	27	6.535 - 6.895 μ m	1.16 (240K)
	28	7.175 - 7.475 μ m	2.18 (250K)
Cloud Properties	29	8.400 - 8.700 μ m	9.58 (300K)
Ozone	30	9.580 - 9.880 μ m	3.69 (250K)
Surface/Cloud Temperature	31	10.780 - 11.280 μ m	9.55 (300K)
	32	11.770 - 12.270 μ m	8.94 (300K)
Cloud Top Altitude	33	13.185 - 13.485 μ m	4.52 (260K)
	34	13.485 - 13.785 μ m	3.76 (250K)
	35	13.785 - 14.085 μ m	3.11 (240K)
	36	14.085 - 14.385 μ m	2.08 (220K)

Source: <http://modis.gsfc.nasa.gov/about/specifications.php>.

The detection criteria are based on the temperature of an each potential fire pixel and the difference between the temperature brightness of the fire pixel and its background temperature (Giglio et al., 2003). The detection algorithm identifies pixels with one or more actively burning fires that are commonly referred to as “hotspot.” Each detected fire represents the center of an (approximately) 1 km pixel that contains one or more hotspots. The actual pixel size varies depending on the location of an observation in the swath. Pixels farther away from nadir will grow larger. The coordinates of the fire in the attribute table does not represent the exact location of the fire, but the center point of the pixel (Giglio et al., 2010). The size of the fire can be much smaller than the pixel size (Figure 2.5). The detection probability of hotspot depends on a number of factors, among others on fire temperature and satellite viewing angle.



Source: <http://maps.geog.umd.edu/firms/faq.htm>.

Figure 2.5 Fire pixel detection using MODIS.

Hotspot can detect flaming fires (~1000 K) as small as 100 m² under ideal conditions with a 50% detection probability, or a 1000-2000 m² smouldering fire

(~600 K). Detection rates are higher when the daily peak fire activity coincide with the time of satellite overpass. Also, fires in degraded forests are easier to detect than fires in primary forests, because degraded forests burn hotter due to more dry fuel and the open canopy. Ultimately, the algorithm assigns to each pixel one of the following classes: missing data, water, cloud, fire, non-fire or unknown.

The hotspots are derived from multiple MODIS channels to detect the thermal anomalies on a per-pixel basis. They produce very sophisticated fire information, which is based on the algorithms developed. Hotspots are calculated by the MODIS Rapid Response system and reported by FIRMS with multiple reported fields. These fields include latitude and longitude (center point location), brightness temperature in Kelvin (BT) of either channel 21, 22 or 31, scan and track (actual spatial resolution of the scanned pixel), acquisition date and time of the overpass of the satellite, satellite name (Terra or Aqua), confidence percentage, version of algorithm, and brightness temperature of channel 31 (Appendix A). Hotspot detected by Terra satellite is denoted as MOD14 and that of Aqua satellite as MYD14 (Giglio, 2010).

2.7.2 MODIS fire detection algorithm

The accuracy of fire information (hotspot) is a common concern for all user groups that is determined primarily by fire detection algorithms. The MODIS fire detection algorithms are based on those developed for AVHRR, but they bring some new capability to the remote sensing field. In the MODIS design, the 3.75 μm channel was shifted to 3.95 μm to avoid the variable water vapor absorption and to reduce reflected solar radiation by 40%. MODIS visible and NIR channels (0.66 and 0.86 μm) both have a resolution of 250 m, which is advantageous for more accurate remote sensing of vegetation and burn scars. MODIS has a 1.65 μm channel (with a resolution

of 500 m) that has been shown to be very sensitive to burn scars (Kaufman et al., 1998b). MODIS smoke detection employs the blue (0.41 and 0.47 μm) and mid IR (2.1 μm) channels in addition to the AVHRR red channel (0.66 μm) for better detection and discrimination of smoke from soil dust (Kaufman et al., 1997).

In order to detect the presence of fire in a non-interactive fashion, a set of detection criteria different for the day and night fire observations are prescribed. Fire detection algorithm is performed using a contextual algorithm that exploits the strong emission of mid infrared radiation from fires. The algorithm examines each pixel of the MODIS swath, and ultimately assigns to each one of the following classes: missing data, cloud, water, non-fire, fire, or unknown. The algorithm uses brightness temperatures derived from the MODIS 4 and 11 μm channels, denoted by T4 and T11, respectively. The MODIS instrument has two 4 μm channels, numbered 21 and 22, both of which are used by the detection algorithm. Channel 21 saturates at nearly 500 K; channel 22 saturates at 331 K. Since the low-saturation channel (22) is less noisy and has a smaller quantization error, T4 is derived from this channel whenever possible. However, when channel 22 saturates or has missing data, it is replaced with the high saturation channel (21) to derive T4. T11 is computed from the 11 μm channel (channel 31), which saturates at approximately 400 K for the Terra MODIS and 340 K for the Aqua MODIS. The 12 μm channel (channel 32) is used for cloud masking; brightness temperatures for this channel are denoted by T12 (Giglio et al., 2003). The 250 m resolution red and near infrared channels, aggregated to 1 km, are used to reject false alarms and mask clouds. These reflectances are denoted by $\rho_{0.65}$ and $\rho_{0.86}$, respectively. The 500 m resolution of 2.1 μm band, also aggregated to 1 km, is used to reject water-induced false alarms; the reflectance in this channel is denoted by $\rho_{2.1}$

(Giglio et al., 2003). A summary of all MODIS bands used in fire detection algorithm is shown in Table 2.3.

Table 2.3 MODIS channels used in fire detection algorithm.

Channel number	Central wavelength (μm)	Purpose
1	0.65	Sun glint and coastal false alarm rejection; cloud masking.
2	0.86	Bright surface, sun glint, and coastal false alarm rejection; cloud masking.
7	2.1	Sun glint and coastal false alarm rejection.
21	4.0	High-range channel for fire detection.
22	4.0	Low-range channel for fire detection.
31	11.0	Fire detection, cloud masking.
32	12.0	Cloud masking.

Source: Giglio et al. (2003).

To avoid false detection under MODIS fire detection algorithm, Justice et al. (2006) stated that all pixels for which $T_4 < 315 \text{ K}$ (305 K at night) or $\Delta T = T_4 - T_{11} < 10 \text{ K}$ (3 K at night) or $\rho_{0.86} > 0.3$ (daytime only) should be immediately eliminated as possible fires (potential fire pixels). For absolute fire detection, the algorithm requires that at least one of two conditions is satisfied. These are

- (1) $T_4 > 360 \text{ K}$ (330 K at night), and
- (2) $T_4 > 330 \text{ K}$ (315 K at night) and $\Delta T > 25 \text{ K}$ (10 K at night).

If either of these absolute criteria is not met, the algorithm pursues a relative fire detection in which the fire is distinguished from the mean background values by three standard deviations in T_4 and ΔT as

$$T_4 > \text{mean}(T_4) + 3\text{stddev}(T_4), \text{ and } \Delta T > \text{median}(\Delta T) + 3\text{stddev}(\Delta T).$$

The mean, median, and standard deviations (denoted by “mean”, “median”, and “stddev” above) are computed for pixels within an expanding grid centered on the candidate fire pixel until a sufficient number of cloud, water, and fire-free pixels are identified. A “sufficient number” is defined as 25% of all background pixels, with a minimum of six. Water pixels are identified with an external water mask, and cloud pixels are identified with the MODIS cloud mask product (MOD35). Fire-free background pixels are identified as those pixels for which $T_4 < 325$ K (315 K at night) and $\Delta T < 20$ K (10 K at night). If either standard deviation is below 2 K, a value of 2 K is used instead. The background window is allowed to grow up to 21X21 pixels in size. If this limit is reached and the previous criteria regarding the minimum number of valid background pixels are not met, the relative detection tests cannot be used. If the absolute tests do not indicate that an active fire is present in this situation, the algorithm flags the detection result as unknown.

Combining all tests into a single expression, a pixel is classified as a fire pixel in daytime if the following conditions are satisfied:

$\{T_4 > \text{mean}(T_4) + 3\text{stddev}(T_4) \text{ or } T_4 > 330 \text{ K}\}$, and $\{\Delta T > \text{median}(\Delta T) + 3\text{stddev}(\Delta T) \text{ or } \Delta T > 25 \text{ K}\}$, or $T_4 > 360 \text{ K}$.

For the nighttime, following condition is applied.

$\{T_4 > \text{mean}(T_4) + 3\text{stddev}(T_4) \text{ or } T_4 > 315 \text{ K}\}$, and $\{\Delta T > \text{median}(\Delta T) + 3\text{stddev}(\Delta T) \text{ or } \Delta T > 10 \text{ K}\}$, or $T_4 > 330 \text{ K}$.

Finally, for daytime observations when sun glint may cause false detections, a fire pixel is rejected if the MODIS 250 m red and near infrared channels have a reflectance above 30% and it lies within 40° of the specular reflection position.

2.7.3 Caveats of the hotspot

There are few limitations of hotspot being reported despite its vast applications in many research fields. The textural component of the detection algorithm causes problems with false detections in areas where the canopy cover exhibits strong differences in surface temperatures. Cloud cover obstructs fire detection and may lead to high errors of omission (undetected fires). The size of a particular fire cannot be calculated from hotspot data and no distinction can be made between large fires and small fires. The hotspots do not allow distinguishing, if one or more fires were actively flaming within a pixel on the same day and burned areas cannot be derived from the hotspots (Giglio et al., 2003).

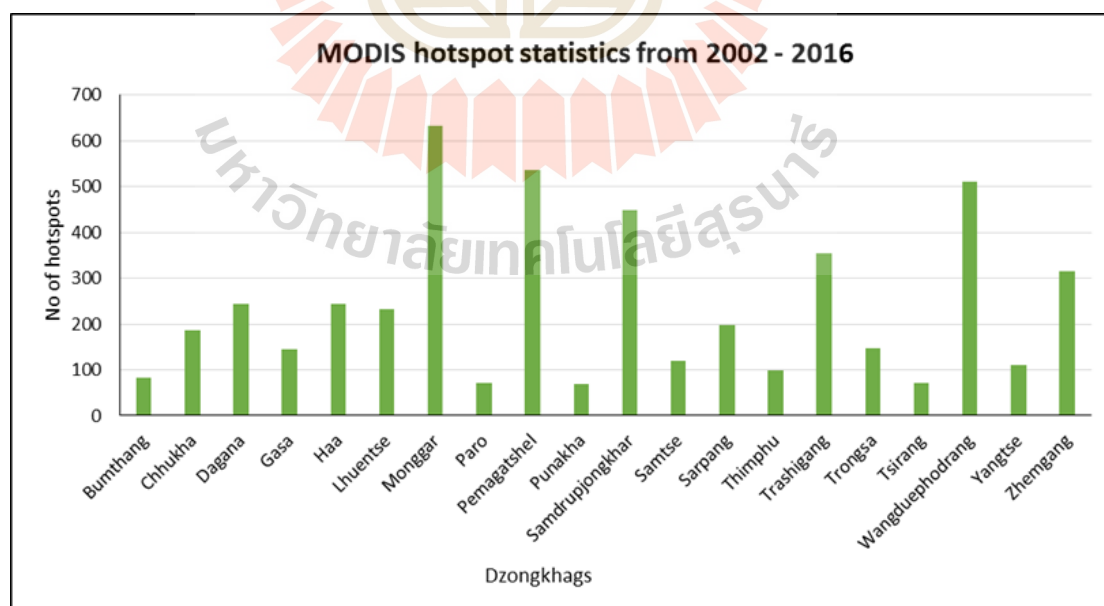
2.7.4 Statistics of MODIS hotspot in Bhutan

The statistic of MODIS Hotspot data in 20 districts of Bhutan (2002-2016), detected by MODIS Terra and Aqua satellite onboard are presented below (Table 2.4). According to the overall statistics, it is observed that the majority of wildfires have occurred in eastern Bhutan, particularly in Mongar, Pema Gatshel, Samdrup Jongkhar and Trashigang districts. Likewise, Wangdi Phodrang district in the west and Zhemgang district in the central Bhutan also have experienced high frequency of wildfires (Figure 2.6). Tsirang, Bumthang and Paro has low wildfire frequency while remaining districts has a moderate wildfire frequency. The distribution of hotspot with their spatial location for 20 districts of Bhutan are displayed in Figure 2.7.

Table 2.4 Statistics of MODIS Hotspot in Bhutan (2002-2016).

SI No	Dzongkhag	No. of hotspots detected	Percentage (%)
1	Bumthang	82	1.70
2	Chhukha	186	3.86
3	Dagana	243	5.04
4	Gasa	145	3.01
5	Haa	243	5.04
6	Lhuentse	232	4.82
7	Monggar	634	13.16
8	Paro	72	1.49
9	Pemagatshel	536	11.13
10	Punakha	69	1.43
11	Samdrupjongkhar	450	9.34
12	Samtse	119	2.47
13	Sarpang	198	4.11
14	Thimphu	98	2.03
15	Trashigang	354	7.35
16	Trongsa	147	3.05
17	Tsirang	72	1.49
18	Wangduephodrang	512	10.63
19	Yangtse	110	2.28
20	Zhemgang	315	6.54

Note: NRT files and VIIRS are not included

**Figure 2.6** Graphical representation of hotspot in Bhutan (2002-2016).

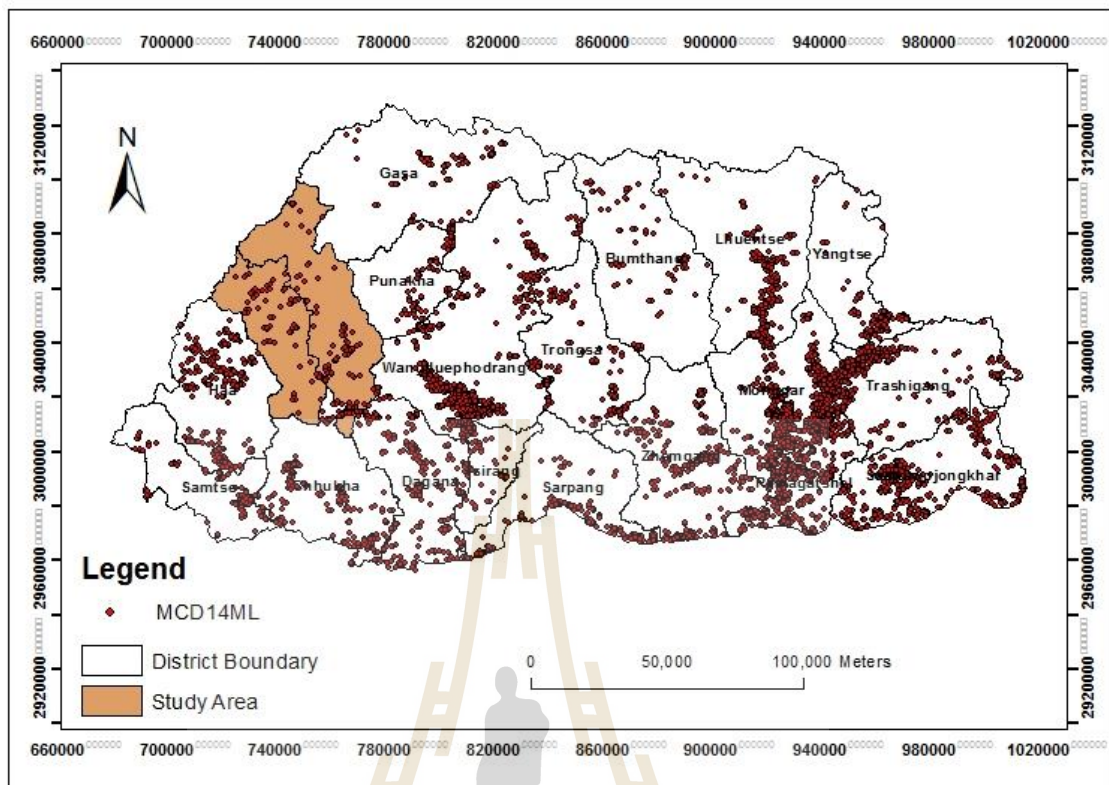


Figure 2.7 Distribution of MODIS hotspot in 20 districts of Bhutan (2002-2016).

2.8 Literature review

To assess the wildfire susceptibility and understand the relationship between various influential variables, a good knowledge of spatial distribution and temporal variation of wildfire hotspot data in the study area is required. The primary task is to identify the areas that have high probability of wildfire that is useful for wildfire management and planning. To achieve this, remote sensing and GIS are two components applied based on spatial data for biophysical factors, climatic factors and human factors in combination with fire-behaviour models. Remote sensing technologies provides an efficient and economical means of acquiring fire information over large areas on a routine basis, despite various limitations and shortcomings (Setzer

and Malingreau, 1996). Along with remote sensing and GIS tools, different GIS based statistical and probabilistic methods, models and algorithms are being tested and applied in many wildfire researches to determine the effects of various factors. For example, various approaches from simple to sophisticated models have been applied for forest fire assessments, such as expert knowledge, statistical methods such as linear regression, multiple regression, logistic regression, geographically weighted regression, frequency ratio, and evidential belief function. The expert knowledge method is clearly subjective and the accuracy of the results is questionable. Therefore, statistical approaches are widely used to develop fire models based on the statistical assumption that the relationship between input variables and forest fire will be the same in the past and in the future. However, forest fire regimes are complex and influenced multiple factors; therefore, the accuracy of the models is not always satisfactory.

In general, GIS-based LR and FR models have given a promising result in different parts of the world with a high prediction accuracy (Lee and Talib, 2005). Both models make use of fire inventory and fire influential factors to come up with a certain wildfire susceptibility map. For instance, Mohammadi, Bavaghar and Shabanian (2013) integrated logistic regression and geographic information systems (GIS) to study the risk of forest fires and to identify the factors that most influenced the occurrence of forest fires in the forests of western Iran. The correlation between forest fires and climatic variables, human factors and physiography were analyzed. A method based on spatial GIS analysis and logistic regression was also used by Zhang, Zhang and Zhou (2009) to predict the probabilities of human caused grassland fires in Inner Mongolia. Likewise, many fire risk researchers and scholars have used LR and FR to predict and analyze forest fire occurrence earlier studies (Pradhan et al. 2007; Intarawichian and

Dasananda, 2010; Zhang, Han, and Dai, 2013; Pourtaghi, Pourghasemi and Rossi, 2014 and Guo et al., 2015). LR examines relations between historical fire data and their influential factors and applies this knowledge to determine probability of having fire at a particular location. Thus, LR model developed from historical fire data are found valuable for understanding general historical fire trends and wildfire prediction. FR model provides how each factor's class affects fire occurrence while the LR gives a clear picture about the degree of influence the causative factors that have on fire occurrence. Though, LR and FR models take different approaches to identify fire risk area the comparison of their results may give us more insight on the complicated interaction between fire events and the environmental conditions in the study area. Herein, the reviewed literature are briefly summarized.

Pradhan et al. (2007) used remote sensing and GIS technology to evaluate forest fire susceptibility and risk mapping at Selangor, Malaysia together with FR method. The main objective was to develop an a fire susceptibility map and determine the level of severity of forest fire hazard zones by assessing the relative importance between fire factors and the location of fire ignition. Forest fire locations were identified from historical hotspots data (2000-2005) from AVHRR data of NOAA 12 and NOAA 16 satellite. A total of 112 hotspots were compiled and various other supporting data such as soil map, topographic data, and agro climate were collected and created using GIS software. A total of 6 factors that influence fire occurrence: NDVI, land use, soil, agro climate, slope and aspect were derived. The fuel map from NDVI was derived using Landsat-7 ETM imagery. The factors were converted to a raster grid with 30 m cells. The study area by grid was 2,418 rows by 1,490 columns (i.e. total number is 3,033,610 cells) and 112 cells had forest fire occurrences. The FR was calculated from analysis of

the relation between hotspot and the attributing factors and then Forest Fire Susceptibility Index was calculated. The validations of results showed prediction accuracy of 73.18% indicating a good prediction accuracy for forest fire susceptibility mapping. The, results obtained was expected to help the concerned authorities for forest fire management and mitigation.

Zhang, Zhang and Zhou (2009) examined the probability of human caused grassland fires in the east of Inner Mongolia, China using GIS spatial analysis and LR. The study highlighted the importance of understanding the fire factors like weather, vegetation, topography and socio-economic factors. It focused mainly to improve the understanding of spatial dynamics of human caused wildfires and more importance was given to anthropogenic variables. The study mentioned that humans are the primary cause of forest fire according to the historical records. They found LR model very appropriate for fire prediction and to analyze complex relationship between fires and associated factors. A total 2,611 fires incidences for 20 years were located and converted to shape files. Out of this, 1,537 human-caused grassland fires were used in the study. The study assumed that the probability of occurrence of human caused fire will increase with proximity to human infrastructure, as a greater number of human activities will lead to grassland fire ignition. A total of 13 predictor variables were prepared: elevation, aspect, slope, and distance to the nearest isolated building, village, railroad, dirt road, paved road. Dynamic variables included mean temperature, precipitation, relative humidity, mean sunlight time, and mean wind speed. All these variables were resampled to 500 m grid files. LR model was developed using SPSS software to statistically test the relationship of grassland fires with the predictor variables and predict the probability of location of human caused grassland fires. The

model was developed using half of burned points and equal number of un-burned points chosen randomly. The LR model was separately applied for two variable groups: static and dynamic variables. That means, the first probability (P1) of occurrence of fire was obtained using the proximity and topographic variables and in the second probability (P2) was tested using topography and climatic variables. Finally, the probability of grassland fire was obtained by the product of two probabilities by overlaying P1 and P2 and the probability of a grassland fire occurring at a given location and day (P3) was calculated. The prediction accuracy of the model was 80.48% indicating that LR can produce a meaningful model of the probability for human caused grassland fire. The correlations between the human-caused grassland fires and the logistic model variables were positive with temperature and elevation, and negative with relative humidity, precipitation, distances to dirt roads, railroad, villages, and isolated buildings. The results are expected to help other grassland fire studies, such as fire ecology, fire weather, and fire cycles. These results will also help to identify locations with a high risk of fire occurrence, and prepare plans for grassland utilization. The study did not include the fuel characteristic and the socio-economic variables.

Intarawichian and Dasananda (2010) used both LR and FR to produce fire susceptibility map for protected areas in Chiang Mai province of northern Thailand. In the LR method, five factors most related to the occurrences of active fire spot were considered (slope, rainfall intensity, population, NDVI and elevation, and in the FR method, nine factors were used (vegetation, slope, aspect, distances from road/village, temperature, rainfall, population, NDVI). Based on 213 samples of active fire spots FR matrix of fire variables were constructed using FR equation. The fire risk scores for each image's pixel were then computed and fire susceptibility map with four levels of

the severity are categorized: (1) low, (2) moderate, (3) High, and (4) very high. Meanwhile, the LR model was applied and the fire severity was categorized as in the FR method. Under LR model, 1,229 fire spots were used to find the relation with the chosen variables and R^2 was found to be 0.70. The factors were then normalized and LR model was applied to get the probability map. Resulting susceptibility maps from both FR and LR methods indicated a similar pattern of susceptibility level. The output maps were validated using the area under the curve (AUC) method where the accuracy rate of 75.88% (for FR) and 70.87% (for LR) were achieved. Herein, 47 fire spots, which were not used in model development, were applied to validate both methods. The results indicated that prediction accuracies from both methods are relatively high with FR method performing slightly better. Bases on the result 77.16% was classified as moderate level of fire susceptibility by FR method while LR method classified only 36.06% as moderate level and 28.38% as high level of susceptibility. In contrast, only 0.5% of the area was at high level of susceptibility by FR method. However, since the accuracy obtained from both methods were quite high, the authors recommend that these methods are reliable and the results obtained can be used to reduce forest fire hazard and assist in proper planning of land use activity in the future.

Zhang, Han, and Dai (2013) used binary LR analysis to map the fire occurrence probability of Northeast China. Ten predictor variables including altitude, slope, aspect, distance to the nearest village, distance to the nearest path, distance to the nearest water bodies, land cover, fuel moisture content, LST and NDVI were employed. NDVI, LST and burned area data are downloaded from NASA website. MOD13 NDVI data, MOD11 LST data and MOD14 8-day composite fire products data are here used. The study tried to include the human factors apart from natural factors such as topographic,

climatic and fuel characteristics. All variable maps were rasterized with the spatial resolution of 1 km and all continuous variables are rescaled to ensure easy interpretation of the LR result. To obtain the unbiased estimate of model prediction performance, two independent data subsets were proportionally defined, 70% for training and 30% for validation test. Firstly, all the continuous and categorical variables were included in the model. Next, with backwards stepwise procedure, some variables are eliminated from the initial model in an iterative process. At each iteration step, the significance of variables included in the initial model is tested, and those insignificant variables are eliminated. Finally, a model was developed and estimated coefficients are allocated to the significant variables. The performance of the model was evaluated using ROC technique and the model's fitness accuracy was found to be 84.2%, which indicates a good correlation between independent variables and dependent variable. Except for altitude, all other 9 variables were found significant and it was used in the model. The interpretations of the estimated coefficients from the LR showed that NDVI best explain fire occurrence in the region. The study highlighted that among the quantitative techniques, the LR model is considered as a valuable tool for predicting fire events. The resulting fire probability maps can assist fire managers in locating spatial potential fire danger areas, so that fire managers can act according to circumstances in fire prevention operations. Weather variables was excluded in this study and recommended for future studies to further improve predictive performance.

Mohammadi, Bavaghar and Shabanian (2014) used LR and GIS for fire risk zone mapping in western Iran. The main objective was to generate a forest fire risk zone map and to utilize GIS coupled with spatial LR analysis to define the relationship between physiographic and climate characteristics and human activities related to forest

fire patterns. The fire map was prepared from the field data available for 6 years and field reconnaissance survey. In this study, it was hypothesized that the forest fires are related to 6 influential variables including elevation, slope, and distance to streams, distance of farmlands, temperature and annual precipitation. All these variables were collected from different sources and converted from vector to raster format with 20 m grid cells. Spatial interpolation of annual precipitation based on existing datasets was carried out using IDW to generate the rainfall distribution layer for the study area. LR was used to determine weights of variables as well as to investigate relationships between occurrence of forest fire and explanatory variables. In the investigation of forest fire risk assessment, fire presence (hotspots) was the dependent variable, while the environmental and human factors were the independent variables.

In this study, 100 sample points each were selected randomly, where fire has occurred and not occurred respectively for the same period. To decrease the spatial autocorrelation, the points should be separated by distance of at least 1,000 m (Koenig, 1999). However, the burned areas were composed of small polygons, and therefore at least 100 m separation distance between samples was considered adequate. The spatial characteristics of each sample points were obtained by extracting data from each 6 factors and the data were exported to SPSS software. Before applying LR, all the explanatory variables were standardized or normalized to uniform scale. Finally, LR was applied. Herein, 80% of data points were used for modeling and 20 % for validation. The ROC method was employed to assess the discrimination ability of the model. The Wald and Chi square test was used to examine the statistical significance of the individual regression coefficients. The ROC value of 0.794 was obtained which indicates that the model is fit. The results revealed that the probability of forest fire was

significant and negatively related to elevation, slope and distance from farmlands whereas annual precipitation was found positively related to fire occurrence. This indicated that the areas with low elevation, low slope, and short distance from farmland to higher precipitation have higher values in fire probability map, and therefore are more prone to forest fire. According to the model, there is a positive relationship between probability of fire and annual precipitation. Authors observed that higher rainfall leads to further growth of grasses on the forest floor. In such circumstances, with drying grasses covering the forest floor in summer, the incidence of fire occurrence increases in wet sites. This research further demonstrates that LR model and GIS are suitable for determining the forest fire risk zone. The analysis has revealed that the elevation, slope, annual precipitation and distance to farms have high significant correlation with fires. Authors recommended that the model quality could be improved if further variables that may affect the forest fire are imported into the LR analysis. The relationships between variables may change over time, so periodic updating the model is desirable.

Pourtaghi, Pourghasemi and Rossi (2014) evaluated forest fire susceptibility mapping using remote sensing and GIS technology in the Minudasht forests, Golestan province, Iran using FR method. Various fire influential factors included NDVI, land use, slope, aspect, topographic wetness index (TWI), topographic position index (TPI), curvature, distance to roads, distance to rivers, distance to villages, soil texture, wind effect, annual temperature and annual rain. Forest fire locations were specified from MODIS data and extensive field surveys. 106 (70 %) out of 151 forest fire identified, were used for modelling the forest fire susceptibility maps, while the remaining 45 (30%) cases were used for the validation. Before applying the model, a multicollinearity

test among the fire inducing factors was applied. No multicollinearity issue was observed, so all the independent variables was used in FR model. The fire map achieved from the FR method showed 31.50% of the total area as very high FFM class. On the other hands, the area related to low, moderate and high Forest Fire Map (FFM) zones are 16.39, 21.85, and 30.26%, respectively. The findings revealed that the most important conditioning factors were NDVI, land use, soil and annual temperature. The model was validated using the ROC technique and was found to be 83.16% with the standard error of 0.044. This further confirms that FR method provides a good result in mapping the forest fire susceptibility mapping.

Guo et al. (2015) analyzed the spatial pattern and drivers of wildfire in Fujian province, southeastern China (2000-2008). LR model was used to predict the likelihood of wildfire. Herein, forest fires were divided into two categories: anthropogenic fires and naturally induced fire. Unlike in other studies it has considered socio-economic indicators and human activity as very important. The main objectives were: (1) to identify the spatial distribution of fire ignitions; (2) to understand the comprehensive and individual effects of ignition factors and (3) to produce spatially explicit statistical models and maps predicting patterns of fire ignitions by combining biophysical and human variables. For dependent variable, a certain percentage of random points (non-fire points) were created to satisfy the requirements of the binomial LR model using 13,185 satellite fire points collected between 2000 and 2008. Herein, a total of 14,965 random points (non-fire) were generated about the same number of ignition points. Independent variables included topography, vegetation, weather, infrastructure, and social and economic data. A total of 25 factors were prepared including 15 climate variables. Multicollinearity test was performed using VIF test and 18 variables were

selected for modelling. In total, 28,150 fires (13,185 fire points +14,965 random point as non-fire points) were assigned as validation set (60%) and calibration set (40%). To reduce the influence of a random division of samples on the selection of model parameters, the division and model fitting were performed three times by generating three intermediate models. Variables that are significant in at least two of the three intermediate models was selected to use in analysis of the complete dataset. After analyzing the model fitting with 18 variables again 11 best variables were selected that met the requirements after testing with three intermediate models and were used in the final stage of model development. The model was calibrated using the ROC technique and results showed AUC value of 0.843, indicating a high goodness of fit proving that the model is a good candidate for predicting forest fire occurrence in Fujian Province. The study revealed that fire ignition was mainly clustered in space due to the comprehensive influence of different factors. Elevation, daily precipitation, and daily relative humidity were negatively associated with fire ignitions, whereas distance to settlement, population density and per capita gross domestic product (GDP) influenced fire occurrence positively. The study also found that the model overestimated forest fire occurrence rate in some areas, while it underestimated in other areas. Authors reasoned that this might have happened because LR do not consider spatial correlation among fire points.

CHAPTER III

RESEARCH METHODOLOGY

The present study on wildfire susceptibility analysis applied the innovative approach of remote sensing and GIS technology by integrating with reliable geospatial models (LR and FR) which is very significant component in the effective wildfire management system. The main objective of the research is to determine the impact of environmental, climatic and anthropogenic factors on wildfire occurrence and to develop a susceptibility map of the study area.

The framework of research methodology consists of three major components (Figure 3.1): (1) data collection and preparation; (2) wildfire susceptibility analysis based on LR and FR models; and (3) accuracy assessment and validation of wildfire probability maps to determine the optimum model for final wildfire susceptibility mapping. Details of each component with major steps involved in each component are separately described in the following sections. In addition, concepts and process of resampling and cell size of raster dataset and its standardization are also summarized under Section 3.1 of this chapter.

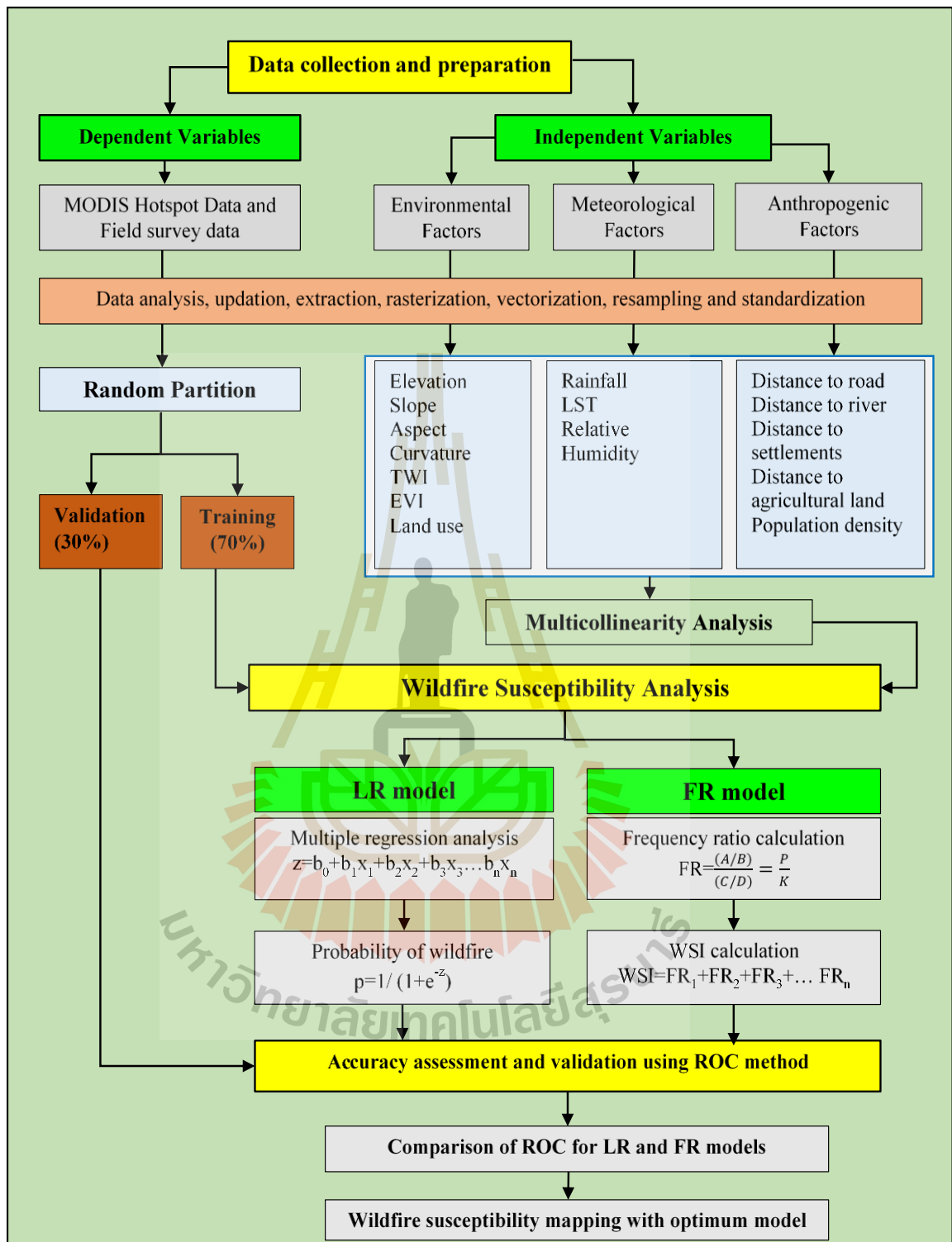


Figure 3.1 Flow chart of research methodology for wildfire susceptibility mapping.

3.1 Data collection and preparation

The data collection and preparation phase consist of two parts: (i) collection of MODIS hotspot as data dependent variable and (ii) collection of environmental, meteorological and anthropogenic factors as independent variables. The process begins with the preliminary analysis of raw input data obtained from various sources at varying scales/resolution by classifying and mapping the dependent and independent variables that are directly or indirectly related to wildfire occurrence. The main steps involved in preliminary analysis includes, projection and defining proper coordinate system, extraction, data updating and editing, conversion, vectorization, rasterization, resampling and data standardization using remote sensing and GIS software (ERDAS Imagine and ESRI ArcGIS) to establish the standard input for wildfire susceptibility analysis. Herein, the process for preparation of dependent and independent variables are discussed in details separately.

3.1.1 Dependent variable (MODIS hotspot/active fire data)

The wildfire inventory map of the study area depicts the spatial location of wildfire points and represents the dependent variable in the analysis. However, the spatial data for the wildfire incidences in the study area was not available and did not exist at all. The study used spatial locations of the wildfire hotspots from the MODIS active fire data. MODIS active fire data (Hotspot), MCD14ML Collection 5, of both Terra and Aqua satellites was obtained from the NASA FIRMS (<https://firms.modaps.eosdis.nasa.gov>) for 15 year time series (2002-2016) via E-mail. The MCD14ML is a standard science quality MODIS thermal analysis/active fire locations processed by University of Maryland with three months lag and it is distributed by NASA FIRMS.

The hotspots data acquired from the MODIS sensor are re-projected to a standard coordinate system (UTM Coordinate System Zone 45N for Bhutan) and then extracted. Extracted hotspot points are then overlaid to a high resolution Google Earth images, analyzed, processed and finally converted to raster format consisting of hotspot and non-hotspot to be used as the dependent variable. The output cell size of 100 m is considered adequate after the analysis of various resolution/scales of other relevant factors used in the analysis.

The statistics of wildfire hotspots obtained from MODIS sensor and its monthly distribution during the active fire season is presented in the Figure 3.2 and Figure 3.3 respectively. The distribution of number of hotspot (2002-2016) reflects the frequency of wildfire incidence in the study (Figure 3.2). It is observed that the number of hotspots has increased from 2002 until 2009, with only few incidences observed in 2004 and 2005. From 2010 until 2015, a slight decreasing trend is observed with sudden drop in 2015. During this period only 3 hotspots were detected, but notably a sudden increase of hotspots was again observed in 2016 with 18 fire incidents. This varying distribution in the frequency of hotspots in the study area is attributed to various associated factors addressed in the result. In addition, it is also observed that February is peak wildfire season with 64 hotspot incidences (Figure 3.3). The information revealed by the hotspots statistics is observed rationale and reliable, because the actual fire season in the study area usually begins in the mid of October and continues until May, where the peak fire season normally falls in January, February and March. Thus, the data is consistent with the actual fire situation in the study area.

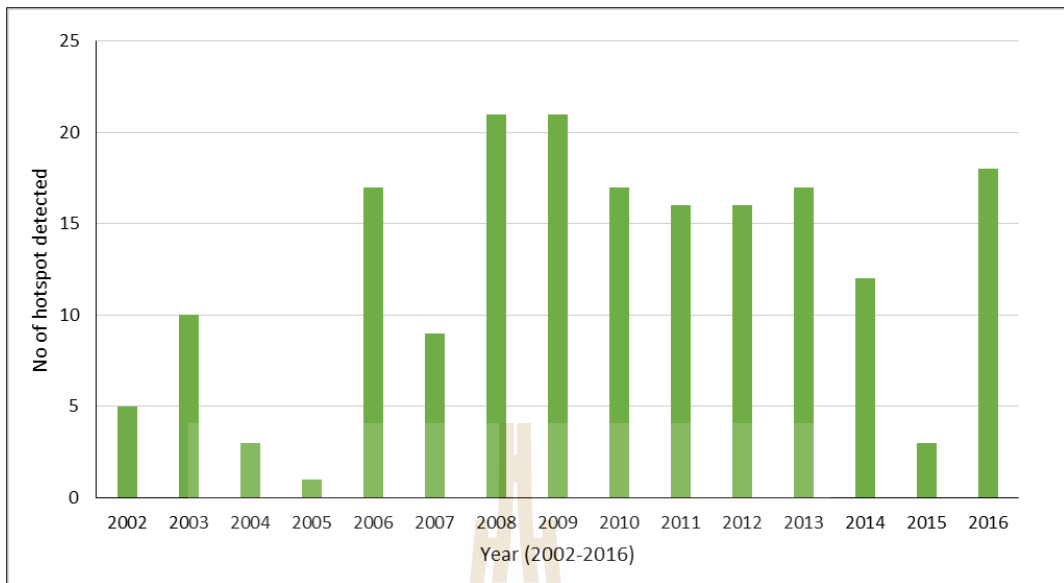


Figure 3.2 MODIS Hotspot data from 2002-2016 in the study area.

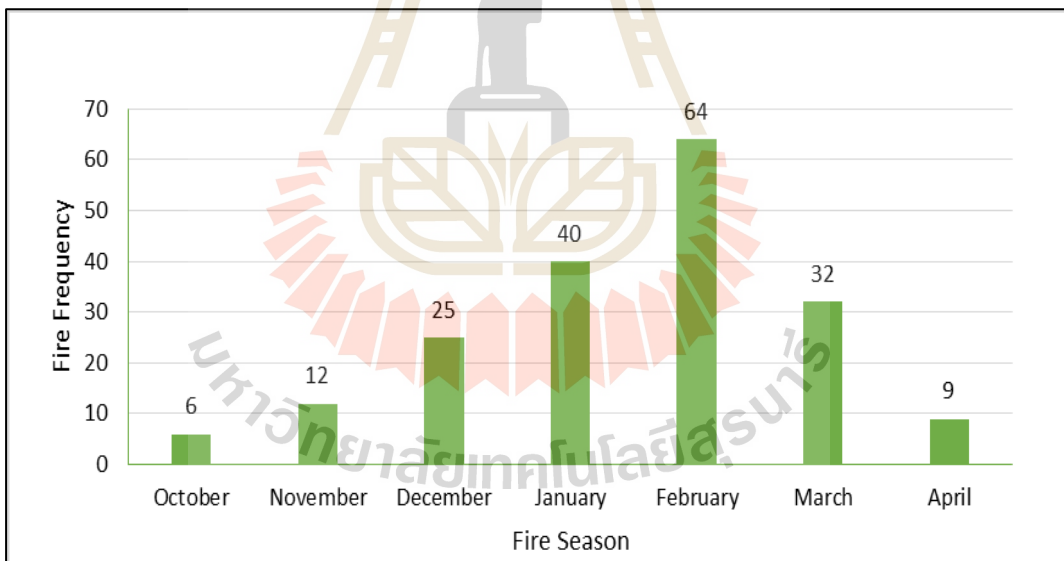
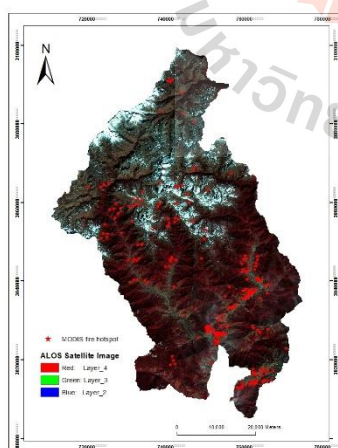


Figure 3.3 Monthly distribution of MODIS hotspot in the study area.

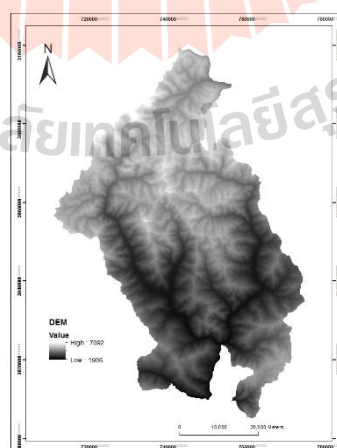
The basic information on remote sensing and GIS input data used in the current study is provided in Table 3.1 and the input maps in Figure 3.4 respectively.

Table 3.1 Basic remote sensing and GIS input data for wildfire susceptibility analysis.

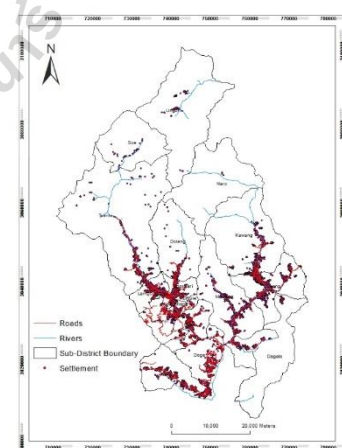
No	Input Data	Data Format	Scale/Resolution	Source
1	MODIS hotspot	Vector	1 km	NASA FIRMS (LANCE)
2	ALOS DEM	Raster	10 m	NLCS, Bhutan
3	ALOS image	Raster	10 m	NLCS, Bhutan
4	Topographic map	Vector	1:25,000	NLCS, Bhutan
5	LULC map	Vector	10 m	MoAF, Bhutan
6	NCRP map	Vector	10-20 cm	NLCS, Bhutan
7	Meteorological data	Excel	NA	Meteorology department, Bhutan
8	Population data	Excel	NA	NSB (PHCB-2010), Bhutan
9	EVI data	Raster	250 m	NASA, MODIS vegetation indices
10	LST data	Raster	1 km	NASA, MODIS LST product
11	Google satellite images	Raster	65 cm	Digital globe (Quickbird), 2016



(a) MODIS hotspot



(b) DEM



(c) Topographic map

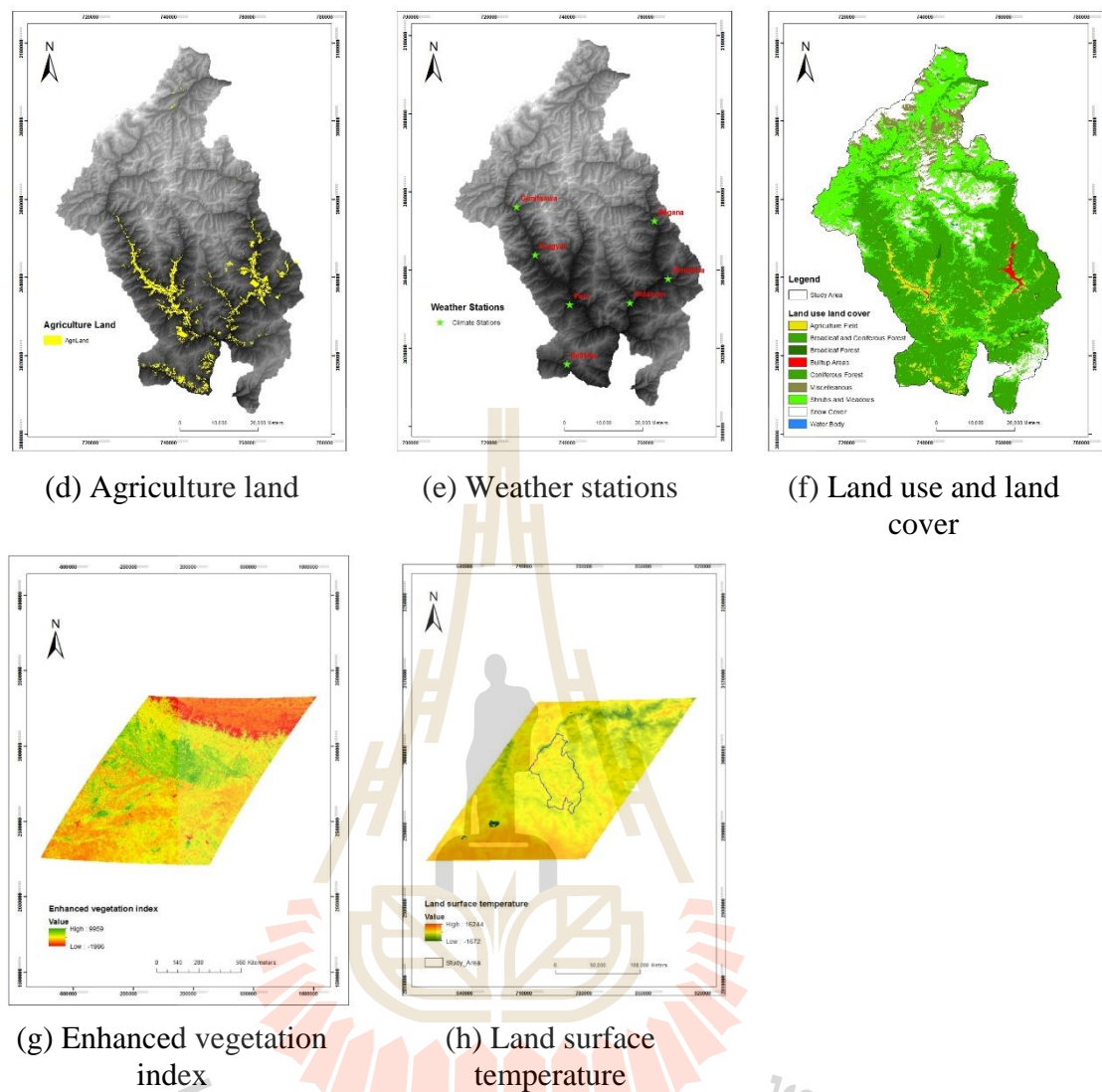


Figure 3.4 Basic input maps for wildfire susceptibility analysis.

3.1.2 Independent variables (Wildfire influential factors)

A total of 15 predictor variables that constitute three key influential factors (environmental, climatic and anthropogenic) are presented in Table 3.2 with quoted references from the literature reviews. In addition, these factors are further reclassified into different classes according to the objectives and scale of the input data used in the analysis. Characteristics of input wildfire influential factors for LR

and FR analysis is presented in Table 3.3. These factors are prepared from basic input data obtained from different agencies at varying scales/resolutions using remote sensing and GIS tools. Various steps and process of preparation are summarized below.

Environmental factors include topographic features and fuel characteristics. Topographic variables including elevation, slope, aspect, curvature and TWI are derived from 10 m resolution ALOS DEM (Appendix B), using surface analysis and hydrological functions under Spatial Analyst tools in ESRI ArcGIS Version 10.3 software. All topographic variables are firstly derived from the original DEM at original cell size using surface analysis tools and then resampled to 100 m cell size. MODIS vegetation indices, EVI produced on 16 days intervals at 250 m resolution is downloaded, re-projected and extracted prior to the active fire season to represent fuel. Meanwhile, land use data are extracted from the Bhutan Land Cover Assessment 2010 (LCMP-2010) provided by MoAF. Herein, nine major land use classes are prepared: coniferous forest, broadleaf forest, broadleaf and coniferous forest, shrubs and meadows, agricultural field, built-up areas, snow cover, water bodies and miscellaneous classes. Land cover is sometimes used as proxy for fuel types because they reflect the possible interactions with the humans.

Weather conditions affects fuel accumulation and moisture. Considering the temporal scale of the current study, climatic variables are derived from the average weather conditions over the period of 11 years (2005-2015) from Meteorological Department of Bhutan (Appendix C). Climatic factors including rainfall and relative humidity are generated through IDW interpolation technique using available gauge stations. Meanwhile, level-3 MODIS global LST with 8-day

composite of 1-Km LST product (MOD11A1) is downloaded from NASA's website and extracted to represent as a proxy for fuel temperature. It is converted to appropriate unit (Celcius) using the scale factor (0.02) provided in metadata file.

Anthropogenic-induced factors include proximity and socio-economic factors, which are the most significant driving factor for wildfire occurrence, since most of the wildfire incidences related to human activities. The proximity variables represent the accessibility to the areas where fires can occur and many previous researchers have pointed out as an important factors in wildfire occurrence. Proximity factors like distance to roads, rivers, settlements and agricultural land are obtained using the Euclidean distance tool in ESRI ArcGIS software. In this study, roads, rivers and settlements are extracted from the topographic map obtained from the NLC at 1:25,000 scale. The missing features and some new features are updated according to the recent National Cadastral Survey Program (NCRP) data. Missing rivers and streams are generated from the DEM using the hydrological tools in ESRI ArcGIS software. Few road networks are digitized and extracted using Google Earth image. Agricultural field class is updated according to the latest NCRP data, obtained from NLC of Bhutan. In addition, population density represents the distribution of potential human influence, considering that fires in Bhutan are mainly caused by humans. Thus, population density is generated at sub-district level using the Population and Housing Census (PHCB-2010) data obtained from National Statistical Bureau (NSB) of year 2010 (Appendix D). The density value is computed by raster interpolation using the IDW method, considering the major towns and cities as the center point of highly populated areas.

Table 3.2 Selected influential factors for wildfire susceptibility analysis.

Category	No	Factor	Reference
Environmental factors	1	Elevation	Zhang et al. (2009); Intarawichian and Dasananda (2010); Zhang et al. (2013); Frouzan et al. (2013); Guo et al. (2015)
	2	Slope	Pradhan et al. (2007); Zhang et al. (2009); Intarawichian and Dasananda (2010); Zhang et al. (2013); Frouzan et al. (2013); Pourtaghi et al. (2014); Guo et al. (2015)
	3	Aspect	Pradhan et al. (2007); Zhang et al. (2009); Intarawichian and Dasananda (2010); Zhang et al. (2013); Pourtaghi et al. (2014); Guo et al. (2015)
	4	Curvature	Pourtaghi et al. (2014)
	5	EVI	Pradhan et al. (2007); Intarawichian and Dasananda (2010); Zhang et al. (2013); Pourtaghi et al. (2014)
	6	TWI	Pradhan et al. (2007); Pourtaghi et al. (2014)
	7	Land use	Zhang et al. (2013); Pourtaghi et al. (2014); Guo et al. (2015)
Meteorological factors	8	Rainfall	Zhang et al. (2009); Intarawichian and Dasananda (2010); Frouzan et al. (2013); Pourtaghi et al. (2014); Guo et al. (2015)
	9	MODIS Land Surface Temperature (LST)	Zhang et al. (2009); Intarawichian and Dasananda (2010); Zhang et al. (2013); Frouzan et al. (2013); Pourtaghi et al. (2014); Guo et al. (2015)
	10	Relative humidity	Zhang et al. (2009); Guo et al. (2015)
Anthropogenic factors	11	Distance to road	Zhang et al. (2009); Pourtaghi et al. (2014); Guo et al. (2015)
	12	Distance to river	Zhang et al. (2013); Frouzan et al. (2013); Pourtaghi et al. (2014); Guo et al. (2015)
	13	Distance to settlement	Zhang et al. (2009); Zhang et al. (2013); Pourtaghi et al. (2014); Guo et al. (2015)
	14	Distance to agricultural land	Frouzan et al. (2013)
	15	Population density	Intarawichian and Dasananda (2010); Guo et al. (2015)

Table 3.3 Characteristics of input variables for LR and FR analysis.

No	Factors	Class for FR	Original Scale/ Resolution	Remarks
1	Elevation	<2,500 m 2,500-3,500 m 3,500-4,500 m 4,500-5,500 m >5,500 m	10 m	Reading from DEM
2	Slope	<8° 8–15° 15–25° 25-50° >50	10 m	Generate from DEM
3	Aspect	Flat North Northeast East Southeast South Southwest West Northwest	10 m	Generate from DEM
4	Curvature	Concave(+) Flat(0) Convex(-)	10 m	Generate from DEM
5	TWI	<0 0-2 2-4 4-6 >6	10 m	Generate from DEM
6	EVI	<0.1 0.1-0.2 0.2-0.3 0.3-0.4 >0.4	250 m	Extraction for study area.
7	Land use	Coniferous Forest Shrubs and meadows Broadleaf Forest Agriculture Field Water Body Snow Cover Miscellaneous Built-up Areas Miscellaneous	10 m	Extraction and updating for study area.

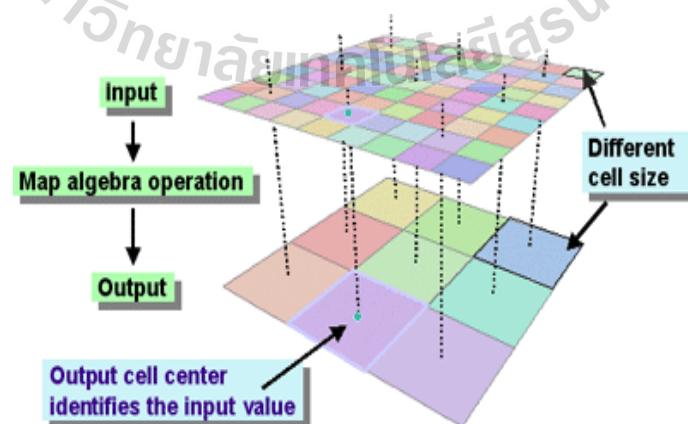
Table 3.3 Characteristics of input wildfire influential factors for LR and FR analysis

(continued).

No	Factors	Class for FR	Original Scale/ Resolution	Remarks
8	Rainfall	<1,000 mm 1,000-1,500 mm 1,500-2,000 mm 2,000-2,500 mm >2,500 mm	Not apply	Spatial interpolation
9	LST	< 0°C 0–10°C 10–20°C 20-25°C >25°C	1 km	Extraction for study area
10	Relative humidity	<68% 68-70% 70-72% 72-74% >74%	Not applicable	Spatial interpolation
11	Distance to road	<5,000 m 500-1000 m 1000-1,500 m 1,500-2,000 m >2,000 m	1:25,000	Euclidean distance calculation
12	Distance to river	<5,000 m 500-1000 m 1000-1,500 m 1,500-2,000 m >2,000 m	1:25,000	Euclidean distance calculation
13	Distance to settlement	<5,000 m 500-1000 m 1000-1,500 m 1,500-2,000 m >2,000 m	1:25,000	Euclidean distance calculation
14	Distance to agricultural land	<5,000 m 500-1000 m 1000-1,500 m 1,500-2,000 m >2,000 m	10-20 cm	Euclidean distance calculation
15	Population density	<50 person/sq.km 50-100 persons/sq.km 100-200 persons/sq.km 200-300 persons/sq.km >300 persons/sq.km	Not applicable	Density calculation and interpolation

3.1.3 Resampling and cell size of raster dataset.

Raster datasets from different sources are stored in different cell sizes according to their cell resolutions. However, to process between multiple datasets in ESRI ArcGIS environment, the cell resolution, like the registration, needs to be the same. When multiple raster datasets of different resolutions are input into any ESRI ArcGIS Spatial Analyst function, one or more of the input datasets are automatically resampled using the nearest neighbor assignment to the coarsest resolution from input datasets. By default, the nearest neighbor resampling technique is used since it is applicable to both discrete and continuous value types. A resampling technique is necessary because it is rare that an output cell center will align exactly with any cell center of the input raster. Thus, to align the cell centers of input raster exactly with that of output cell of desired resolution, different techniques have been used and the values assigned to the cells of an output raster may differ according to the technique used. The default resampling method can be changed to a specific cell size of desired resolution in ESRI ArcGIS software. Figure 3.5 shows an example of how the input raster is resampled to the coarser resolution.



Source: ESRI, 2016

Figure 3.5 Example of resampling technique.

A raster dataset can always be resampled to have a larger cell size; however, it will not obtain any greater detail by resampling your raster to have a smaller cell size (<https://www.esri.com>). The level of details represented by a raster depends on the cell size, or spatial resolution, of the raster. The cell must be small enough to capture the required detail but large enough so that computer storage and analysis can be performed efficiently. However, smaller cell sizes result in larger raster datasets to represent an entire surface; leading to greater storage space, which often results in longer processing time. Therefore, choosing an appropriate cell size is not always simple and it must be balanced with the application's need for spatial resolution with practical requirements for quick display, processing time, and storage. For the current study, a cell size of 100 meters is considered adequate and appropriate for the analysis based on the following considerations:

- The spatial resolutions/scales of various input data,
- The level of details for the analysis and the objectives of study.
- The size of the resultant database and the processing time according to the extent of study area.
- Cell limitations of the processing software, viz. SPSS and Excel spread sheet.

3.1.4 Standardization of raster dataset

The first step before the main statistical analysis is to normalize/standardize all the raster datasets in a manner LR requires, otherwise, it creates problem during interpretation of the final result (Ayalew and Yamagishi, 2005). Since the independent variables are measured in different scales/resolutions, they do not contribute equally to the analysis, making it difficult to assess the relative

importance. Hence, transforming the data to comparable scales can solve this problem. So, all factor maps are normalized to a uniform scale from 0 to 1 using the Rescale function (Linear scale transformation method) in ESRI ArcGIS software. The linear scale transformation method converts the raw data into standardized criterion scores. The advantage of this method is a proportional (linear) transformation of the raw data. This means, the relative order of magnitude of the standardized score remain equal and the scale of measurement varies precisely from 0 to 1 for each criteria.

3.1.5 Sampling of dependent variable

Selecting an appropriate sample for LR model involves considerations of the sample size and the proportion of hotspot and non-hotspot pixels (Schicker and Moon, 2012). Thus, an appropriate number of samples should be considered to create dependent variable. Basically, there are three methods of sampling that is generally applied in LR analysis (Zhu and Huang, 2006). The first one is using data from all over the study area. This method leads to unequal proportions of hotspot and non-hotspot pixels (Ohlmacher and Davis, 2003) and involves large volumes of data which is sometimes very difficult to process. The second approach is using all the hotspot pixels and equal proportions of non-hotspot pixels. This may decrease number of data to be used but it eliminates the associated bias in the data sampling process (Zhu and Huang, 2006). For example, Yesilnacar and Topal (2005) used all hotspot pixels and equal number of randomly selected non-hotspot pixels. The third method is considered as the most reasonable approach. Herein, it divides hotspot pixels into two parts, i.e. training and validation dataset. In this approach, there are two cases. The first one is the application of unequal pixels (Atkinson and Massari, 1998) and the

second one is to use equal proportion of hotspot and non-hotspot pixels (Dai and Lee, 2002).

In the current study, since the number of hotspot pixels is comparatively less than the non-hotspot pixels, all hotspot pixels are taken into account. To avoid the drawbacks attributed to the application of unequal proportion of hotspot and non-hotspot pixels, equal numbers of non-hotspot pixels are randomly selected from hotspot free area (non-hotspot) and then it is combined with equal number of hotspot pixels. Thus, equal number of samples of hotspot and non-hotspot pixels are considered for the analysis. These samples (dependent variable) is further partitioned into training and validation dataset by applying random sampling technique to the proportion of 70% and 30% respectively. The random sampling is performed using the Geostatistical Analysis Tools in ESRI ArcGIS software. For LR model, dependent variable include randomly sampled hotspot and non-hotspot pixels while for FR model, it requires only hotspots pixels as dependent variable.

3.1.6 Input data preparation for LR and FR model

For LR analysis, first the entire study area is converted to grids of points with 100 m cell size using the fishnet tools in ESRI ArcGIS software, such that the cells are exactly registered with hotspot map by applying the processing extent and Mask function under raster analysis option. The fishnet points are then used to extract the values of dependent variable (0 and 1) from the entire study area which is divided into hotspot and non-hotspot pixels using the 70% training dataset. Herein, the binary values of dependent variable are extracted using the Spatial Analyst Tools. These points are in turn used to extract the values of independent variables for the corresponding locations of each training dataset and they are exported to MS-Excel

spread sheet. Next, a tabular database is designed in the Excel containing the status of dependent variable (hotspot and non-hotspot) for 70% training locations, represented by 1 (hotspot pixels) and 0 (non-hotspot pixels). The corresponding values of all the independent variables, which are extracted for the sample locations is appended to the tabular database at their respective locations for each pixel. Thus, this tabular database which contains equal proportion of hotspot and non-hotspot locations (dependent variable) together with the corresponding values of all independent variables is considered as the input for LR model (Appendix E).

For FR model, all the factor maps are further reclassified into various classes using the reclassify function of ESRI ArcGIS software. Herein, factor classes are defined according to the objective, accuracy and scale of the data and based on standard practice deduced from various literature reviews (Table 3.3). Once all classes of factors are finalized, all the hotspot pixels containing the 70% training dataset are superimposed over the predictor maps to determine the frequency ratio of respective classes of each factor.

3.1.7 Multicollinearity analysis

After defining the predictor variables, one of the important keys in any research is consideration of multicollinearity problem among predictor variables to obtain the best result from the LR analysis. Multicollinearity refers to the correlation among the predictor variable in a linear regression model. Multicollinearity happens when the correlation among the predictor variables have perfect linear relationship, therefore the estimation of the model coefficients cannot be possibly computed (Odzemir, 2011). The existence of correlation among the predictor variables may distort the model estimation or interfere with accurate estimation. Chatterjee and Hadi

(2006) also reported that multicollinearity indicates some of the explanatory variables may be highly correlated. In some case, if multicollinearity between two variables are very high, but not perfectly correlated, the model regression coefficients become more sensitive to individual predictor that can cause result of model coefficient to appear insignificant (Rogerson, 2006).

Tolerance (TOL) and variance inflation factor (VIF) are two important indexes widely used for multicollinearity diagnosis. TOL is the amount of variance in an independent variable and is not explained by the other independent variable (Rogerson, 2006). Mernard (2002) reported that if TOL value is less than 0.2, multicollinearity occurs and becomes more serious when TOL value is smaller than 0.1. Meanwhile, VIF value is a reverse/reciprocal of TOL value. Thus, if VIF value to be equal or over 10, multicollinearity will occur (Rogerson, 2006). O'Brien (2007), also reported that TOL of less than 0.20 or 0.10 and/or a VIF of 5 or 10 and above presented a multicollinearity problem. The TOL and VIF value can be calculated using the following Equation:

$$TOL = 1 - r^2 \quad (3.1)$$

$$VIF = \frac{1}{1 - r^2} \quad (3.2)$$

Where, r^2 is associated with the regression of the independent variable on all other independent variables. In this research, a TOL value of less than 0.1 and VIF index of greater than 10 is applied to detect the multicollinearity problem (O'Brien, 2007).

3.2 Wildfire susceptibility analysis using LR and FR models

Wildfire susceptibility analysis is performed using GIS based LR and FR models and optimum model for final susceptibility mapping was selected based comparative assessment and validation. The various procedure and steps involved in applying the two probabilistic models in the analysis are separately summarized in the following sections for each model.

3.2.1 Wildfire susceptibility analysis using LR model

In general, the main aim of LR is to find the best fitting model to describe the relationship between a dependent variable and a set of independent variables (Ayalew and Yamagishi 2005). For LR, the dependent variable is dichotomous whereas, independent (predictor) variables are either categorical (nominal, ordinal) or continuous (interval or ratio scale).

In the analysis “wildfire occurrence” or presence of dependent variable (hotspot) is coded as “1” ($y = 1$), while “non-occurrence” or absence of dependent variable (non-hotspot) is coded as “0” ($y = 0$). Furthermore, we can assume that the probability of occurrence of wildfire ($y = 1$) as P , and the probability of no wildfires ($y = 0$) as $(1 - P)$. This allows LR to model the probability of occurrence of wildfire in association with each variable. Since the outcome of LR model is binary, the probability value cannot be expressed as the linear function of the explanatory variables. Thus, the predicted probability is transformed to linear function of predictors applying the logit transformation by executing the logarithm of $P / (1 - P)$ known as odds. Thus, in the case of “n” independent variables, the logistic regression equation is expressed as shown below in Equation 3.2.

$$\text{Logit}(y) = \text{Ln}\left(\frac{P}{1-P}\right) = \beta_0 + \beta_1x_1 + \beta_2x_2 + \beta_3x_3 \dots \dots \beta_nx_n \quad (3.3)$$

The logit transformation of the equation effectively linearizes the model so that the dependent variable of the regression is continuous in the range of 0 to 1. Thus, the linear regression equation is the natural log-odds of the probability of occurrence divided by the probability of non-occurrence of wildfire hotspot. Here, the “ P ” represents the probability of an event occurrence and “ $1-P$ ” represents the non-occurrence of an event, and $P/(1-P)$ is the odds ratio. Quantitatively, relationship between the probability of wildfire occurrences and its influential variables can be expressed as (Preisler et al., 2004):

$$P = \frac{1}{1+e^{-(\beta_0 + \beta_i x_i)}} \approx \frac{1}{1+e^{-z}} \quad 0 < P < 1 \quad (3.4)$$

and

$$Z = \beta_0 + \beta_1x_1 + \beta_2x_2 + \beta_3x_3 \dots \dots \beta_nx_n \quad (3.5)$$

Where, P is the probability that wildfire occurs ($Y=1$) at given location and varies from 0 to 1. β_0 is the intercept/constant of the model and the β_i are the coefficients associated with the independent (X_i) variables. Z is the linear combination of the independent variables (X_i) in use weighted by their regression coefficients and e is the base of the natural log and n is the number of the variables used. The coefficients of variables with positive values indicate a positive correlation while those with negative coefficients indicate a negative correlation with wildfire occurrence (Yalcin, et al., 2011).

Prior to LR analysis, the categorical variables has to be converted from nominal to numeric. The conversion of parameters from nominal to numeric can be done through the creation of dummy variables or by coding and ranking the classes based on the relative percentage of the area containing hotspots. Though, both methods are similar the latter is preferred because it avoids the creation of an excessive number of dummy variables and allows consideration of previous knowledge of hotspot susceptibility (Yesilnacar and Topal, 2005). If there are many parameters, it would create a long regression equation that may even create numerical problems and even lead to multicollinearity (Yesilnacar and Topal, 2005). Thus, considering the advantage of later method, the categorical variables are coded and ranked based on the relative percentage of hotspot density using SPSS software.

Using LR procedure in SPSS statistical software, the constant and the coefficients of independent variables are obtained. The intercept also known as constant represents the value of dependent variable when the values of all independent variables are zero, and the parameter coefficients explains the change in response (Y) for a unit increase in the corresponding predictor variable (X).

(a) Goodness of fit of LR model (Likelihood ratio test)

The most common assessment of overall model fit in LR is the goodness-of-fit test. A LR model is said to provide a better fit to the data if it shows an improvement over a model with fewer predictors. This is performed using the likelihood ratio test, which compares the likelihood of the data under the full model against the likelihood of the data under a model with fewer predictors. That is, simply the chi-square difference between the null model and the model containing one or more predictors. Removing predictor variables from a model will always make the

model fit less, but it is necessary to test whether the observed difference in model fit is statistically significant with the given null hypothesis $H_0: \beta = 0$. If the estimated coefficients (β) is statistically different from 0, then a p-value for the overall model fit statistic less than 0.05 rejects the null hypothesis. This indicates that selected variables are significant (Sig.).

Unlike in linear regression with ordinary least square (OLS) estimation, there is no true coefficient of determination (R^2) statistic in LR which explains the proportion of variance in the dependent variable that is explained by the predictors. The R^2 measure is only appropriate to linear regression with continuous dependent variables. However, For LR, an equivalent measure called ‘Pseudo R^2 ’ measure is developed, which take a different conceptual approach but aims to mimic R^2 found in OLS and it is used to measure the variance between two or more variables. Due to the binary nature of dependent variable, the pseudo R^2 measure will tend to be lower than OLS R^2 measure (Bio et al. 1998). The pseudo R^2 in LR model are represented by Cox and Snell R^2 and Nagelkerke R^2 that generally have lower values than the OLS R^2 , but they are interpreted in the same manner. However, Cox and Snell R^2 cannot reach the maximum value of 1 and it recommended to report Nagelkerke R^2 which is modified to attain the R^2 value to 1. The pseudo R^2 value greater than 0.2 indicates a relatively good fit (Clark and Hosking, 1986). The Cox and Snell R^2 is computed as follows:

$$f(x) = \frac{1 - \exp\left(\frac{-2(LL_m - LL_0)}{N}\right)}{1 - \exp\left(\frac{2LL_0}{N}\right)} \quad (3.6)$$

Where LL_m and LL_0 are the log-likelihood for the fitted model and intercept (the model without any predictors) respectively, and N is the sample size.

(b) Wald statistics (Statistical tests for individual predictors)

A Wald test is used to determine statistical significance of each coefficient (β) in the model. It is calculated by taking the ratio of the square of the regression coefficient to the square of the standard error of the coefficient. The idea is to test the hypothesis that the coefficient of an independent variable in the model is significantly different from zero. If the test accepts the null hypothesis, this suggests that removing the variable from the model will not substantially harm the fit of that model. But, if the null hypothesis is rejected that means the coefficient is different from zero, then it gives some evidence that the variable is significant to understand dependent variable (Rogerson, 2010). The Wald statistic is computed as given below (IBM SPSS, 2012; Menard, 2002):

$$Wald = \frac{\beta^2}{(SE_\beta)} \quad (3.7)$$

Where, β is a coefficient of independent variable and SE_β is a standard error that measures predictive accuracy.

Wald statistic is interpreted that if the coefficient (β) is more than twice (approximately) its corresponding standard error (SE_β), it may be regarded as significantly different from zero (Rogerson, 2010). So, in other words, if the Wald statistic value is bigger than 4, the independent variables (X) are significant and it can influence the model outcome of dependent variable (Y) because the Wald value

bigger than 4 gives a level of significance (P-value) of less than $\alpha=0.05$ (chi-square distribution table). Therefore, in backward LR method, the variable that has P-value greater than the confidence interval $\alpha=0.05$ are considered as insignificant and removed from the model. After removing, the calculation is repeated again until the remaining variables have P-value lower than the value of confidence interval (IBM SPSS, 2012).

(c) Odds Ratio

In general, most LR analysis outputs odds ratios (OR) along with the regression coefficients (β). These odds ratios are the exponential of the corresponding regression coefficient (e^β). The OR indicates the change in “odds” of being in one of the categories of the dependent variable for every unit increase of any given variable in the model. It represents the ratio of the probability that an event will occur (hotspot) to the probability that it will not occur (Non-hotspot). While coefficient (β) is convenient for testing the usefulness of predictors, odds ratios can be used to interpret as much easier than coefficient (β). (IBM SPSS, 2012). OR shows how the odds changes for one-unit increase in the value of predictor variable. OR is expressed as:

$$OR = \frac{odds(x+1)}{odds(x)} = \frac{\frac{P(x+1)}{1-P(x+1)}}{\frac{P(x)}{1-P(x)}} = \frac{e^{\beta_0+\beta_1(x+1)}}{e^{\beta_0+\beta_1(x)}} = e^\beta \quad (3.8)$$

If the coefficients (β) is positive, the corresponding value of OR is greater than 1, which means the wildfire event is more likely to occur or for every unit increase of a given variable the odds of the probability of wildfire occurrence increases. If coefficients (β) is negative, the corresponding OR is less than 1

indicating that the odds of event will decrease or for every unit increase of a given variable, the odds of the probability of wildfire occurrence decreases. If coefficient (β) is zero, a value of OR is equal to 1 indicating that there is no change in odds as the variable increases (IBM SPSS, 2012).

Using the coefficients of LR model, the linear combination of the independent variables of Z function is determined using Equation 3.5. This process is performed using the raster calculator function of Spatial Analyst tools in ESRI ArcGIS software. The next step is to calculate the predicted probability (P) of the wildfire occurrence for the entire study area. Herein, the final probability values of the P function as shown by Equation 3.4 is calculated to generate the probability map, which ranges between 0 and 1.

3.2.2 Wildfire susceptibility analysis using FR model

Under FR model, based on the observed spatial relationship between the hotspot locations (training dataset) and each hotspot related factors, the FR of each hotspot related factors classes (see Table 3.3) are calculated using FR equation given below:

$$FR = \frac{\text{Hotspot Ratio}}{\text{Area Ratio}} = \frac{A/B}{C/D} = \frac{P}{K} \quad (3.9)$$

Where, A is the number of hotspot pixels in each class of factor; B is the total number of hotspot pixels in the entire study area; P represents % of hotspot pixels for entire study area; C is the number of pixels (hotspot and non-hotspot) in each class of factor; D is the total number of pixels (hotspot and non-hotspot) for the entire study area; K represents the % of pixels (hotspot and non-hotspot) in each class for the factor.

3.3 Accuracy assessment and validation

The accuracy assessment and validation of predicted wildfire susceptibility maps is the most important component, otherwise the prediction models has no scientific significance (Chung and Fabbri, 2003). The accuracy assessment of the wildfire probability maps from the LR and FR models is performed using ROC method based on the independent validation dataset (30%). The model that provides better ROC value, is selected for the final wildfire susceptibility mapping.

Basically, ROC determines whether the model is fit or not by checking the prediction performance of the model. It determines the accuracy of classification model at a user defined threshold value using Area under Curve (AUC) of ROC. The AUC, also referred to as index of accuracy (A) or concordant index, represents the performance of the ROC curve. Higher the area, better is the model. In general, the ROC graph is plotted with true positive rate (sensitivity) on Y-axis against false positive rate (1-specificity) on X-axis for possible classification thresholds (Figure 3.6). The true positive rate (sensitivity) is the proportion of hotspot that are correctly classified, while true negative rate (specificity) is the proportion of non-hotspot correctly classified. Here, false positive rate (1-specificity) and false negative rate (1-sensitivity) are the proportion of non-hotspot and hotspot pixels that are erroneously classified. Both true positive rate (sensitivity) and false positive rate (1-specificity) ranges from 0 to 1. The result of ROC measured by area under ROC curve varies from 0.5 to 1. If ROC value is equal to 1, it indicates a perfect fit and ROC value of 0.5 indicates a random fit.

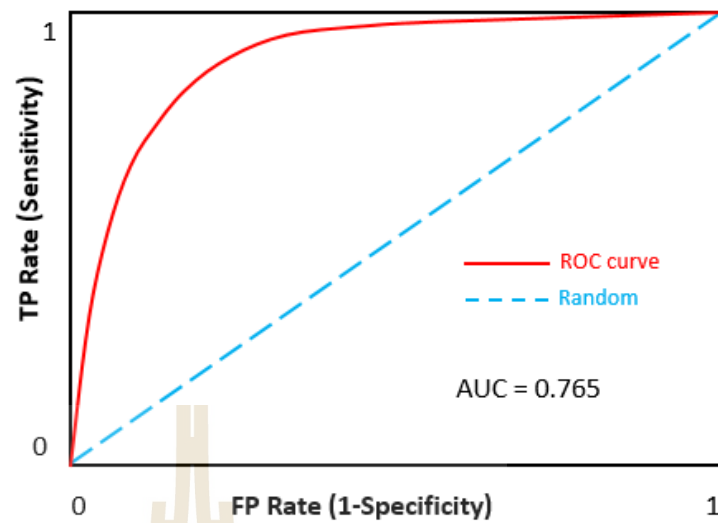


Figure 3.6 Characteristics of ROC curve.

Practically, the derived probability maps of LR and FR models from GIS environment were firstly exported to ERDAS Imagine software in IMG format. Then, it is imported to IDRISI software and converted to RST format. Subsequently, the training and validation dataset are also imported to IDRISI environment to compute the ROC from both the datasets. Herein, the probability maps represent the input image while the training and validation map is used as reference image for the calculation of ROC in IDRISI software. The probability map is then compared with the training and validation dataset to obtain the respective ROC values and consequently the success and prediction rate curves are constructed for both datasets.

CHAPTER IV

RESULTS AND DISCUSSION

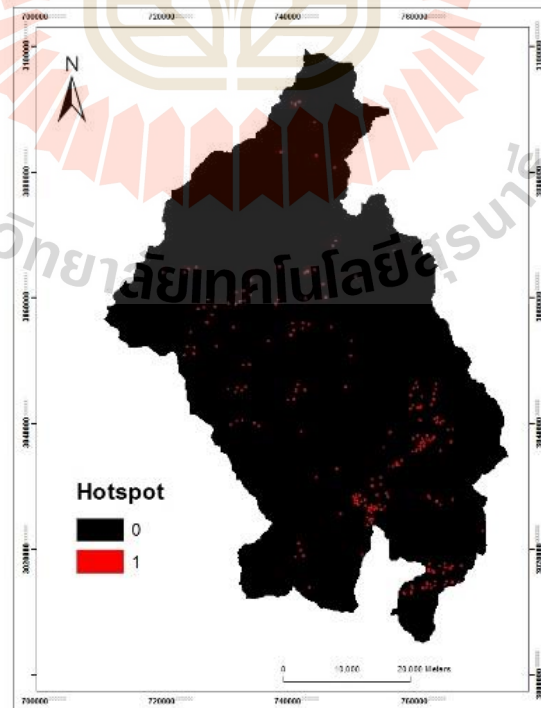
The combination of geoinformatics technology with relevant geospatial models can be a reliable tools to identify the wildfire susceptibility zones of particular area. The study applied these novel approach to conduct a wildfire susceptibility analysis in Thimphu and Paro districts of Bhutan using historical wildfire inventory from remote sensing satellite data and the three key influential factors (environmental, climatic and anthropogenic) of wildfire. Wildfire hotspots are obtained by Aqua/Terra MODIS of NASA's EOS while various influential factors are derived from collected input database. The LR and FR models are the primary analysis applied with remote sensing and GIS tools. In this chapter, the major results of the wildfire susceptibility analysis are reported and discussed. Herein, the results and analysis for LR and FR models are presented separately.

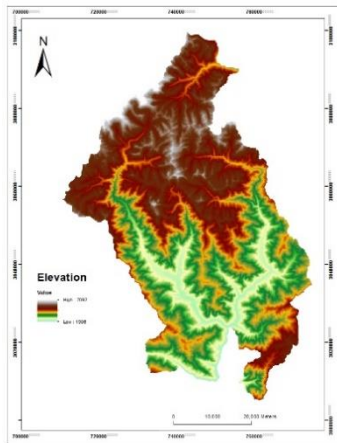
4.1 Input variables for LR model

The input for LR analysis comprise of fifteen influential factors as described in the Section 3.1.2. The summary of input variables used in the LR model is presented in the Table 4.1 with abbreviations, descriptions and data types for three different category of variables. The input raster maps of dependent and independent variables are shown in Figure 4.1 and Figure 4.2.

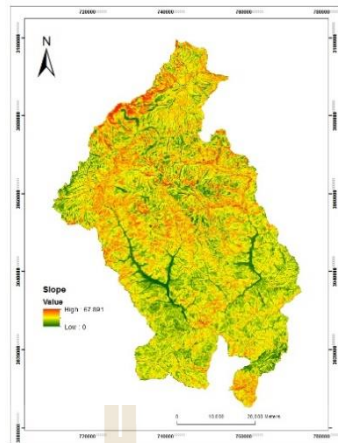
Table 4.1 Input variables used for LR analysis.

Factors	No	Abbreviations	Description	Data type	
Dependent	1	Y	1 = Hotspot	Dichotomous	
	2	X	0 = Non-Hotspot		
Independent	1	ELV	Elevation	Continuous	
	2	SLP	Slope	Continuous	
	3	ASP	Aspect	Categorical	
	Environmental factors	4	CRV	Curvature	Continuous
		5	TWI	Topographic wetness index	Continuous
		6	EVI	Enhanced vegetation index	Continuous
	Meteorological factors	7	LU	Land use	Categorical
		8	RF	Rainfall	Continuous
		9	LST	Land surface temperature	Continuous
	Anthropogenic factors	10	RH	Relative humidity	Continuous
		11	Dist_Road	Distance to road	Continuous
		12	Dist_River	Distance to river	Continuous
		13	Dist_Sett	Distance to settlement	Continuous
		14	Dist_AgriL	Distance to agricultural land	Continuous
		15	Pop_Density	Population density	Continuous

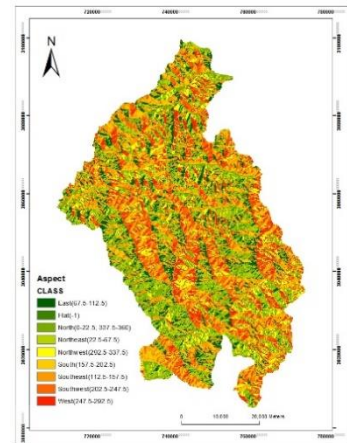
**Figure 4.1** Dependent variable (Hotspot map) used in the LR analysis.



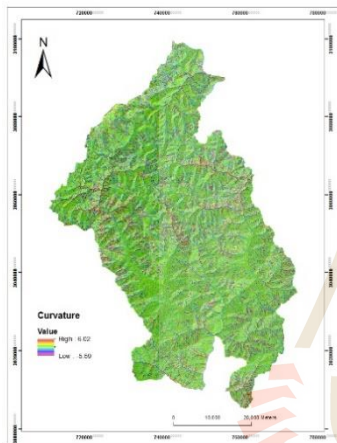
Elevation



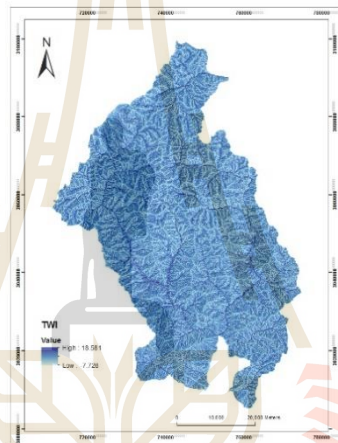
Slope



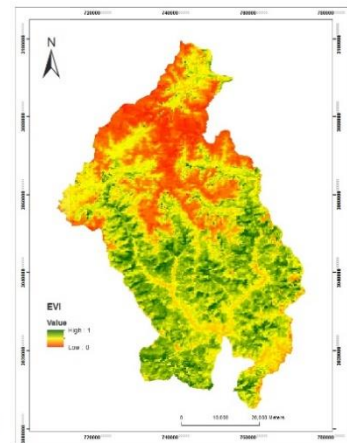
Aspect



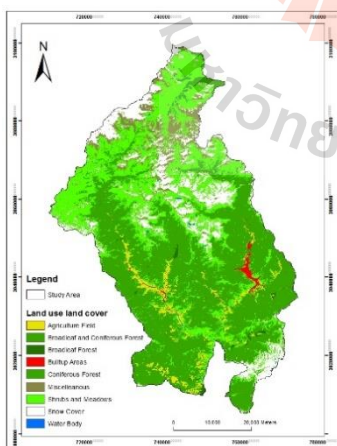
Curvature



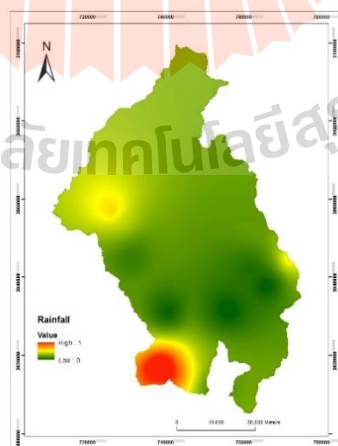
TWI



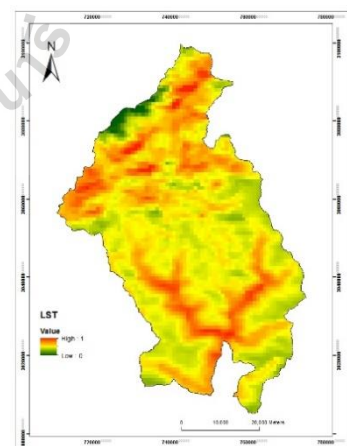
EVI



Land use



Rainfall



LST

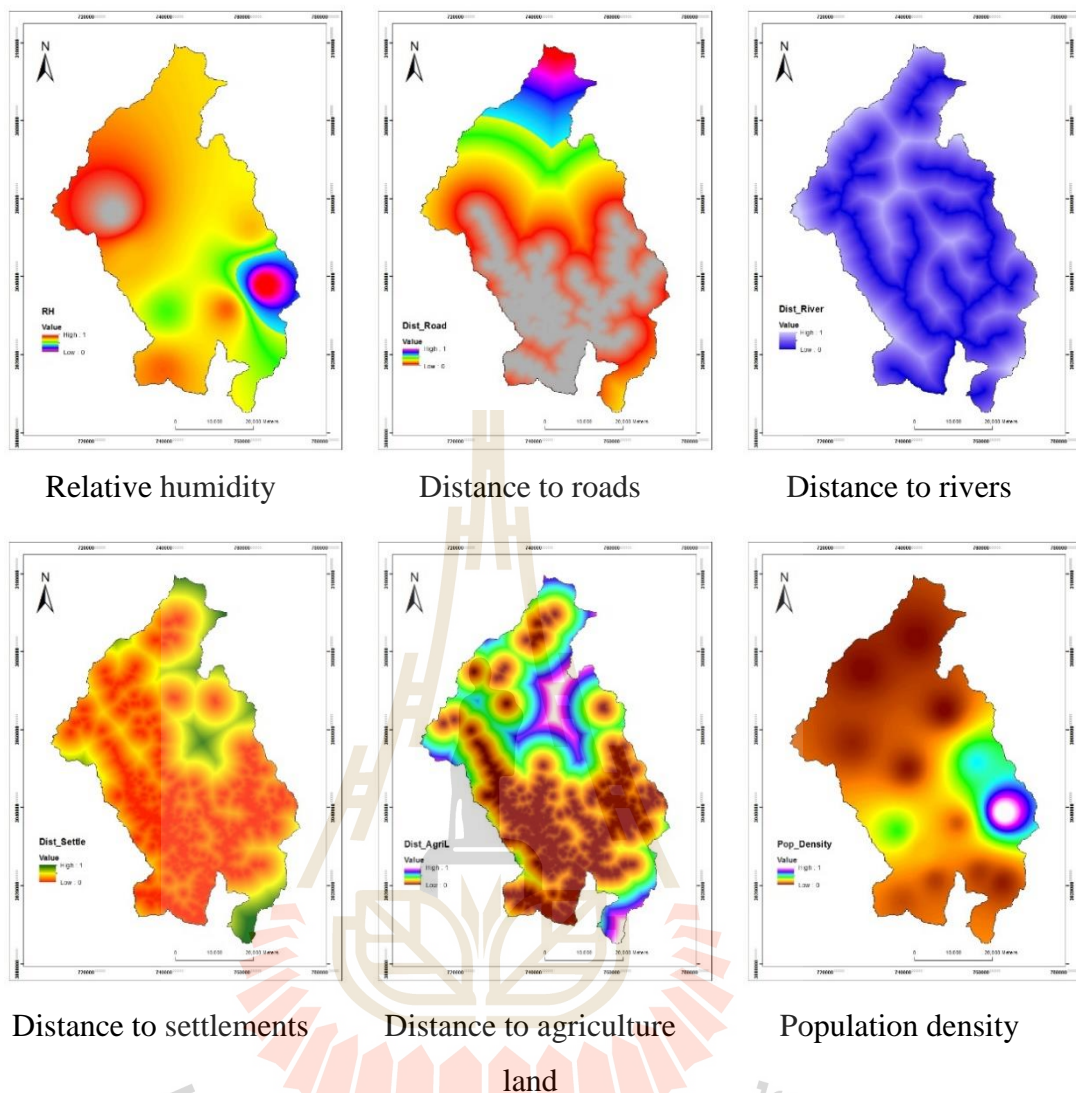


Figure 4.2 Independent variable (predictor maps) used in the LR analysis.

4.2 Multicollinearity analysis

To detect the multicollinearity problem among predictor variables, TOL value of 0.1 and VIF index 10 were set as benchmark. If the TOL value is less than 0.1 and VIF value is greater than 10, the variables are considered to have high correlation/multicollinearity (Section 3.1.7). The results of multicollinearity analysis which is performed in SPSS statistical software is reported in Table 4.2.

Table 4.2 Results of multicollinearity diagnostic test of independent variables

No	Wildfire influential factors	Collinearity Statistics	
		TOL	VIF
1	Elevation (ELV)	0.161	6.218
2	Slope (SLP)	0.840	1.190
3	Aspect (ASP)	0.855	1.170
4	Curvature (CRV)	0.506	1.974
5	Topographic wetness index (TWI)	0.496	2.016
6	Enhanced vegetation index (EVI)	0.624	1.602
7	Land use (LU)	0.875	1.143
8	Rainfall (RF)	0.684	1.461
9	Land surface temperature (LST)	0.543	1.842
10	Relative humidity (RH)	0.184	5.443
11	Distance to road (Dist_Road)	0.546	1.830
12	Distance to river (Dist_River)	0.515	1.943
13	Distance to settlement (Dist_Set)	0.282	3.541
14	Distance to agriculture land (Dist_AgriL)	0.270	3.697
15	Population density (Pop_Density)	0.174	5.753

The test results confirmed that there is no multicollinearity among the independent variables. In fact, the lowest TOL value is 0.161 and the highest VIF index is 6.218 for elevation which is greater than TOL threshold (0.1) and less than VIF threshold (10). Meanwhile, all other variables have TOL and VIF values within the threshold value which indicates there is no multicollinearity problem among the independent variables. Hence, all independent variables are applied for LR and FR analysis.

4.3 Wildfire susceptibility analysis using LR model

For LR analysis, the input for dependent variable consists of equal number of samples for the presence and absence of hotspot. Based on the random partition of dependent (2,546 pixels) into training and validation dataset to the proportion of 70% and 30% respectively, 1,782 hotspot pixels (70%) are selected for the analysis and another 764 hotspot pixels (30%) are retained for accuracy assessment and validation of result. An equal number of non-hotspot pixels (1,782 pixels) are also randomly selected from the non-hotspot pixels and then combined with hotspot pixels. Therefore, total number of hotspot and non-hotspot comprise of 3,564 pixels for the entire study area as training dataset. Meanwhile, the corresponding values of independent variables for 3,564 pixels at the same location of hotspot and non-hotspot were extracted and finally combined in MS-Excel spreadsheet as the input for LR analysis. Before LR analysis, the relative percentage of hotspot density is used to transform nominal variable to numeric variable since this avoids the creation of an excessive number of dummy variables (Section 3.2.1).

The LR analysis in the SPSS statistical software program includes all fifteen influential factors of wildfire: elevation (ELV), slope (SLP), aspect (ASP), curvature (CRV), topographic wetness index (TWI), enhanced vegetation index (EVI), land use (LU), rainfall (RF), land surface temperature (LST), relative humidity (RH), distance to road (Dist_Road), distance to river (Dist_River), distance to settlement (Dist_Set), distance to agriculture land (Dist_AgriL) and population density (Pop_Density). The LR model in SPSS offers several variable entry methods, namely, Enter, Forward Conditional, Forward LR, Forward Wald, Backward Conditional, Backward LR, and Backward Wald.

In this research, a Backward LR with stepwise analysis using the maximum likelihood method is employed. Maximum likelihood estimation involves finding the value(s) of the parameter(s) that give rise to the maximum likelihood of occurrence of wildfire (IBM SPSS, 2012). The backward stepwise process first starts by entering all fifteen predictor variables into the model and then sequentially eliminates the predictor variable based on the probability of the likelihood-ratio statistic, based on conditional parameter estimates. A variable is retained in the model if the probability of its score statistic is less than the “Entry value” (0.05) and it is removed if the probability is greater than the “Removal value” (0.01) i.e., it removes the predictor variable with largest p-value (i.e. the variable with least statistically significant) greater than the significant threshold value one by one. After removal, it refits the model and the same process is repeated until all the p-values are less than the cutoff value. The backward elimination process of variable removal terminated after the 4th step. In the process, three insignificant predictor variables including curvature (CRV), slope (SLP) and distance to river (Dist_River) were removed while twelve significant predictor variables were retained by the model.

The model statistics and classification summary of LR analysis reported in Table 4.3 conveys that the number of hotspots (presence) and non-hotspots (absence) which are coded as 1 and 0 respectively are observed as the dependent variable, while the predicted output of the dependent variable based on the full LR model suggests how many observed hotspot and non-hotspot are correctly predicted. The classification summary table shows that, the predicted accuracy of hotspot is approximately 69% and that of non-hotspot is 71% respectively. Thus, the overall percentage of correct classification is approximately 70%. In other words, the model predicted that the

probability of wildfire occurrence (presence) is correctly classified or predicted by 69% (1,226/1,782) and the probability of non-occurrence of wildfire (absence) is correctly predicted by 71% (1,262/1,782). The former is called the sensitivity of prediction, that is, the percentage of hotspot occurrence correctly predicted and the latter is known as specificity of the prediction, that is, the percentage of non-occurrence (non-hotspot) correctly predicted. Overall, the model predicted correctly for 2,488 pixels out of 3,564 pixels with an overall success rate of 70%. The cutoff value is 0.50 which means that if the predicted probability of a case being classified into "hotspot" category is greater than or equal to 0.50, then that particular case is classified as "hotspot" category. Otherwise, the case is classified as the "non-hotspot" category.

Meanwhile, the LR goodness of fit measured by the Nagelkerke R^2 statistic of 0.267, which is the pseudo- R^2 , indicates that the estimated LR model can approximately explain 27% of variance in wildfire occurrence. The value of pseudo- R^2 (>0.2) indicates that the performance of the model is good (Clark and Hosking, 1986). Thus, the derived LR model can efficiently explain and interpret the relationship between the independent variables and the occurrence of wildfire.

Table 4.3 Model statistics and classification summary of LR analysis.

Observed		Predicted		Percentage Correct
		Hotspot		
		Absence	Presence	
Hotspot	Absence	1,262	520	70.8%
	Presence	556	1,226	68.8%
Overall Percentage				70%
Nagelkerke R Square : 0.267				
Cox & Snell R Square : 0.20				
ROC : 0.76				
SE : 0.008				

Note: The cutoff value is 0.50

Similarly, Cox & Snell R^2 can explain the variance of wildfire occurrence, however, the Cox & Snell R^2 value cannot attain the maximum value as Nagelkerke R^2 (Section 3.2.1a). The ROC value of 76% with the standard error of 0.008 indicates that the performance of the model is good with the training dataset. Meanwhile, the chi-square statistics and its significance level indicates that the overall model is statistically significant since the p-value is less than the critical value (0.05).

The final results of LR analysis is provided in Table 4.4. The variables in the equation provides the estimated regression coefficient (β), the Wald statistic and the Odds Ratio ($\text{Exp}(\beta)$) for each variable category. They indicate the contribution of each independent variable to the model and its statistical significance. All the variables have the estimated coefficients (β) statistically different from 0 with the given null hypothesis $H_0: \beta = 0$. The twelve retained variables have a significance value (Sig.) less than 0.05 and they are considered as significant. The Wald with Chi square test is used to examine the statistical significance of the individual regression coefficients (β) at 95% confidence interval for the corresponding degree of freedom (df). The test indicates that all twelve variables are significant, because all the Wald values are greater than 4 which give the level of significance value (p-value) less than 0.05 (Table 4.4).

The coefficient (β) of LR model indicates the contribution of each factor to wildfire occurrence and its statistical significance. The relative importance of independent predictor variables are assessed and the coefficients (β) are used to predict the probability of wildfire. The parameter coefficients (β) explains a change in the dependent variable (probability of occurrence of wildfire) for a unit increase in the corresponding independent variables. The variables with positive coefficients indicate

positive correlation while negative coefficients indicate negative correlation to wildfire occurrence.

4.3.1 Impact of influential factors on wildfire occurrence (LR)

The results of LR analysis revealed that the probability of wildfire occurrence have a significant positive correlation with LST, ASP, Dist_AgriL, Dist_Set and LU variables, while Dist_Road, ELV, Pop_Density, EVI, RH, RF and TWI have significant negative correlation. Meanwhile, the variables including CRV, SLP and Dist_River were eliminated during the process of stepwise LR analysis.

Table 4.4 Variables in the equation retained by LR analysis (LR result).

No	Factors	β	S.E.	Wald	df	Sig.	Exp(β)
1	Land surface temperature (LST)	5.099	0.480	112.995	1	0.000	163.778
2	Distance to agriculture land (Dist_AgriL)	1.769	0.320	30.562	1	0.000	5.862
3	Aspect (ASP)	1.540	0.137	125.692	1	0.000	4.663
4	Distance to settlement (Dist_Set)	0.997	0.354	7.921	1	0.005	2.709
5	Land use (LU)	0.805	0.225	12.851	1	0.000	2.237
6	Topographic wetness index (TWI)	-0.680	0.231	8.671	1	0.003	0.507
7	Rain fall (RF)	-0.790	0.328	5.792	1	0.016	0.454
8	Relative humidity (RH)	-1.388	0.446	9.668	1	0.002	0.250
9	Enhanced vegetation index (EVI)	-1.798	0.565	10.135	1	0.001	0.166
10	Population density (Pop_Density)	-1.841	0.436	17.786	1	0.000	0.159
11	Elevation (ELV)	-2.937	0.563	27.238	1	0.000	0.053
12	Distance to road (Dist_Road)	-3.261	0.366	79.312	1	0.000	0.038
	Constant	-1.785	0.601	8.833	1	0.003	0.168

Note: β = logistic coefficient; S.E. = standard error of estimate; Wald = Wald chi-square values;

df = degree of freedom; Sig. = Significance; Exp(β) = exponentiated coefficient.

This suggests that they have very weak correlation with the wildfire occurrence or their influence on the occurrence of wildfire is negligible compared to those factors retained by the model. The variables with positive coefficients have more explanatory capability than variables with negative coefficients in terms of causing wildfire in the study area. The variables with negative coefficients will tend to suppress the probability of wildfire occurrence, which means, for a unit increase in the variables with negative coefficients, the probability of wildfire occurrence will decrease. The results indicate that the most significant influential factors of wildfire are LST and Dist_Road followed by ELV, Pop_Density, EVI, Dist_AgriL, ASP and RH. These factors have very high degree of correlation/influence as indicated by their coefficients. The remaining factors have relatively low influence. Consequently, areas with high land surface temperatures at lower elevations with low rainfall and relative humidity, and areas closer to the roads will have high probability values of wildfire, and therefore are more prone to wildfire.

Further, the weight of each independent variable can be interpreted from the exponentiated coefficients “ $(\text{Exp}(\beta))$ ” referred as odds ratio (OR) (Section 3.2.1c). All variables with positive coefficients have OR values greater than 1, indicating a positive influence. i.e., the probability of wildfire occurrence will increase with every one unit increase in this parameters. In contrast, all variables with negative coefficients have OR value less than 1 indicating negative influence. In general, the current analysis of LR model revealed that the influence of variables including LST, ASP, LU, Dist_Road, ELV, Pop_Density, EVI, RH, RF and TWI principally agree with basic characteristic of wildfire and found consistent with the previous works of Zhang et al. (2009); Mohammadi et al. (2014); Pourtaghi et al. (2014); Guo et al. (2015); Zhang,

Han, and Dai (2013) and Abdi et al. (2016). The details on impact of each variables and their degree of correlation to the occurrence of wildfire is interpreted and summarized in the following sections:

The value of the odds of LST indicates that, as the LST increases, the odds of occurrence of wildfire increase by a factor of 163.788. Here, it can be observed that LST is the most notable influential factor of wildfire compared to all other variables. This signifies that temperature plays an important role in predicting wildfires which is true because LST has significant impact on the moisture content of the fuels. So areas with high LST can dry fuels and surrounding areas more quickly, making more susceptible to fires. The result is consistent with the previous work of Zhang et al. (2009); Mohammadi et al., (2014) and Pourtaghi et al., (2014).

The positive linear relationship of the proximity variables Dist_AgriL and Dist_Setl indicates that as the Euclidean distance increases the occurrence of wildfire fire increases. This is an unexpected result because generally areas closer to the agriculture land and settlement areas are more likely to initiate the wildfire due to human activities like burning of debris (agriculture/orchards/waste). To verify the result, the wildfire hotspots were overlaid with the raster maps of agriculture land and settlement. It was observed that for certain areas closer to the agriculture lands and settlements, show high density of hotspot while more fires are also seems scattered farther away from the agriculture and settlement areas in the northern part of Paro and southeastern part of Thimphu. As a result, the overall impact seems to show positive correlation to the Euclidean distance of agriculture land and settlements. Wu et al. 2015 also reported that all variables do not necessarily show a consistent linear relationship with the wildfire occurrence and instead it is important to focus on the possible reasons

for such type of surprising outcomes. The other possible reason could be here mentioned, because unlike in the past where farmers used to clear their registered land for agriculture, burn grasslands and practice shifting cultivation that caused more fire incidences, nowadays such traditional practices have declined with improved farming techniques and more awareness on fire has deviated the traditional practice of using fires. Ultimately this may have reduced fires incidences in agriculture lands. Moreover, in the analysis, all those registered lands irrespective of cultivation status are considered as agriculture land which may have accounted for less number of fires compared to overall area. In addition, majority of agriculture land are paddy field, especially in the lower valleys which may have resulted to less numbers of wildfire unlike other farmlands. Most fires are suspected to have occurred along the periphery or away from the agriculture lands. Likewise, most of the settlements are more or less concentrated in lower valleys while wildfires usually occurs on either side of the valleys above the settlement areas spreading uphill. Furthermore, nearby the settlement areas, people collect fallen leaves and debris of pines and deciduous trees resulting in less accumulation and concentration of litter and duff on the forest floor. This practice also in turn may have resulted in the positive correlation to the Euclidean distance.

In general, the aspect (ASP) variable which determines the intensity and direction of sunlight received by the face shows a significant positive correlation/influence to wildfire with OR value of 4.663 ($\beta=1.540$) as expected. This implies that aspect plays an important role in determining the probability of wildfire in the study area.

Likewise, land use (LU) further contributes to the occurrence of wildfire with positive influence. This indicates that the overall impact of the land use have a

positive influence to the occurrence of wildfire. The study area is characterized by a rugged topographic terrain with varieties of vegetation cover. The dry shrubs and meadows on the sloppy valleys and mountain bases are more susceptible to fires. In addition, Thimphu and Paro are the fastest developing districts in Bhutan where many developmental activities are taking place at a rapid pace, and many people from the rural areas of Bhutan migrate to these areas looking for jobs and better opportunities. As a result, a significant change in the land use may have taken place with increased population over the time, which in turn may have a positive impact on the occurrence of wildfire. The OR indicated that the probability of wildfire occurrence in the area increases by the factor of 2.237 for land use variable.

One of the most important human factor, distance to road (Dist_Road) revealed a negative correlation as expected. This shows that, as the Euclidean distance to the road decreases, the probability of occurrence of wildfire increases, indeed a positive influence, i.e., the more closer to the vehicle road, it is more likely that the incidence of wildfire will increase. The results signifies a strong evidence that road access is a significant contributing factor in the probability of wildfire occurrence. Most human-caused wildfires start along roads and these fires constitute the majority of the wildfires that burn across many areas. While roads do improve access for firefighters and sometimes even act as breaklines for fuel, those same roads provide access to careless people including drivers, campers, smokers and arsonists which increases in human-caused wildfire. Due to this, the overall influence of access to road system on wildfire is quite important and need to analyze properly. In addition, wildfires are initiated by the road side laborers while burning the bitumen and it is also reported as one of the causes of wildfire in Bhutan. Moreover, in the current study area, the

topography is not uniform and most of the major roads are located along the sloppy mountain bases following the main rivers. So most fires starts from the base of hilly terrain spreading uphill where access to road and water becomes very difficult to contain the fire. As a result, the probability of wildfires are high within the proximity of roads.

The negative coefficient value of elevation (ELV) indicates that, as the altitude of the place above the mean sea level increases, the probability of wildfire occurrence decreases. This is because, places at higher elevation normally experience more rainfall and remains much cooler and wetter than the places at lower elevation that experience higher temperature and lower rainfall. Moreover, places at higher altitudes experience frequent snow falls during the winter season coinciding with the fire season. As a result, fire behaviour trends are less severe at higher altitude while more fires occur at lower altitudes as indicated by the negative correlation of elevation. The OR of less than 1 (0.053) also indicates that odds of wildfire event will decrease for every unit increase of an elevation by a factor of 0.053. The results is true and consistent with the findings of the previous researches (Zhang et al., 2009 and Mohammadi et al., 2014).

The topographic wetness index (TWI) shows a negative correlation with the wildfire occurrence. This means, the areas with low TWI values are more susceptible to wildfires than those areas that have high TWI values. The results is true because TWI represents the measure of potential wetness in any portion of the landscape. It identifies and locates areas where water bodies, ponds or any wet areas exist in a landscape. Therefore, wetter areas will have lower probability to ignite a fire

than the dry areas, hence TWI indicates a negative influence in the occurrence of wildfire.

The mean annual rainfall (RF) and relative humidity (RH) are two important factors which determine the moisture content and fuel accumulation which in turn effects on the probability of wildfire occurrence. Higher rainfall and high relative humidity contribute to fuel moisture, decreasing the possibility of fire ignition. This is confirmed by both variables showing a negative correlation. This indicates that, places that experience lower annual rainfall have higher chance of wildfire while places with higher annual rainfall have less chance of wildfire. This implies that, areas associated with high rainfall may have reduced the fire occurrence by increasing the fuel moisture content, limiting the fire ignition and spread; On the contrary, rains falling outside the fire season may influence wildfire by favouring seasonal growth of vegetation/grass lands resulting in an increase availability of dry fuels, where fires can easily start and spread during the fire season. Likewise, as the relative humidity in the air decreases, the moisture content of the fuels in the surrounding area tend to dry faster, increasing the probability of ignition. Though, influence of relative humidity is relatively low compared to other variables, the result is consistent with the findings of previous studies (Zhang et al. 2009 and Guo et al., 2015). The OR value indicates that, for every unit increase in the RF and RH values, the probability of wildfire occurrence decreases by the factor of 0.454 and 0.25 respectively.

The enhanced vegetation index (EVI) which represents the amount of fuel available for ignition shows a negative influence, meaning that as the EVI values increases the probability of wildfire ignition decreases. In general this is not always true, because the high value of EVI means there is more vegetation cover and normally

should have a higher chance of wildfire occurrence due to more concentration of ground biomass. However, the result seems true and reasonable because majority of the wildfire are found in the lower sloppy valleys where the area is mostly covered by shrubs and meadows, and in sparsely vegetated areas with small trees and high concentrations of dry bushes. Certainly, the EVI values of shrubs and meadows will be lower than those with highly vegetated areas like coniferous and broad leaf forest. Thus, the result is agreeable because the overall impact of EVI in the current study indicates a negative correlation due to low EVI values of shrubs and meadows compared to highly vegetated areas.

The population density which represents the local socioeconomic activity indicates a negative correlation. This illustrates that wildfires are less frequent in areas that have higher population density. In general, the impact of population density in the particular area can have both positive and negative impact on the frequency of fires. The positive influence would be that, with rise in population density it is more likely that people may induce more fires. On the other hand, more people and more resources can be deployed to contain the fire and help in the reduction of fire severity and prevent it from spreading. Hence, it can have a negative impact on fire frequency as well as in spreading and fire severity. In addition, when an area has no human or less population, there is a risk that the fires may increase and spread without any interference. In the present study, the negative impact of population density on probability of wildfire is agreeable. Thimphu and Paro being one the most developed districts constitute the population with high literacy rates and have more awareness on the consequences and impacts of fire. Consequently, the overall impact of population density have negative correlation in the wildfire occurrence. Meanwhile, the study on

the impact of human population density on the fire frequency at the global scale also found that the assimilated charcoal records and analysis of regional fire patterns from remote sensing observations showed a decline in fire frequency with increase in human population (Knorr et al., 2014). Thus, the result is consistent with this finding.

In summary, LR model demonstrates that, while most of the fires are induced by the human activities along the roads, the probability of wildfire occurrence are mainly influenced by environmental, climatic and fuel variables. This indicates that the spread of wildfire is ultimately a function of various factors described in section 2.5 of Chapter 2. While the frequency of wildfire was observed higher closer to the road, more fires are also predicted away from the agriculture and settlement areas. In addition, the population density have a negative correlation. Although this result seems contradictory based on the location of wildfire hotspots, it appears to be true because once the fire is ignited, it tends to burn more frequently when there is less or no human interference with continuous flow of fuels in faraway places. So wildfires can consistently sustain burning when they spread beyond their ignition source into more remote areas. Although fires start closer to roads, the areas that actually burn most frequently are the non-urban areas where fires spread after ignition. Another reason could be because, for the current analysis the anthropogenic variables only represents for a temporary time period, whereas the hotspot data used for the analysis spanned a period of last 15 years. Despite the temporal mismatch, the current results are found consistent with most of the previous research as discussed. This is supported by the fact that, while anthropogenic variables are the best predictors for the number of fires that start, biophysical variables are better at explaining the variation in area burned. Therefore, the most important predictors for the LR analysis also include environmental

variables, especially topographic data that remains constant over the temporal extent of the fire frequency data. As a result, high number of fire incidence in the particular area does not always need to have a positive influence with all considered variables. This can be further explained by the fact that, although Thimphu district has the highest number of fire incidence compared to other areas of Bhutan, the overall acreage damaged is relatively moderate or low compared to other areas. This indicates that there are certain factors that may have accounted for negative influence to the occurrence of wildfire. For instance, in the core urban areas of Thimphu and Paro, there is more support from the sectors like armed forces, police personals, volunteers, Desups, fire fighters etc. to contain the fire as soon as it is detected. In addition, accessibility to the wildfire is facilitated by the existence of numerous approach roads, while this may not be the case in other remote areas. Nevertheless, majority of the areas that are away from the human influences have low probability of fire occurrence. Therefore, although fires spread away from ignition sources and burn more frequently outside urban and settlement areas, there are also even more remote areas that burn with much less frequency or no fire incidence at all. However, areas closer to the road associated with high human activities are found more conducive to fire and they are more likely to experience high number of fire incidences.

The results of LR model revealed that, the most significant influential factors of wildfire are LST and Dist_Road followed by ELV, Pop_Density, EVI, Dist_AgriL, ASP and RH. These factors have very high degree of correlation/influence as indicated by their coefficients.

4.3.2 Wildfire probability map generation

Using the coefficients (β) values of LR analysis, the predicted probability of the entire study area for the observed values of independent variables is calculated. For each cell in the study area, the values of independent variables are multiplied by their respective coefficients and then they are summed up including the estimated constant (β_0). Finally the estimated probability map of wildfire hotspot is obtained using the probability equation. As described in Section 3.2.1, this is achieved using multiple regression and the probability equation of LR model in the following steps:

First the multiple regression equation is applied in three steps for environmental, climatic and anthropogenic variables separately and then later added together with the estimated constant of the model to complete the multiple regression equation all variables. These combined Z values which represents the linear combination of all variables weighted by their regression coefficients is then applied to formulate the probability equation for the entire study area as shown below:

$$Z_E = 1.54(ASP) - 2.937(ELV) + 0.805(LU) - 1.798(EVI) - 0.68(TWI) \quad (4.1)$$

$$Z_C = 5.099(LST) - 1.388(RH) - 0.79(RF) \quad (4.2)$$

$$Z_A = 1.769(Dist_{AgriL}) - 3.261(Dist_{Road}) + 0.997(Dist_{Sett}) - 1.841(Pop_{Density}) \quad (4.3)$$

$$Z = -1.785 + Z_E + Z_C + Z_A \quad (4.4)$$

Now, by applying the value of “Z” in the following LR probability equation

$$Logit(Y) = \log \frac{p}{(1-p)} = \frac{e^{(\beta_0 + \beta_1x_1 + \beta_2x_2 + \beta_3x_3 + \dots + \beta_nx_n)}}{1 + e^{(\beta_0 + \beta_1x_1 + \beta_2x_2 + \beta_3x_3 + \dots + \beta_nx_n)}} \quad (4.5)$$

$$\Rightarrow P = \frac{1}{1+e^{-(\beta_0 + \beta_1x_1 + \beta_2x_2 + \beta_3x_3 \dots \beta_nx_n)}} \approx \frac{1}{1+e^{-z}} \quad (4.6)$$

Where, Z_E , Z_C and Z_A are the parameters which represents the linear combination of environmental, climatic and anthropogenic variables in use weighted by their individual regression coefficients respectively, and P is the probability of occurrence of wildfire hotspot.

In practice, the probability map was generated using the Model builder in ESRI ArcGIS software with the relevant tools (Figure 4.3). This technique is very efficient and convenient which enables to run the model interactively whereby a user can input the regression coefficients or change variables efficiently. The model consist of three main components. The process first starts with the calculation of multiple regression for three categories of independent variables which include environmental, climatic and anthropogenic variables. The regression coefficients of each independent variable for respective categories were assigned separately by using the raster calculator tool in the model. In the second step, the weighted independent variables for all the three components are then summed up by applying multiple regression equation in raster calculator tool. The result obtained from these process is three raster's (Z_E , Z_C and Z_A) for three categories of independent variables.

In the next step, all three raster's are added together to obtain the Z value, the linear combination of all the independent weighted by their respective regression coefficients. Herein, the constant of LR model was included in the summation. Finally, the probability equation of LR is applied to obtain the wildfire probability map of the entire study area.

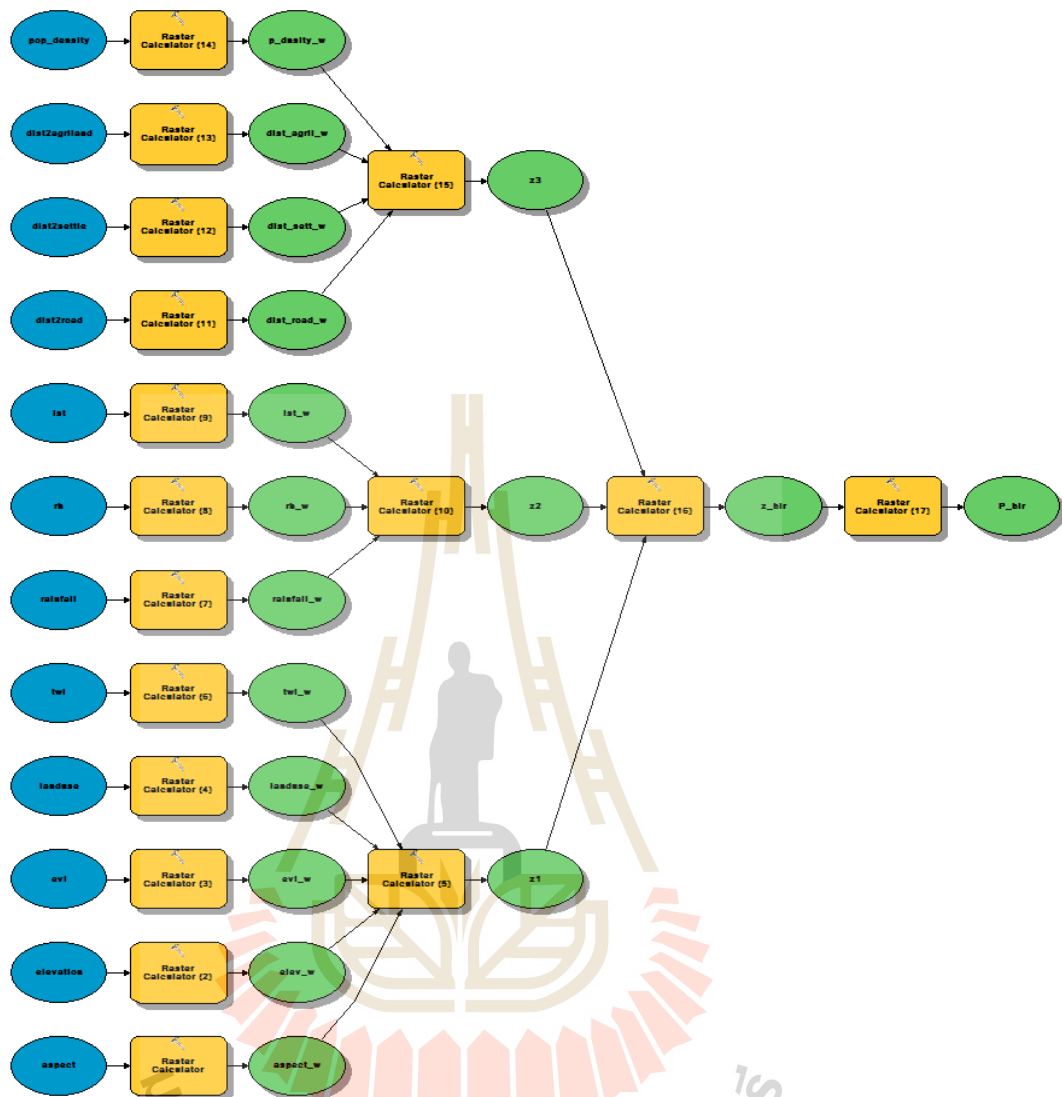


Figure 4.3 Model structure for LR analysis in ESRI ArcGIS 10.3 software.

The result is a raster layer with the cell values representing the estimated probability of wildfire occurrence, which vary from 0 to 0.945. The wildfire probability map obtained based on the formulated LR model is presented in Figure 4.4.

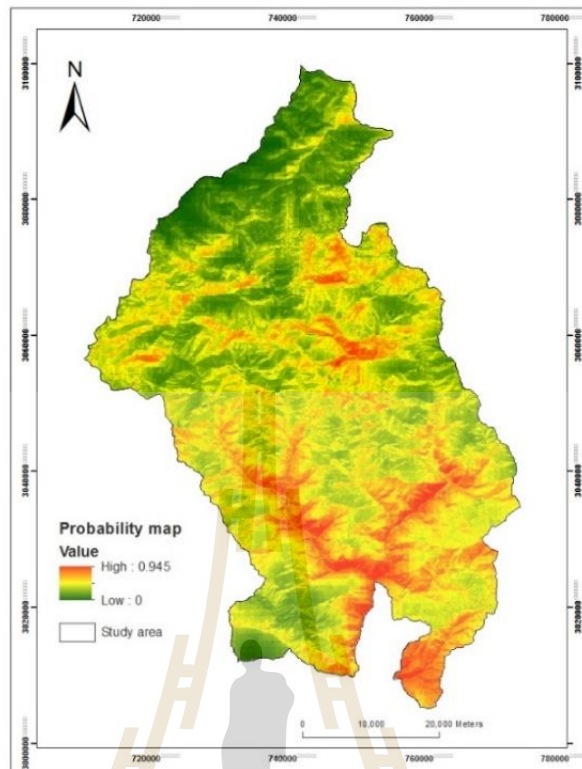


Figure 4.4 Wildfire probability map from LR model.

The probability map derived from LR model demonstrates the impact of different factors with different degree of influence to the occurrence of wildfire. As indicated by the regression coefficients (β), the probability is observed higher at lower elevation that corresponds to high land surface temperature, low rainfall and low relative humidity. The probability values are very high closer to the roads and in places where the vegetation is dominant with dry grasslands, shrubs and meadows, and therefore are more susceptible to wildfire occurrence. Hence, the findings from LR analysis revealed that the most significant predictor variables of wildfire are LST followed by Dist_Road, ELV, Pop_Density, EVI, Dist_AgriL, RH and ASP. Other variables have relative low influence.

4.4 Wildfire susceptibility analysis using FR model

The FR analysis employed all the fifteen influential factors and the classified maps are presented in the Figure 4.5. The classification of each factor maps are done based on the objective, accuracy and scale of the input data and also based on extensive literature reviews.

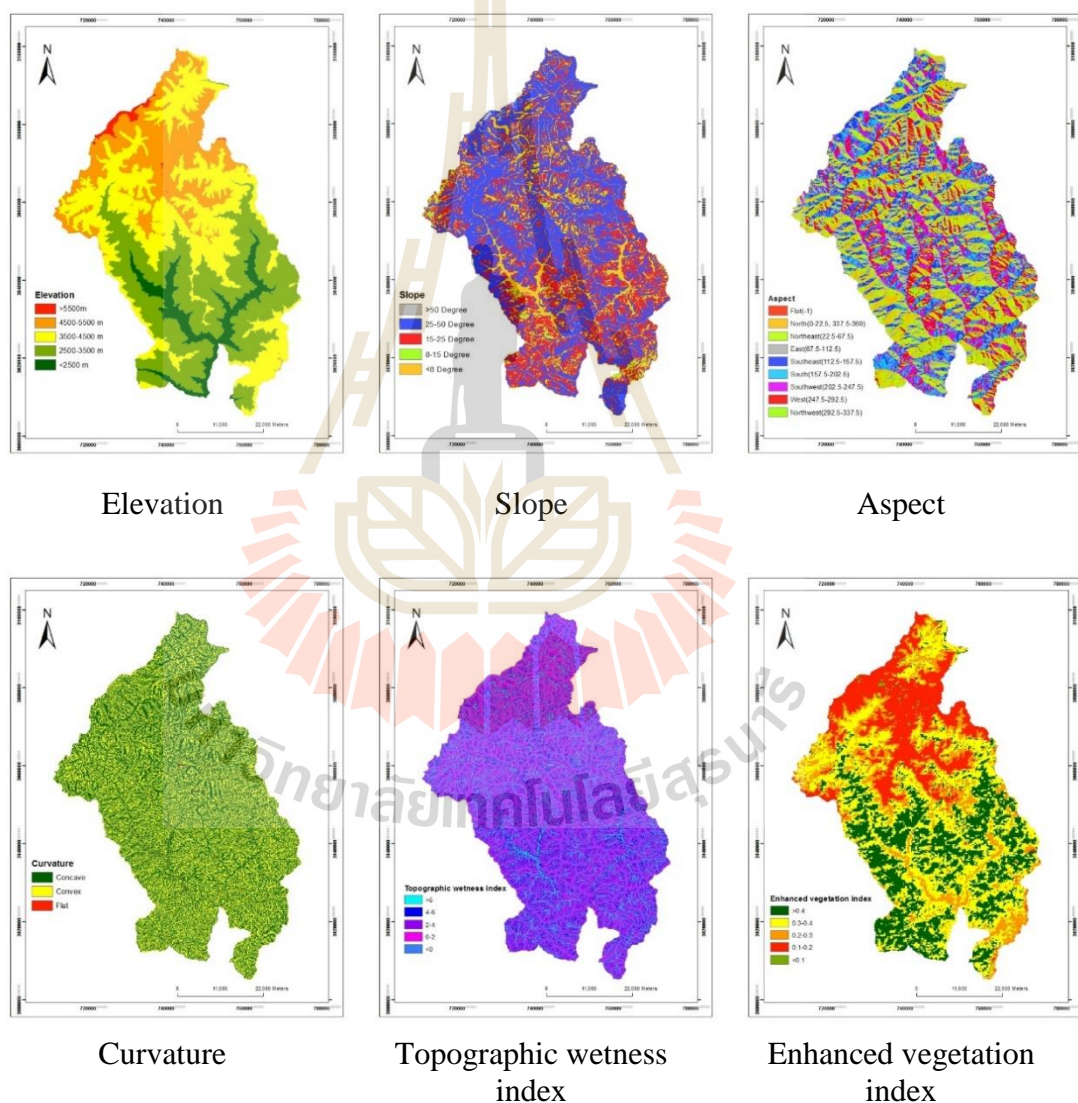


Figure 4.5 Input factor maps for FR analysis.

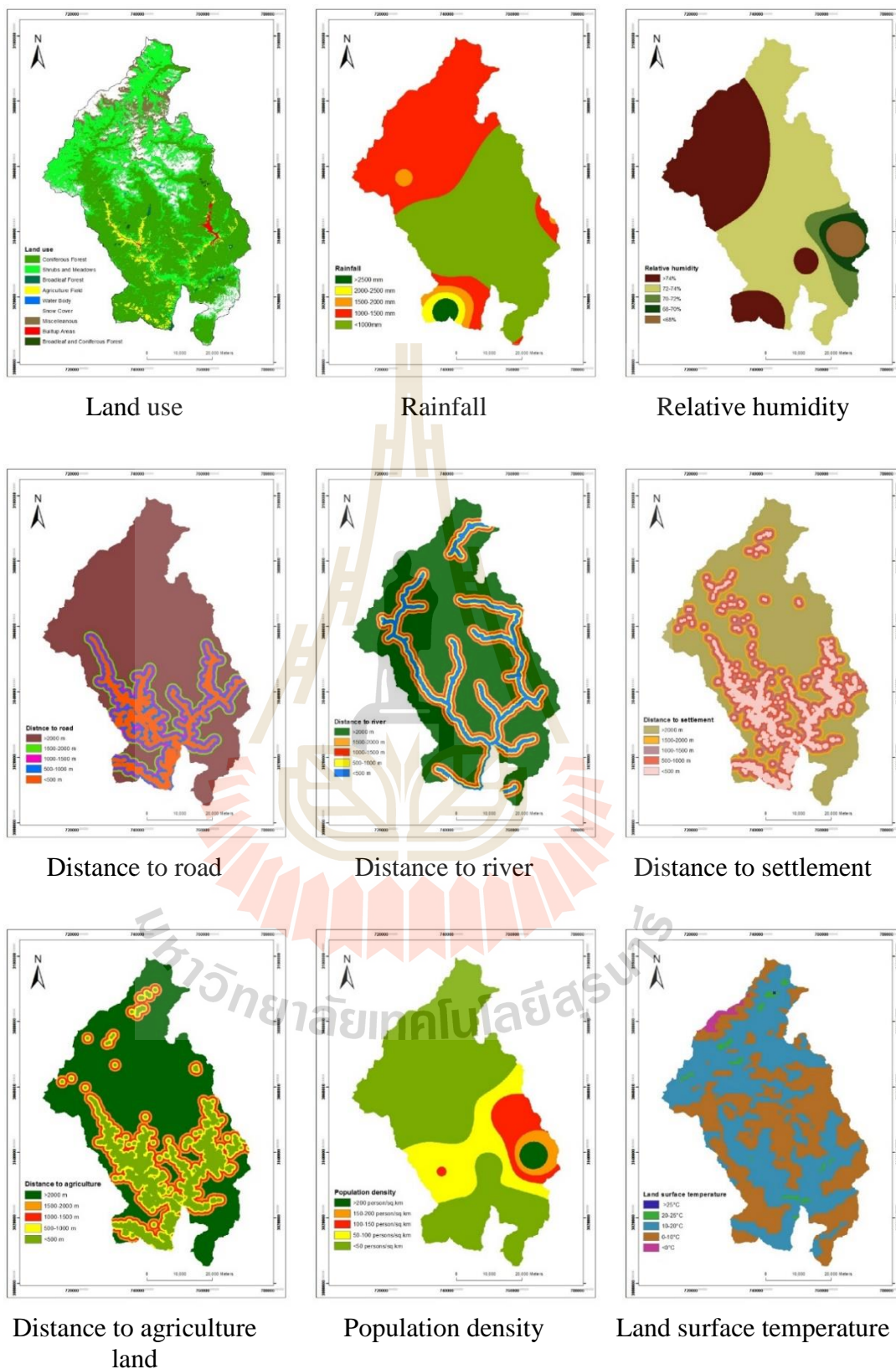


Figure 4.5 Input factor maps for FR analysis (Continued).

To calculate the FR of each factor class, the hotspot pixels of entire training dataset are overlaid/superimposed with the classified factor maps individually and the number of hotspot pixels in each class is cross tabulated and examined using the Spatial Analyst Tool in ESRI ArcGIS software. It is then imported to MS-Excel spreadsheet to calculate the FR values. Herein, the FR of each factor's class are calculated in three steps. First, the area ratio of each class of factor is calculated, followed by the calculation of hotspot ratio. Finally, the FR is computed by dividing the hotspot ratio by the area ratio for each factor's classes. The results of FR values determined using FR model is provided in Table 4.5

Table 4.5 Frequency ratio of each class of independent factors (FR result).

Factor	Class	No. of pixels in each class	% of pixels in each class (B)	No of hotspot pixels	% of hotspot pixels (A)	FR = A/B
Elevation	<2500 m	22507	7.3%	272	15.3%	2.092
	2500-3500 m	107241	34.8%	711	39.9%	1.148
	3500-4500 m	112812	36.6%	734	41.2%	1.126
	4500-5500 m	63253	20.5%	65	3.6%	0.178
	>5500 m	2661	0.9%	0	0.0%	0.000
Slope	0-8°	13473	4.4%	45	2.5%	0.578
	8-15°	34880	11.3%	172	9.7%	0.854
	15-25°	104848	34.0%	592	33.2%	0.977
	25-50°	153493	49.8%	970	54.4%	1.094
	>50	1780	0.6%	3	0.2%	0.292
Aspect	Flat(-1)	59	0.0%	0	0.0%	0.000
	North(0-22.5; 337.5-360)	36565	11.9%	103	5.8%	0.488
	Northeast(22.5-67.5)	43033	14.0%	131	7.4%	0.527
	East(67.5-112.5)	40158	13.0%	217	12.2%	0.935
	Southeast(112.5-157.5)	39793	12.9%	421	23.6%	1.831
	South(157.5-202.5)	39760	12.9%	376	21.1%	1.637
	Southwest(202.5-247.5)	37175	12.1%	300	16.8%	1.397
	West(247.5-292.5)	36587	11.9%	147	8.2%	0.696
Northwest	35344	11.5%	87	4.9%	0.426	

Table 4.5 Frequency ratio of each class of independent factors. (Continued).

Factor	Class	No. of pixels in each class	% of pixels in each class (B)	No of hotspot pixels	% of hotspot pixels (A)	FR = A/B
Curvature	Concave	158018	51.2%	862	48.4%	0.944
	Flat	3001	1.0%	16	0.9%	0.923
	Convex	147455	47.8%	904	50.7%	1.061
TWI	<0	108949	35.3%	635	35.6%	1.009
	0 - 2	101073	32.8%	667	37.4%	1.142
	2-4	62128	20.1%	311	17.5%	0.867
	4-6	20944	6.8%	108	6.1%	0.893
	>6	15380	5.0%	61	3.4%	0.687
EVI	<0.1	827	0.3%	0	0.0%	0.000
	0.1-0.2	58858	19.1%	78	4.4%	0.229
	0.2-0.3	54116	17.5%	364	20.4%	1.164
	0.3-0.4	113695	36.9%	1009	56.6%	1.536
	>0.4	80978	26.3%	331	18.6%	0.708
Land Use	Coniferous Forest	149563	48.5%	798	44.8%	0.924
	Shrubs and Meadows	95445	30.9%	735	41.2%	1.333
	Broadleaf Forest	1388	0.4%	1	0.1%	0.125
	Agriculture Field	8638	2.8%	45	2.5%	0.902
	Water Body	972	0.3%	0	0.0%	0.000
	Snow Cover	34686	11.2%	185	10.4%	0.923
	Miscellaneous	15397	5.0%	16	0.9%	0.180
	Built-up Areas	1975	0.6%	1	0.1%	0.088
	Broadleaf and Coniferous Forest	410	0.1%	1	0.1%	0.422
Rainfall	<1000 mm	154940	50.2%	1271	71.3%	1.420
	1000-1500 mm	135384	43.9%	429	24.1%	0.549
	1500-2000 mm	8150	2.6%	39	2.2%	0.828
	2000-2500 mm	5546	1.8%	34	1.9%	1.061
	>2500 mm	4454	1.4%	9	0.5%	0.350
LST	< 0°C	3081	1.0%	0	0.0%	0.000
	0 – 10°C	140505	45.5%	460	25.8%	0.567
	10 – 20°C	160574	52.1%	1234	69.2%	1.330
	20-25°C	4233	1.4%	88	4.9%	3.599
	>25°C	81	0.0%	0	0.0%	0.000
Relative humidity	<68%	10226	3.3%	125	7.0%	2.116
	68-70%	8719	2.8%	134	7.5%	2.660
	70-72%	15076	4.9%	139	7.8%	1.596
	72-74%	161191	52.3%	809	45.4%	0.869
	>74%	113262	36.7%	575	32.3%	0.879

Table 4.5 Frequency ratio of each class of independent factors. (Continued).

Factor	Class	No. of pixels in each class	% of pixels in each class (B)	No of hotspot pixels	% of hotspot pixels (A)	FR = A/B
Distance to road	<500 m	41450	13.4%	351	19.7%	1.466
	500-1000 m	22578	7.3%	363	20.4%	2.783
	1000-1500 m	17514	5.7%	123	6.9%	1.216
	1500-2000 m	15186	4.9%	74	4.2%	0.844
	>2000 m	211746	68.6%	871	48.9%	0.712
Distance to river	<500 m	31233	10.1%	229	12.9%	1.269
	500-1000 m	27100	8.8%	300	16.8%	1.916
	1000-1500 m	26676	8.6%	218	12.2%	1.415
	1500-2000 m	26368	8.5%	212	11.9%	1.392
	>2000 m	197097	63.9%	823	46.2%	0.723
Distance to settlement	<500 m	50630	16.4%	487	27.3%	1.665
	500-1000 m	41601	13.5%	372	20.9%	1.548
	1000-1500 m	34438	11.2%	173	9.7%	0.870
	1500-2000 m	28846	9.4%	97	5.4%	0.582
	>2000 m	152959	49.6%	653	36.6%	0.739
Distance to agricultural land	<500 m	54186	17.6%	582	32.7%	1.859
	500-1000 m	32447	10.5%	292	16.4%	1.558
	1000-1500 m	26166	8.5%	74	4.2%	0.490
	1500-2000 m	21770	7.1%	54	3.0%	0.429
	>2000 m	173905	56.4%	780	43.8%	0.776
Population density	<50 person/sq.km	215810	70.0%	1255	70.4%	1.007
	50-100 persons/sq.km	56084	18.2%	167	9.4%	0.515
	100-150 persons/sq.km	21856	7.1%	166	9.3%	1.315
	150-200 persons/sq.km	9023	2.9%	105	5.9%	2.014
	>200 persons/sq.km	5701	1.8%	89	5.0%	2.702

In practice, the equation 3.9 and 3.10 of FR model (Section 3.2.2) are used to calculate the FR values of each class of factors. The computed FR values determines the spatial relationships between distribution of hotspot and each hotspot related factors, and it explains the level of correlation between hotspot locations and influential factors in a certain area. The FR values greater than 1 indicates higher correlation with the wildfire occurrence while FR value lower than 1 indicates lower correlation, and if

the FR value is 1, it means an average correlation. The correlation of each factor class based on the computed FR is interpreted and explained in details in the next section.

4.4.1 Impact of influential factors on wildfire occurrence (FR)

Based on the deduced results from FR analysis (Table 4.5), the relation of wildfire occurrence and elevation shows a negative correlation. A gradual decrease in the FR values shows that the frequency of wildfire occurrence decreases as the elevation increases. Most wildfires seems to occur below the elevation of 2,500 meters above msl as indicated by highest FR (2.092) value in this class. This is correct because places at higher elevation are much cooler than the places at lower elevation making the fire behavior trends less severe. In addition, at higher altitudes it encounters higher rainfall and remains wet. No incidence of wildfires are observed at elevations greater than 5,500 m as indicated by FR value (FR=0). This is because of the general trend that as temperature reduces, the humidity increases with increased elevation. This implies that the moisture content of fuels on the highest elevation is high reducing the flammability of the fuels eventually reducing the chances of fire incidences. In addition, at the highest elevations, vegetation are non-existent or very low, because they are covered by rocks and bare soils which cannot support the growth of most tree species and most of the time they are covered by snow and permanent glaciers, hence the chance of fire is very rare.

For slope class, there is a positive correlation with the wildfire occurrence as indicated by a progressive increase in FR values as the slope angle increases. Thus slope plays a significant role in the spread of fire, where fires usually spreads rapidly up slope than down slope. The slope class between 25°–50° have highest frequency (FR=1.09) of wildfires supporting the fact that, a fire burning up to a slope

of +20% to +39% will spread twice as first a fire on level terrain (Brown and Davis, 1973). Since the study area is mountainous, the steep slopes have contributed to increase the spread of wildfires compared to very rare flat slopes.

Though aspect does not have an effect on ignition of the wildfire, it can influence on the rate at which fuels dry consequently affecting fire behaviour. The result revealed that aspect classes facing Southeast (112.5-157.5), South (157.5-202.5) and Southwest (202.5-247.5) slopes show the highest frequency of wildfire occurrence with FR values of 1.831, 1.637 and 1.397 respectively. The other aspect classes show relatively less frequency of fire incidences with low FR values. The result is true because, south aspects receive more sun light and have higher temperatures with robust winds, low humidity, and low fuel moistures in the Northern Hemisphere. Moreover, vegetation is typically drier and less dense on south-facing slopes than north-facing ones which hold more moisture and stay green longer and support more vegetation (Prasad et al., 2008). Thus, drier fuels with less moisture content are more exposed to ignition. Hence, south facing slopes are more susceptible to wildfires. Meanwhile, convex curvature shows high wildfire frequency compared to concave and flat curvatures. The topographic wetness index is found negatively correlated with the wildfire occurrence as indicated by decreasing trend of FR values as TWI values increases. This indicates that the frequency of fire decreases as wetness or moisture content in the surrounding area increases.

For EVI, the high frequency of wildfire occurrence is observed between 0.2 and 0.4. As the EVI values falls below 0.2 and rise above 0.4, the probability of wildfire occurrence is decreased. This shows that most fire occur in the moderately vegetated areas that comprise of shrubs and meadows, dry grasslands or bushy areas in

sloppy valleys. EVI values lower than 0.2 may indicate the presence of bare soils and snow covered areas where there is less chance of fire occurrence, hence the results show no incidence of fires in these areas.

The type of land use which represents vegetation and the forest type have strong influence in the ignition and spread of fire because some forest types are highly flammable as compared to others hence increasing the chances of fire occurrence. The ignition of a fire depends on fuel flammability. Though the environment may be suitable for a fire to start, it cannot start without the flammable material. The results shows that FR values are high in shrubs and meadow class (FR=0.924) and in coniferous forest class (FR=1.333) indicating higher probability of wildfire occurrence compared to other land use types. The result is consistent with the findings of Carmoa, Moreiraa, Casimirob and Vaza (2011). This result further supports the occurrence of wildfire on intermediate EVI class as discussed. Land use classes like agriculture land and snow cover also indicate a moderate correlation with wildfires. While this is agreeable with the agriculture land class, the correlation with the snow cover class seems doubtful. However, this can also be true because the incidence of fire may have happened in the area before it was covered by the snow, because, the fire season in the study area begins in early October and continues until the end of May, while the peak winter lies in between the mentioned period. In addition, snow cover is one of dynamic variable that characterizes spatial-temporal phenomena that results in the mismatch with temporal scale of hotspot data. This may provide an unexpected result (FR=0.923) as observed. The frequency of wildfire in other classes like broadleaf forest, broadleaf and coniferous forest, miscellaneous and built-up areas show relatively low, while the water body class shows no incidences.

The climatic variables that includes rainfall and relative humidity show negative correlation with the wildfire as expected. It can be seen that the FR values gradually decrease as the rainfall and relative humidity increase, indicating the decreasing trend in wildfire incidences. In particular, the frequency of wildfire is seen high in areas where the mean annual rainfall is less than 1,000 mm and relative humidity is less than 70% respectively. The findings are acceptable because high rainfall and high relative humidity will result in the high fuel moisture content in the surrounding areas eventually reducing the risk of fire occurrence.

Land surface temperature (LST) is seen as one of the most influential factor with highest FR value indicating a positive correlation to wildfire occurrence. The progressive increase in the FR values of the LST indicate that the frequency of wildfire increases as LST increases. The frequency of wildfire occurrence is relatively high in places where the LST is above 25°C as indicated by the FR values of 3.599. The influence of temperature on fire behaviour is to reduce the moisture content of the fuels. When temperatures are low, the moisture content of the fuels is high making the ignition difficult, on the other hand when temperatures are high, the moisture content of the fuels is reduced and the surrounding air and soil temperature is increased resulting into easy ignition of the fire. Thus, positive influence of LST on wildfire is true and consistent with the findings of many other studies (Zhang et al. 2009; Intarawichian and Dasananda, 2010); Zhang et al. 2013).

Likewise, relationship between wildfire occurrence and distance to road shows that most wildfire occurs within the proximity of 1,500 meters. As the Euclidean distance to the road decreases the intensity and frequency of wildfires occurrence increases as shown by the FR values of 2.783 and 1.466 for the classes <500 meters

and 500-100 meters respectively. As the distance to the road increases beyond 1,500 meters the probability is low as indicated by the FR values lower than 1. Relationship of wildfire occurrence with distance to rivers shows that, closer to the river there is high chance of wildfire and the probability increases until the distance range of 1,000 meters. As the distance to rivers increases beyond 1,000 meters, the FR values decreases. The proximity variables like distance to settlements and distance to agriculture land also shows very high correlation within the proximity of 1,000 meters. Within this range, both variables have FR values greater than 1 indicating a high frequency of wildfire. In general the frequency of fires with respect to both variables decrease as the distance increase, however beyond the distance of 2,000 meters, a slight increase in the fire frequency can be noticed. This may be due to the influence of agriculture and settlement in remote areas.

The influence of population density on wildfire occurrence is found very high closer to highly populated areas as shown by the FR values greater than 1 for population density range of 100-150 persons/km², 150-200 persons/km² and >200 persons/km² respectively. For the population density range between 50-100 persons/km², it shows lower correlation, however it is interesting to observe that places with population density less than 50 persons/km² also shows a high correlation with fire. This may due to the people residing in the remote places inducing more fire.

4.4.2 Computation of prediction rates (PR) from FR analysis.

In addition to the calculation of FR values, the relative frequency of each factor class is calculated by dividing the FR values of each class by the total FR values of each factor and then the prediction rates of each factor is computed based on the following equations:

$$RF = \frac{FR \text{ of each class of factors}}{\text{Total FR of factor}} \quad (4.7)$$

$$PR = \frac{(RF_{Max} - RF_{Min})}{(RF_{Max} - RF_{Min})_{max}} \quad (4.8)$$

Where,

RF = Relative frequency of each class of factor;

PR = Prediction rate of each factors;

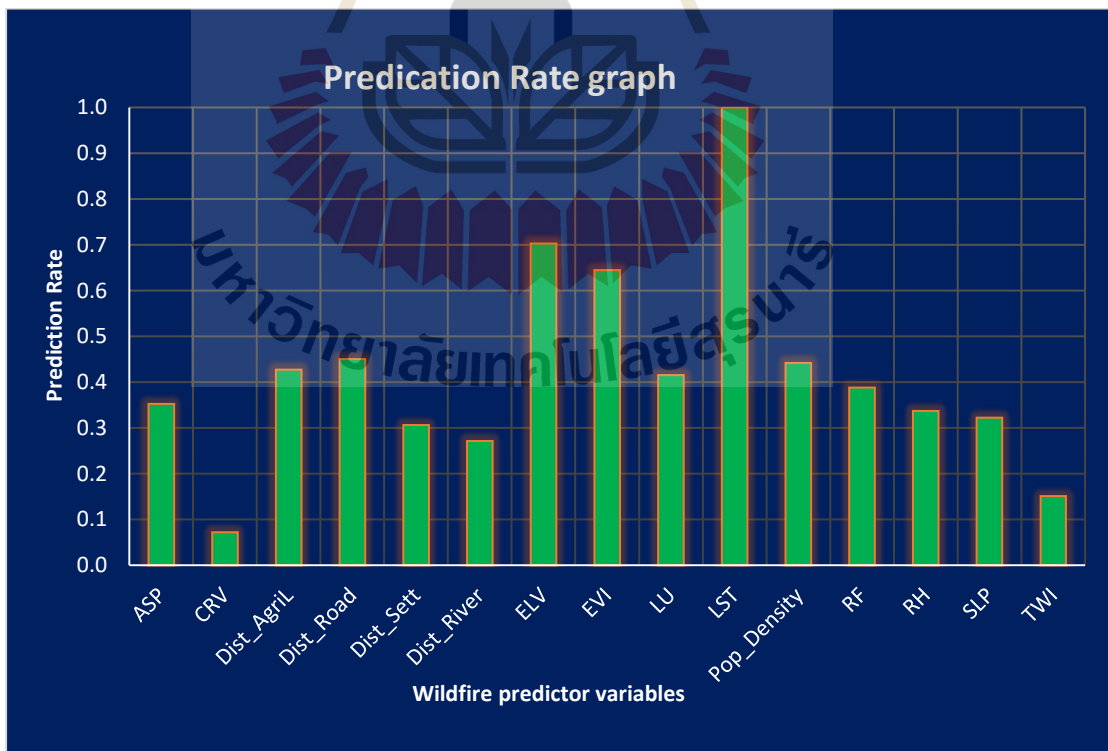
RF_{max} = Maximum RF in a factor class;

RF_{min} = Minimum RF in a factor class.

The relative frequency value for each class of factor represents the standardized FR values which further determine the relative importance of each class in a factor that reveals the level of correlation among each factors with wildfire occurrence. The prediction rates of each factors presented in Table 4.6 and the prediction chart displayed in Figure 4.6 reveals that the land surface temperature followed by elevation, enhanced vegetation index and distance to road have the highest contributing factors to the probability of occurrence of wildfire in the study area. The other factors like population density, distance to agriculture, rainfall, aspect, relative humidity, slope and distance to settlements show a moderate influence in the probability of wildfire occurrence while curvature, topographic wetness index and distance to rivers have negligible influence to the occurrence of wildfire. Curvature and distance to rivers are also eliminated by LR analysis since their contribution to the model is insignificant. This indicates that FR model further confirms their negligible influence or insignificance to wildfire occurrence.

Table 4.6 Prediction rates of wildfire influential factors.

No	Factor	Prediction Rate
1	Elevation (ELV)	0.703
2	Slope (SLP)	0.323
3	Aspect (ASP)	0.352
4	Curvature (CRV)	0.072
5	Topographic wetness index (TWI)	0.151
6	Enhanced vegetation index (EVI)	0.645
7	Land use (LU)	0.416
8	Rainfall (RF)	0.388
9	Land surface temperature (LST)	1.000
10	Relative humidity (RH)	0.337
11	Distance to road (Dist_Road)	0.451
12	Distance to river (Dist_River)	0.271
13	Distance to settlement (Dist_Set)	0.306
14	Distance to agriculture land (Dist_Agril)	0.427
15	Population density (Pop_Density)	0.442

**Figure 4.6** Graphical representation of prediction rate of each factors.

4.4.3 Wildfire susceptibility index map generation

To generate the wildfire susceptibility index (WSI) map of FR model, the computed FR values are assigned as weight values to the classes of each factor map to obtain the weighted factor maps using reclassify function in ESRI ArcGIS software, and then they are overlaid and numerically added using the raster calculator applying the Equation 4.8. Practically, the WSI is obtained by employing a Model Builder in ESRI ArcGIS software (Figure 4.7). Herein, weighted input raster with FR values in the field of respective classes are first converted to a new raster by using Lookup Tool in FR field, then the relative frequency of each class is calculated using the Raster calculator. Finally, the WSI is calculated using the Cell Overlay Statistics tool under Spatial Analyst function in ESRI ArcGIS software (Figure 4.8).

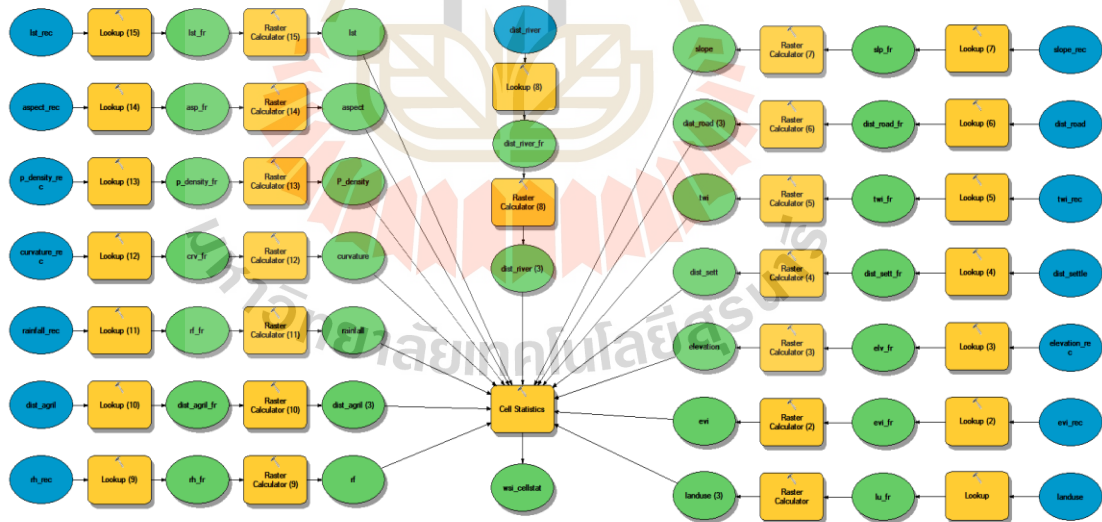


Figure 4.7 Module structure for FR analysis in ArcGIS 10.3.

The wildfire WSI map represents the relative susceptibility to the occurrence of wildfire in the entire study area. The higher values of WSI indicates high susceptibility to wildfire occurrence while lower values of WSI represents low susceptibility. The WSI values here ranges between 1.699 and 5.103.

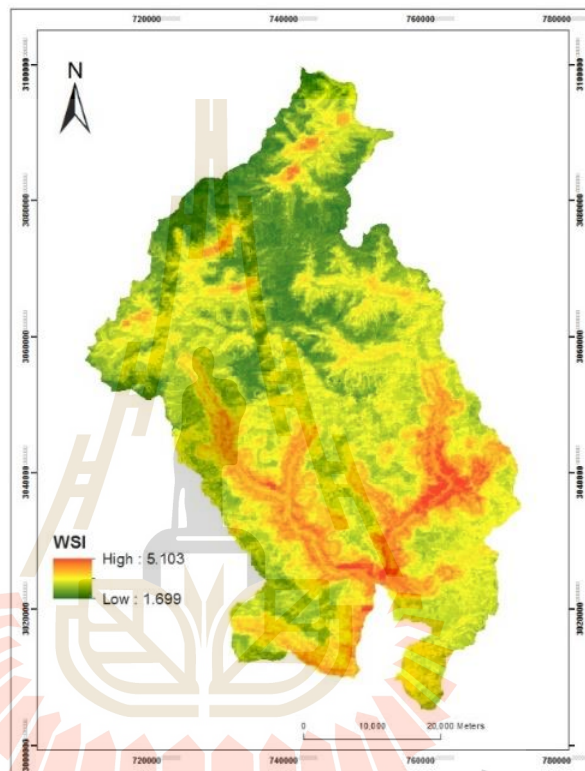
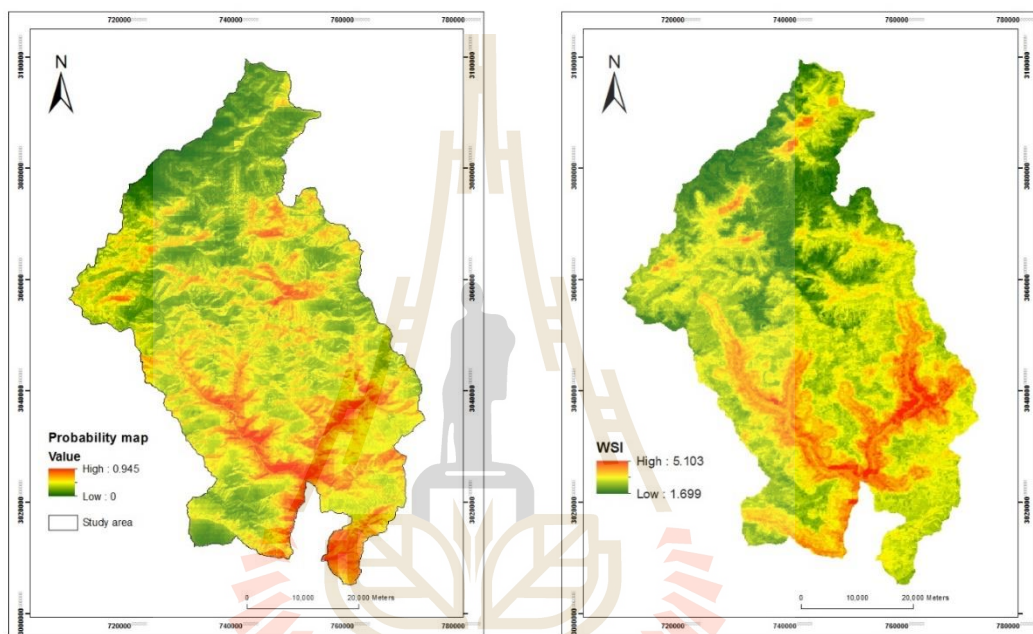


Figure 4.8 Wildfire susceptibility index (WSI) from FR model.

4.5 Comparative assessment of probability map of LR and FR models

The comparative appearance of wildfire probability map from LR model and wildfire susceptibility index (WSI) map from FR model, which both represents the probability of wildfire occurrence is displayed again in Figure 4.9. The two probability maps show a similar pattern along the valley and lowland areas, and present slightly dissimilar pattern in hilly and mountain areas. This is because the representation of

input data for LR model as continuous format and FR model as discrete format are different. In addition, classification system of influential factors plays an important role for FR analysis. However, there is no significant difference between the two probability maps which implies the performance of both LR and FR models are reliably good in predicting the wildfires in the study area.



(a) Probability map from LR

(b) WSI map from FR

Figure 4.9 Comparative view of wildfire probability maps of LR and FR models.

In addition, in order to identify and relate the pattern of influence and degree of correlation each factors have on wildfire occurrence from the both models, the graphical representation of predictive power (regression coefficients) from LR model and prediction rate from FR model are displayed in Figure 4.10. From the graph, it can be deduced that LST followed by ELV, EVI, Dist_Road and Pop_Density have highest degree of influence in the prediction of wildfire. ASP, RH, Dist_Set, RF and LU have moderate influence while TWI, SLP, CRV and Dist_River show a very low influence.

The graph also demonstrates that, all the influential factors considered in this study for the wildfire susceptibility analysis generally show a similar pattern of influence or correlation in both the models. Thus, from this assessment it can be concluded that the overall influence and correlation of influential factors with the wildfire occurrence generally remains same despite the two methods applied have a different approach of identifying the wildfire susceptible areas.

Overall, from the two probability maps obtained from LR and FR model, it can be observed that the spatial pattern of those areas predicted as having highest probability of wildfire occurrence reflects the significant influence of land surface temperature, distance to roads, elevation, EVI and population density in the study area.

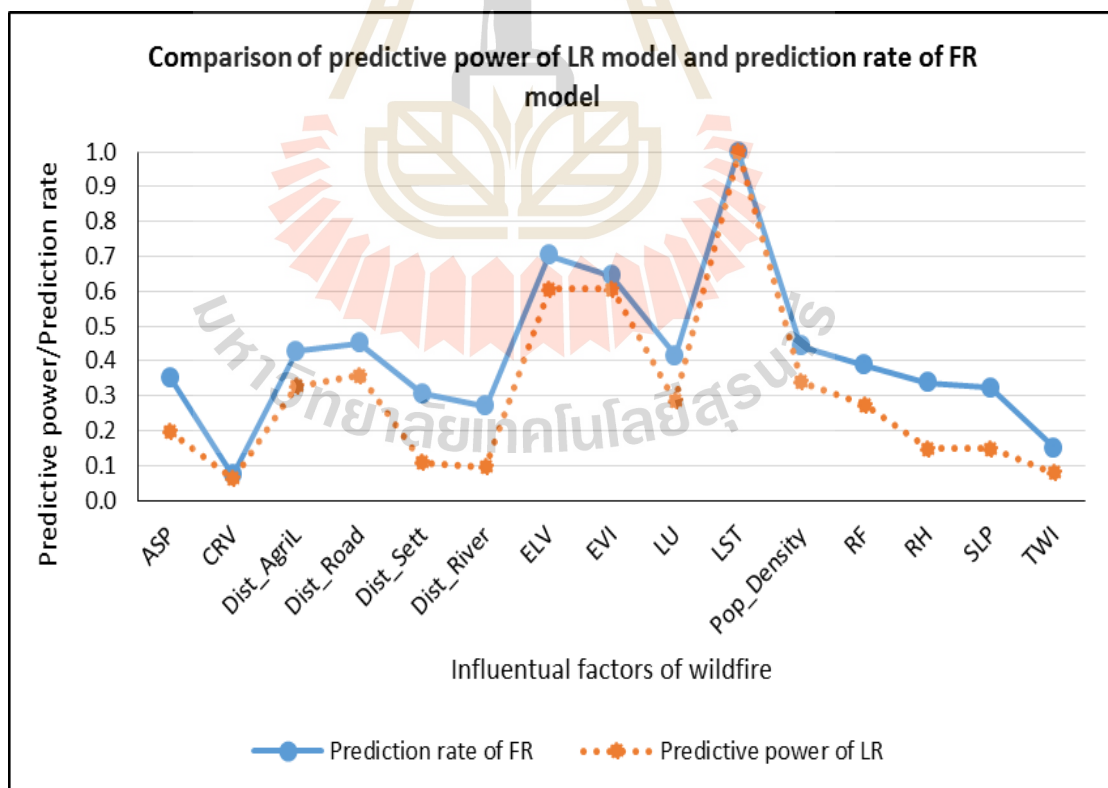


Figure 4.10 Comparison of predictive power of each factors from LR and FR models.

4.6 Accuracy assessment and validation of LR and FR models

The accuracy and validation of the two models were performed using the 30% independent validation dataset by employing ROC method. The deduced results are interpreted and discussed in this section.

The area under ROC which represents the AUC value is calculated using the IDRISI software. Herein, the success-rate curves and the prediction-rate curves are constructed. Practically, the success rates are established by comparing the hotspot pixels in the training dataset (70%) with the wildfire probability maps of LR and FR models respectively. Meanwhile, the prediction rates of LR and FR models are determined by comparing the hotspot pixels in the independent validation dataset (30%) with the wildfire probability maps of both models. Subsequently, the respective ROC curves are constructed with the applied threshold values to obtain the AUC value in IDRISI software from the resulting true positives and false positives.

The results show success rate curves with AUC values of 0.881 and 0.855 for LR and FR models respectively (Figure 4.11). Based on Chung and Fabbri (2003), the results indicate that both LR and FR models have a very good capability of classifying the area, and the models have a high goodness of fit with the training dataset and wildfire variables. The prediction rate curves with AUC values of 0.883 and 0.853 is obtained for LR and FR models respectively (Figure 4.12). The results indicate that both models have a relatively high predictive capability to discriminate the presence (hotspot) and absence (non-hotspot) of wildfire in the study area. Both models performed better with high accuracy compared to previous studies that employed the same model. (Intarawichian and Dasananda (2010); Zhang et al. (2013); Pourtaghi et al., 2014; Guo et al. (2015)).

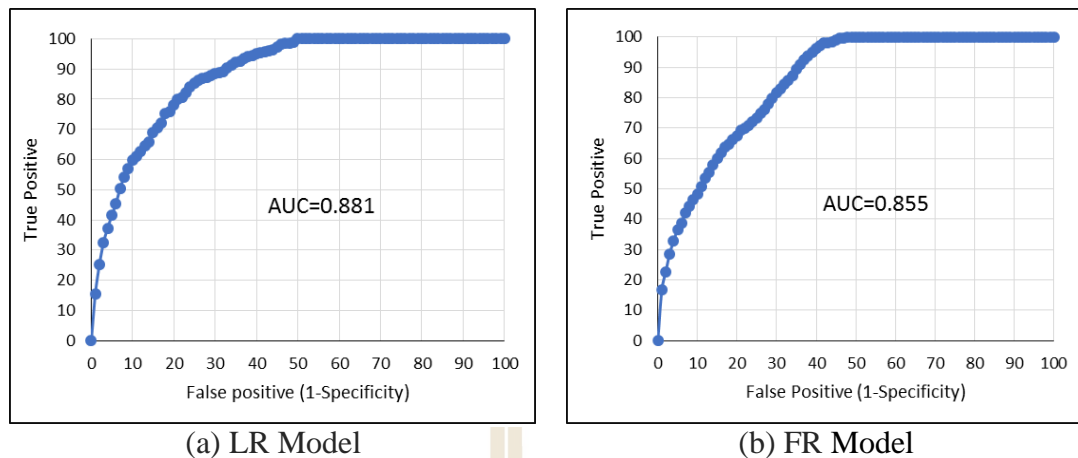


Figure 4.11 Success rate curves of LR and FR model.

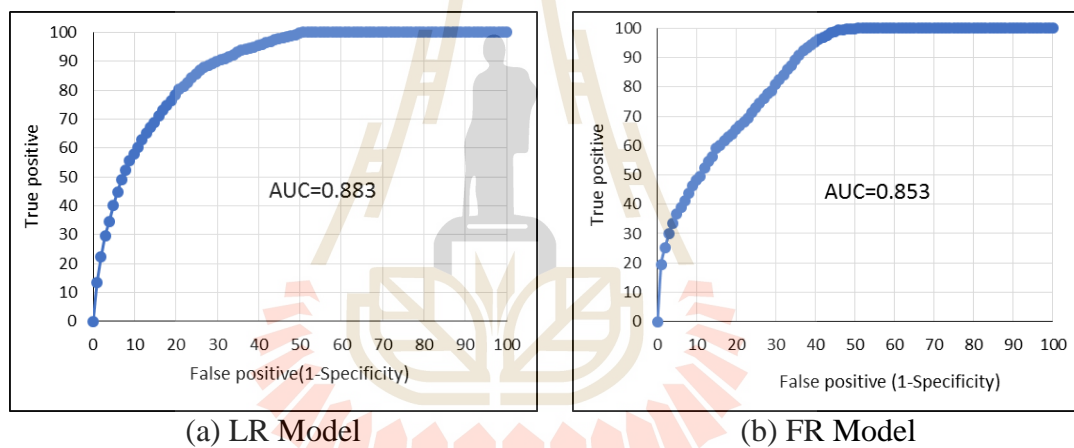


Figure 4.12 Prediction rate curves of LR and FR models.

Although, LR model performed slightly better than FR model as indicated by higher AUC value, the FR model can also be considered as an equally acceptable model that can be applied for susceptibility mapping in the area. A close similarity of success and prediction rate curves of the two models indicate that both models are reliable and can be used in predicting future wildfires (Figure 4.13). However, for the present study, based on the comparative analysis and the validation of final results, LR model is considered as the optimum and suitable model for the final wildfire susceptibility

mapping. The LR model shows slightly high performance in both the training and validation dataset compared to FR model with high AUC value for success and prediction rates of 0.881 and 0.883 respectively. Some studies have also found that LR model has performed better than FR model (Lee and Evangelista, 2008; Meten et al., 2015), while others have found FR model better than LR model (Lee and Pradhan, 2007).

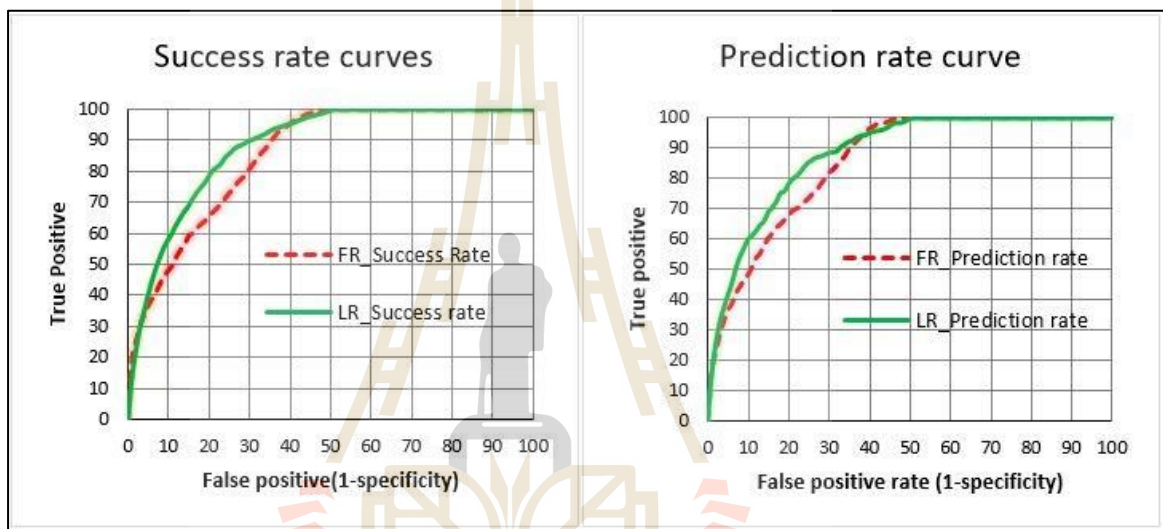


Figure 4.13 Comparison of success and prediction rate curves of LR and FR models.

4.7 Wildfire susceptibility mapping

The optimum LR model is used to generate the final wildfire susceptibility map. To generate the final wildfire susceptibility map of different zones from the probability map, the method adopted in many previous literatures is to divide the histogram of the probability map into different categories based on expert opinions (Dai and Lee, 2002 and Ohlmacher and Davis, 2003) and many studies have chosen and applied different classification methods depending on their interest and the type of data. For instance, Ayalew and Yamagishi (2005) applied four classification methods including quantiles,

natural breaks, equal intervals and standard deviation and selected one that best suits the information depending on the scale of investigation. They found that standard deviation method was suitable and provided good information. In other studies, Meinhardt et al. (2015) and Intarawichian and Dasananda (2010) applied the manual method and natural breaks respectively for better classification.

The present study examined all the available inbuilt classification methods in ESRI ArcGIS software and deduced that the standard deviation method provides the best information that is suitable to study area compared to other methods. The standard deviation method has a certain advantages of using the mean to generate the class breaks (Ayalew and Yamagishi, 2005). Moreover, probability values of the final output map is normally distributed according to the statistics of histogram report (Figure 4.14), where standard deviation is appropriate (ESRI, 2016). Herein, wildfire susceptibility map comprises of five zones: very low, low, moderate, high and very high (Figure 4.15). The computed area and its percentage for each susceptibility zones are presented in Table 4.7.

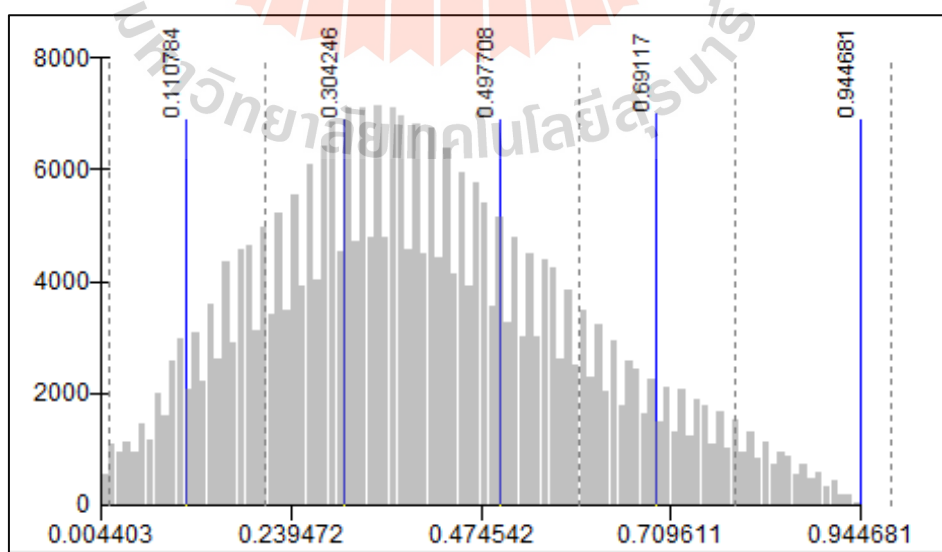


Figure 4.14 Histogram statistics report for wildfire probability map of LR model.

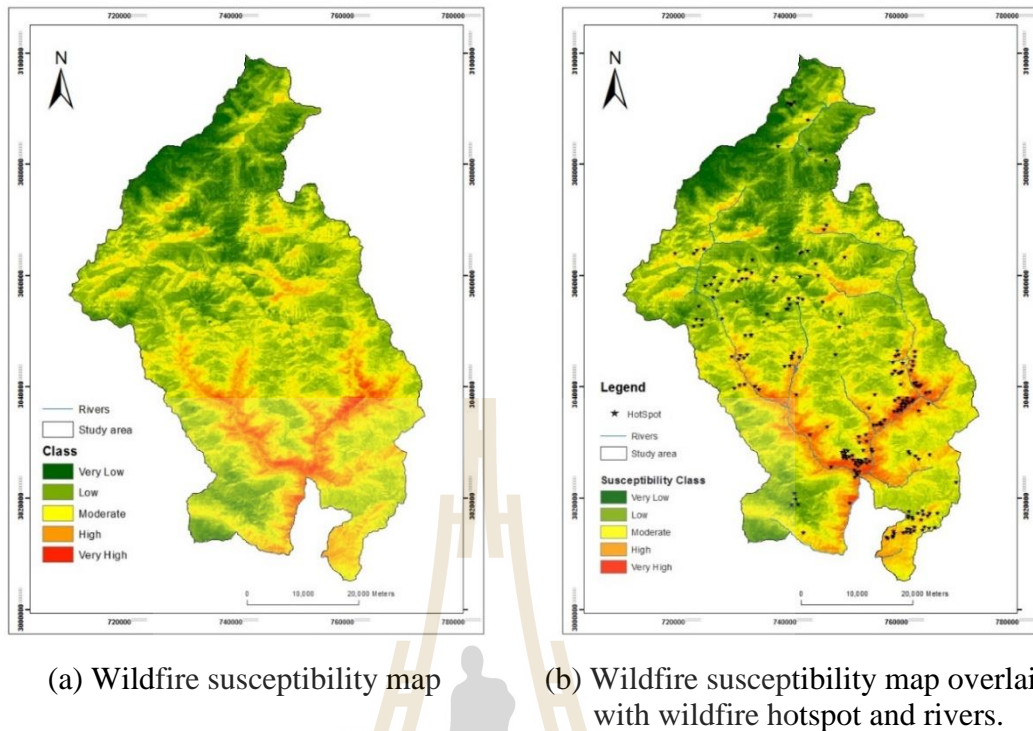


Figure 4.15 Final wildfire susceptibility map of the study area.

The derived wildfire susceptibility map is further examined by overlaying and comparing the hotspot locations under each susceptibility zones to confirm the reliability and to check if it provides any useful information and draw important conclusions.

Table 4.7 Percentage of hotspots and the area coverage of each susceptibility zones.

Probability Range	Susceptibility class	Hotspot (%)	Area (Km ²)	Area (%)
0.000 - 0.110	Very low susceptibility	0	161.530	5
0.110 - 0.300	Low susceptibility	11	860.260	28
0.300 - 0.500	Moderate susceptibility	17	1,146.420	37
0.500 - 0.700	High susceptibility	33	639.150	21
0.700 - 0.945	Very high susceptibility	39	277.380	9

Herein, the percentages of the hotspot pixels falling within each class of susceptibility zone and the covered by each zones are calculated and examined (Table 4.7). According to the classified zones, the majority of the observed hotspots (39%) in the study area are found in very high susceptibility zone that covers about 9% (277.38 km²) of the total study area (3,084.474 km²). Likewise, the high susceptibility zone have 33% of the total hotspots covering the area of 21% (639.150 km²) of the total area. This indicates that the majority of total hotspots (72%) are found in high and very high susceptibility zones covering 30% of the total study area. This demonstrates that the results are reliable. The moderate, low and very low susceptibility zones constitute 17%, 11% and 0% of total hotspots, with the corresponding area coverage of 37% (1,146.420 km²), 28% (860.260 km²) and 5% (161.53 km²) respectively.

Upon the visual interpretation, the deduced wildfire susceptibility map conveys a useful information and it appears to be highly satisfying and rationale. According to the classified zones, most parts of very high and high zones are located in the sloppy valleys at lower elevations and in areas where vegetation is mostly dominant with shrubs and meadows/grasslands that experience high land surface temperatures, low rainfall and relative humidity. These zones are closer to the roads where most of the daily human activities are involved. In addition, most of the agriculture lands also seem to fall under high susceptibility zone. Few patches of high susceptible areas are also noticed in some areas especially nearby the remote settlement areas. The susceptibility of wildfires appear to decrease as the distance from the road increases and in the areas where there is less human interference. Most of the areas that are covered by coniferous forest in the mid-altitude areas seem to fall under moderate susceptibility zone and those areas in the high altitudes covered by snow and bare soils fall under either low or very

low susceptibility zones. The areas that correspond to very low susceptibility zone are in the northern part and few areas with low susceptibility zone are located in the southwest and center of the study area that lie in higher altitudes. Although, the proportion of very high and high susceptibility zones are smaller compared to other susceptibility zones, the resulting map is agreeable and found related to actual fire incidences and situations in the study area. Particularly during winter, when there is no rainfall, the surrounding air becomes very dry with fluctuating wind conditions and the humidity remains very low. The trees shed their leaves adding more fuel to the ground, the grasses, shrubs and meadows become dry. As a result it becomes more susceptible to wildfires.

Overall, the present study demonstrates that the geoinformatics technology, particularly remote sensing and GIS with the integration of LR and FR models is very appropriate for determining and understanding the influence of significant contributing factors of wildfire and eventually develop the wildfire susceptibility map of the study area. The findings provide valuable insights that can guide in effective planning, prevention and mitigation of wildfire, consequently contributing towards effective wildfire management system.

CHAPTER V

CONCLUSIONS AND RECOMMENDATIONS

Wildfires has been and will continue to be the fundamental threat to the rich forest resources and to the people across the country. Nevertheless, its impact and threat can either be prevented or minimized and the communities can always remain alert, cautious and prepared with the availability of reliable wildfire susceptibility map. The present study was an attempt to examine and develop the wildfire susceptibility map using geoinformatics technology with the integration of LR and FR models. This had been achieved by using three key influential factors of wildfire established based on extensive literature reviews. The combination of these factors create a favourable condition that makes highly vulnerable to wildfires. The influence of each factors and their relative importance are analyzed and examined. The conclusions and recommendations drawn from the present study of wildfire susceptibility analysis is discussed in this chapter.

5.1 Conclusions

5.1.1 Logistic regression model

The main influential parameters included in LR analysis are elevation, slope, aspect, curvature, topographic wetness index, enhanced vegetation index, land use, land surface temperature, rainfall, relative humidity, distance to river, road,

settlements and agriculture lands and population density. The aspect and land use variables were transformed from nominal to numeric using the relative percentage of hotspot density in SPSS software program. The primary output of LR analysis were the model statistics and coefficients of regression, which were useful for assessing the accuracy of the regression function and the predictive powers of different parameters on wildfire occurrence. Applying the coefficients of regression, the calculation of probability map was another important outcome of the regression process. However, prior to the use of LR model in wildfire prediction, a multicollinearity diagnostic test has to be performed among the independent variables because if multicollinearity exists, this may interfere in the estimation of model coefficients resulting in erroneous results. So diagnoses and elimination of multicollinearity is important. The diagnostic test was performed using TOL and VIF technique and it was concluded that there was not issue of multicollinearity among the independent variables.

Based on LR analysis result, the probability of wildfire occurrence have a positive correlation with land surface temperature, aspect, distance to agriculture land, distance to settlement and land use variables, while distance to road, elevation, population density, enhanced vegetation index, relative humidity, rainfall and topographic wetness index had a negative correlation to the occurrence of wildfire. On the other hand, curvature, slope and distance to river were eliminated during the process of stepwise LR analysis. This suggested that they had very weak correlation to the wildfire occurrence or their influence on the occurrence of wildfire was negligible compared to those factors that were retained by the model. The variables with positive coefficients had more explanatory capability than variables with negative coefficients in terms of causing wildfire in the study area. The variables

with negative coefficients will tend to suppress the probability of wildfire occurrence. The findings from the LR analysis revealed that the most significant influential factors of wildfire are land surface temperature followed by distance to road, elevation, population density, enhanced vegetation index, distance to agriculture land, aspect and relative humidity while other factors have relatively low influence. Thus, the probability of wildfire occurrence show higher at lower elevations with high land surface temperature and closer to the roads that were associated with high frequency of human activities. The wildfire is more likely to occur in the sloppy valleys where most of the vegetation is covered by shrubs and meadows/grasslands with low humidity and less rainfall.

5.1.2 Frequency ratio model

The FR model employed was another approach to assess the wildfire susceptibility in the study area. All the influential factors that were applied in LR analysis were also applied in FR analysis. Herein, all factors were classified into distinct classes based on the objectives of the study and the scale of spatial data. Using the FR model, the spatial relationship between the hotspot location and each of the factors classes contributing to wildfire occurrence were derived. In addition, relative frequency of each factor class and the prediction rate of each factor was calculated and compared with the predictive power of each factors obtained from LR model.

Based on FR analysis, it revealed that land surface temperature, slope, aspect, curvature, enhanced vegetation index, land use, Euclidean distance to road, river, settlements and agriculture, and population density had a positive correlation to the occurrence of wildfire in the study area, while elevation, rainfall, relative humidity

and topographic wetness index had negative correlation. As the value of positively correlated parameters increases, the frequency of wildfire tend to increase while for negatively correlated variables the frequency of wildfires tend to decrease as their negative influence will suppress the occurrence of wildfire.

Furthermore, the prediction rates revealed that the most significant contributing factors of wildfire are land surface temperature, followed by elevation, enhanced vegetation index and distance to road. Factors like population density, distance to agriculture, rainfall, aspect, relative humidity, slope and distance to settlements showed a moderate influence while curvature, topographic wetness index and distance to rivers showed very little influence to the occurrence of wildfire.

The results from FR model showed similar influence to wildfire occurrence as revealed by the results of LR model. This confirms the reliability of both the models in terms of predicting the wildfire in the study area. In general, it can be concluded that GIS based LR and FR models when integrated with remote sensing and GIS technology can effectively determine the most significant influential variables of wildfire and their degree of influence/correlation and ultimately calculate the wildfire probability.

5.1.3 Accuracy assessment and validation

The accuracy assessment and validation of results showed the success rate with an AUC values of 0.881 and 0.855 for LR and FR models respectively. These shows that both models have a very good capability of classifying the wildfire susceptibility areas with high goodness of fit with the training dataset and wildfire factors. Meanwhile, the prediction rate with AUC values of 0.883 and 0.853 was obtained for LR and FR models respectively indicating both models have a relatively

high predictive capability to discriminate the presence and absence of wildfire in the study area. Nonetheless, based on the comparative analysis and validation results, LR model was chosen as the optimum model for the final wildfire susceptibility mapping.

5.1.4 Wildfire susceptibility mapping

The final wildfire susceptibility map established based on the optimum LR model revealed that the high and very high susceptibility zones covered 30% of the total study area and contained majority of the hotspots (72%). These zones mostly involved sloppy valleys in lower elevations that are associated with high land surface temperatures and in areas where vegetation is dominant with shrubs and meadows, dry grasslands mixed with scattered conifers and blue pines. These zones also lies within the proximity of 1,500 m from vehicle roads where active human activities were involved. This implies that areas closer to the roads are more susceptible to wildfires due to human activities that contribute to starting the fires either accidentally or intentionally. In addition, the low rainfall and humidity in the area had also contributed to high susceptibility to wildfires.

In a nutshell, it can be concluded that the integration of geoinformatics technology with GIS-based LR and FR models can effectively determine the most significant influential factors of wildfire occurrence and their degree of influence, determine its probability and eventually develop the wildfire susceptibility map. The findings may provide valuable information that can guide and help to safeguard our environment and preserve our rich forest resources, thereby enhancing the effective wildfire management system of Bhutan. In addition, the methodology adopted and the results derived in the present study may have the potential to implement in the other areas of Bhutan that share similar influential variables.

The results of this study also demonstrates the feasibility and the robust capability of geoinformatics technology and geospatial models in wildfire mapping. The study can also contribute to address the data requirements and the deficiencies in wildfire studies. This will have advantage towards more focused efforts to provide the data needed for wildfire management system, resulting in the improvement in the efficiency of data reporting and inventorying.

5.2 Recommendations

The current study employed the novel approach of remote sensing and GIS with the integration of suitable geospatial models (LR and FR) to establish reliable wildfire susceptibility map of Thimphu and Paro districts. The study was able to identify the most significant influential factors of wildfire and deduced their degree of relative influence that helped to derive the probability maps with high accuracy and, eventually accomplished the primary objective of the study to develop wildfire susceptibility map of the study area. However, there is a need to highlight for the improvement in the underlying suggested recommendations, particularly the development of comprehensive database on the spatial distribution of wildfire and their characteristics, as well as on the development of spatial information on wildfire predictor variables.

(1) The spatial locations of wildfires were not available and did not exist at all for the present study area. The concerned agency needs to maintain a comprehensive and reliable spatial database of wildfire inventory, rather than just recording the location by place names and area damaged which has no spatial

significance. This will immensely contribute to more accurate and reliable assessment of future wildfire studies in Bhutan.

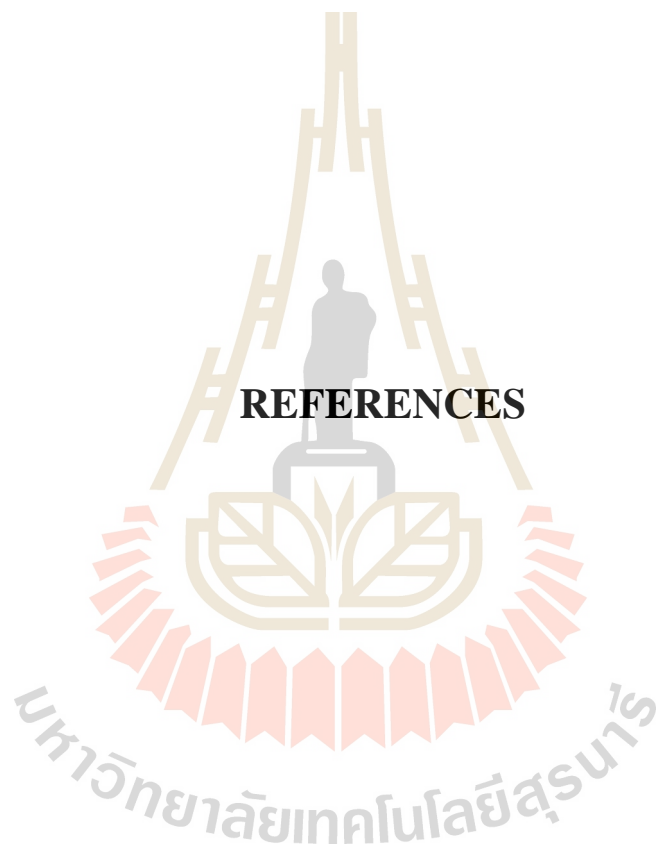
(2) The study also recommends for an improved and reliable meteorological data with fair distribution of weather stations particularly intended for use in the research applications. The improved climatic variables with the incorporation of wind speed/direction and sunshine variables from sufficient number of gauge stations would certainly improve the quality of wildfire studies and other researches related to disaster management.

(3) Considering the current trend of wildfire situation in the country, the need to initiate research in the field of fire detection, behavior and fire ecology for better management of forest fires is seen as necessary and very important.

(4) The results from the present study is expected to help fire managers and planners to identify locations with a high risk of fire occurrence and prepare plans accordingly and ultimately contribute to effective fire management system. In addition, the current study is expected to serve as a guide towards more advanced analysis beyond the susceptibility level including vulnerability and risk assessment applying geoinformatics technology.

(5) The relation between the fire variables may change over time, therefore periodic updating of the model is recommended.

REFERENCES



REFERENCES

- Adab, H., Devi, K. and Solaimani, K. (2013). Modeling forest fire risk in the northeast of Iran using remote sensing and GIS techniques. **Nat Hazards**. 65: 1723-1743.
- Atkinson, P. M., and Massari, R. (1998). Generalised linear modelling of susceptibility to land sliding in the Central Apennines, Italy. **Computers and Geoscience, Department of Geography**. 24: 373-385.
- Ayalew, L., and Yamagishi, H. (2005). The application of GIS-based logistic regression for Landslide susceptibility mapping in the Kakuda-Yahiko Mountains, Central Japan. **Geomorphology**. 65 (1-2): 15-31.
- Bennett, M., Fitzgerald, S., Parker, B., Main, M., Perleberg, A., Schnepf, C., and Mahoney, R. (2010). Reducing Fire Risk on Your Forest Property. **A Pacific Northwest Extension Publication Oregon State University**, University of Idaho, Washington State University.
- Beven, K. J., and Kirkby, M. J. A. (1979). Physically based, variable contributing area model of basin hydrology. **Hydrological Sciences Bulletin**. 24: 43-69
- Bio A.M.F., Alkemende R., Barendregt A. (1998). Determining alternative models for vegetation response analysis: a nonparametric approach. **Journal of Vegetation Science**. 9: 5-16

- Boonchut, P. (2005). Decision Support for Hazardous Material Routing. **International Institute for Geo-Information Science and Earth Observation (ITC)**. M.Sc. Thesis, Enschede, Netherlands.
- Brown, A. A., and Davis, K. P. (1973). **Forest fire: control and use**. (2nd ed). McGraw-Hill: New York. 686 pp.
- Carmo, M., Moreiraa, F., Casimirob, P., and Vaza, P (2011). Land use and topography influences on wildfire occurrence in northern Portugal. **Landscape and Urban Planning**. 100 (1–2): 169-176.
- Castillo, J., and Avendano, E. (2004). **Route Optimization for Hazardous Material Transport**. M.Sc. Thesis, International Institute for Geo-Information Science and Earth Observation (ITC).
- Chang, K. (2014). **Introduction to Geographic Information System**. (7th ed). New York: McGraw-Hill.
- Chatterjee, S., and Hadi, A. (2006). **Regression Analysis by Example**. (4th ed). Canada: A JOHN WILEY & SONS, INC.
- Chung, C. J. F., and Fabbri, A. G. (2003). Validation of Spatial Prediction Models for Landslide Hazard Mapping. **Natural Hazards**. 30 (3): 451-472.
- Chuvieco, E., Aguado, I., Cocero, D., and Rian, O. D. (2003). Design of an empirical index to estimate fuel moisture content from NOAA. AVHRR images in forest fire danger studies. **International Journal of Remote Sensing**. 24: 1621-1637.
- Chuvieco, E., and Congalton, R. G. (1989). Application of remote sensing and geographic information systems to forest fire hazard mapping. **Remote Sensing of Environment**. 29(2): 147-159.

- Clark, W., and Hosking, P. (1986). **Statistical methods for geographers**. New York: John Wiley and Sons.
- Dai, F. C. and Lee, C. F. (2002). Landslide characteristics and slope instability modeling using GIS, Lantau Island, Hong Kong. **Geomorphology**. 42(3-4): 213-228.
- Dorji, T (2006). **Fire situation in Bhutan**. International Forest Fire News (IFFN). No. 34 (January-June 2006, 55-63) ISSN: 1029-0864.
- Drukpa, K. (2015). **Bhutan RNR Statistics**. Royal Government of Bhutan, Ministry of Agriculture and Forests. RNR-SCS, PPD, MoAF.
- ESRI (2016). [On-line]. Available: <http://webhelp.esri.com/arcgisdesktop>.
- Food and Agriculture Organization. (2001). **International handbook on forest fire protection**. Technical guide for the countries of the Mediterranean basin. Le Tholonet: Departement Gestion des territoires, Groupement d'Aix en Provence. 149 pp.
- Ghomi, M. A., Farahi, A. E., Baniyadi, R., and Masoumpoor, C., F. (2013). Rating and mapping mire hazard in the hardwood Hyrcanian forests using GIS and expert choice software. **Forestry Ideas** 19(2(46)):141-150.
- Giglio, J., Descloitres, C. O., Justice, Y. J., and Kaufman (2003). An enhanced contextual fire detection algorithm for MODIS. **Remote Sensing of Environment**. 87: 273-282.
- Giglio, L., Randerson, J. T., Van der Werf, G. R., Kasibhatla, P. S., Collatz, G. J., Morton, D. C., and DeFries, R. S. (2010). Assessing variability and long-term trends in burned area by merging multiple satellite fire products. **Bio-geosciences**. 7: 1171-1186.

- Guo, F., Su, Z., Wang, G., Sun, L., Lin, F., and Liu, A (2015). Wildfire ignition in the forests of southeast China. **Identifying drivers and spatial distribution to predict wildfire likelihood**. 66: 12-21.
- Hushaw, J. (2016, September 20). Wildfire in a Warming World. **Wildfire trends. Climate Smart Land Network Bulletin**. PART I: TRENDS and THE ROLE OF CLIMATE: 1-7.
- IBM-SPSS (2012). **IBM SPSS Statistics 21 Core System User's Guide**. North Castle Drive, Armonk, NY 10504-1785, U.S.A: IBM Corporation.
- Intarawichian, L. S., and Dasananda, S. (2010). Forest fire susceptibility mapping based on logistic regression and frequency ratio methods: a case study of Chiangmai province, Thailand. **33rd Asian conference on remote sensing**.
- ISDR (2002). Disaster Reduction for Sustainable Mountain Development. **International Strategy for Disaster Reduction**. United Nations World Disaster Reduction Campaign: 16 pp.
- Jaiswal, R. K., Mukherjee, S., Raju, K. D., and Saxena, R. (2002). Forest fire risk zone mapping from satellite imagery and GIS. **International Journal on Application of Earth Observation and Geoinformation**. 4: 1-10.
- Janbaz, G., Gholizadeh, B., and Majidi, D. O. (2012). Forest fire risk zone mapping from geographic information system in Northern Forests of Iran. **International Journal of Agriculture and Crop Science**. 4(12): 818-824.
- Johann, G. G., Eduard, P. D., Leonid, G. K., and Nikolai, I. E. (2004). International Forest Fire News (IFFN). **Recent Trends of Forest Fires in Central Asia and Opportunities for Regional Cooperation in Forest Fire Management**. (31): 91-101).

- Kaufman, Y. J., Kleidman, M. D., and King, R. G. (1998b), Fires in the Tropics: properties and their remote sensing from EOS-MODIS. **Journal of Geophysical Research**. 103 (31): 955-31.
- Kaufman, Y. J., Tanré, D., Remer, E., Vermote, A., Chu, B. N., and Holben, L. (1997). Remote Sensing of Tropospheric Aerosol from EOS-MODIS over the Land Using Dark Targets and Dynamic Aerosol Models. **Journal of Geophysical Research**. 102 (17): 51-67.
- Kaufman, Y., Justice, C., Flynn, L., Kendall, J., Prins, E., Ward, D. E., Menzel, P., and Setzer, A. (1998). Monitoring Global Fires from EOS-MODIS. **Journal of Geophysical Research**. 103 (32): 215-338.
- Knorr, W., Kaminski, T., Arneith, A., and Weber, U. (2014). Impact of human population density on fire frequency at the global scale. **Physical Geography and Ecosystem Analysis**. 12: 22-362.
- Koenig, W. D. (1999). Spatial autocorrelation of ecological phenomena. **Trends Ecological Evolution**. 14: 22-26.
- Kuensel (2016, March 12). **Forest fires burning up Bhutan's wilderness**.
- Lee, S., and Evangelista, D. G. (2008). Landslide susceptibility mapping using probability and statistics models in Baguio City, Philippines. **Korea Institute of Geoscience and Mineral Resources**.
- Lee, S., and Pradhan, B. (2007). Landslide hazard mapping at Selangor, Malaysia using frequency ratio and logistic regression models. **Landslides**.4: 33-41.
- Lee, S., and Talib, J. A. (2005). Probabilistic landslide susceptibility and factor effect analysis. **Environmental Geology**. 47(7): 982-990.
- Levine, J. S (1991). **Global Biomass Burning**, MIT Press, Cambridge, MA: 41-46.

- Li, Z., Y., Kaufman, C., Ichoku, R. Fraser, A., Trishchenko, L., Giglio, J. Z. J., and X. Yu, (2001). A review of AVHRR-based fire detection algorithms: Principles, Limitations and Recommendations. **Global and Regional Wildfire Monitoring from Space**. Academic Publishing: 199-225.
- Mckinnell, F. (2000). **Forest fire management in Bhutan: Consultancy report**. Field Document No.FDOO/5/TFDP-TA/FORTECH, Third Forestry Development Project, Khangma, Bhutan. 36 pp.
- Meinhardt, M., Fink, M., and Tünschel H. (2015). Landslide susceptibility analysis in central Vietnam based on an incomplete landslide inventory: Comparison of a new method to calculate weighting factors by means of bivariate statistics. **Geomorphology**. 234: 80-97.
- Menard, S. (1995). Applied logistic regression analysis. Sage University Paper Series on Quantitative. **Applications in Social Sciences**. 106. Thousand Oaks, California, USA. 98 pp.
- Mernard, S. (2002). **Applied logistic regression analysis**. Thousand Oaks, CA: SAGE Publications.
- Meten, M., Bhandary, N.P., and Yatabe, R. J. (2015). GIS based frequency ratio and logistic regression for landslide susceptibility mapping of Sina Debre area in central Ethiopia. **Journal of mountain science**. 12 (6): 1355-1372.
- Mohammadi, F., Bavaghar, M. P., and Shabaniyan, N. (2013). Forest Fire Risk Zone Modelling Using Logistic Regression and GIS: An Iranian Case Study. **Small scale Forestry**. 13: 117-125.

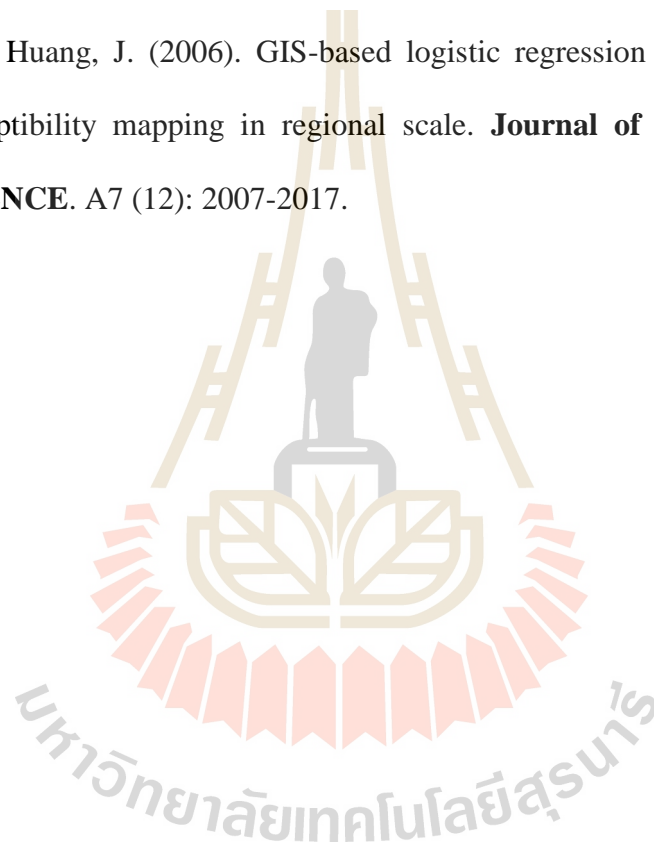
- Moore, I. D., Grayson, R. B., and Ladson, A. R. (1991). Digital terrain modelling, a review of hydro-hydrological, geomorphological, and biological applications. **Hydrological Processes**. 5: 3-30.
- NASA FIRMS (2012). [Online]. Available: <https://firms.modaps.eosdis.nasa.gov/sources.php>.
- O'Brien (2007). A Caution Regarding Rules of Thumb for Variance Inflation Factors. **Department of Sociology, University of Oregon, Eugene, OR 97408, USA.**
- Oh, H. J., Kim, Y. S., Choi, J. K., and Lee, S. (2011). GIS mapping of regional probabilistic ground water potential in the area of Pohang City, Korea. **Journal of Hydrology**. 399: 158-172.
- Ohlmacher, G. C., and Davis, J. C. (2003). Using logistic regression and GIS technology to predict landslide hazard in northeast Kansas, USA. **Engineering Geology**. 69: 331-343
- Ozdemir, A. (2011). Using a binary logistic regression method and GIS for evaluating and mapping the groundwater spring potential in the Sultan Mountains (Aksehir, Turkey). **Journal of hydrology**. 405: 123-136.
- Ozdemir, A., and Altural, T. (2013). A comparative study of frequency ratio, weights of evidence and logistic regression methods for landslide susceptibility mapping. Sultan Mountains. **Journal of Asian Earth Sciences**. 63: 180-197.
- Pourtaghi, Z. S., Pourghasemi, H. R., and Rossi, M., (2014). Forest fire susceptibility mapping in the Minudasht forests, Golestan province, Iran. **Environment and Earth Science**. (2015) 73:1515-1533.

- Pradhan, B., Suliman, M. D. H. B., and Awang, M. AB. (2007). Forest fire susceptibility and risk mapping using remote sensing and geographical information systems. **Disaster Prevention and Management**. 16 (3): 344-352.
- Prasad, P., Pisipati, S., Mutava, R., and Tuinstra, M. (2008). Sensitivity of grain sorghum to high temperature stress during reproductive development. **Crop Science**. 48: 1911-1917.
- Preisler, H. K., David, R. B., Robert, E. B., and Benoit, J.W. (2004). Probability based models for estimation of wildfire risk. **International Journal for Wildland Fire**. 13(2): 133-142.
- Pyne, S.J. (2001). *Fire: A Brief History*; Jeremy Mills Publishing: West Yorkshire, UK; 204 pp.
- Rawat, G. S. (2003). **Fire Risk Assessment for forest fire control management in Chilla forest range of Rajaji National Park Uttaranchal (India)**. M.Sc. Thesis, International Institute for Geoinformation Science and Earth Observation, Enschede of the Netherlands. 74 pp.
- Rogerson, P. (2006). *Statistical methods for geography*. London; Thousand Oaks, Calif.: **SAGE Publications**.
- Royal Government of Bhutan. (1969). **The Bhutan Forest Act**. Ministry of Trade and Industry (MTI).
- Royal Government of Bhutan. (1999). **Vision 2020**. A vision of peace, prosperity and happiness. Planning Commission (PC). Part I: 40 pp.
- San-Miguel-Ayanz, J., and Ravail, N. (2005). Active fire detection for fire emergency management: Potential and limitations for the operational use of remote sensing. **Natural Hazards**. 35: 361 pp.

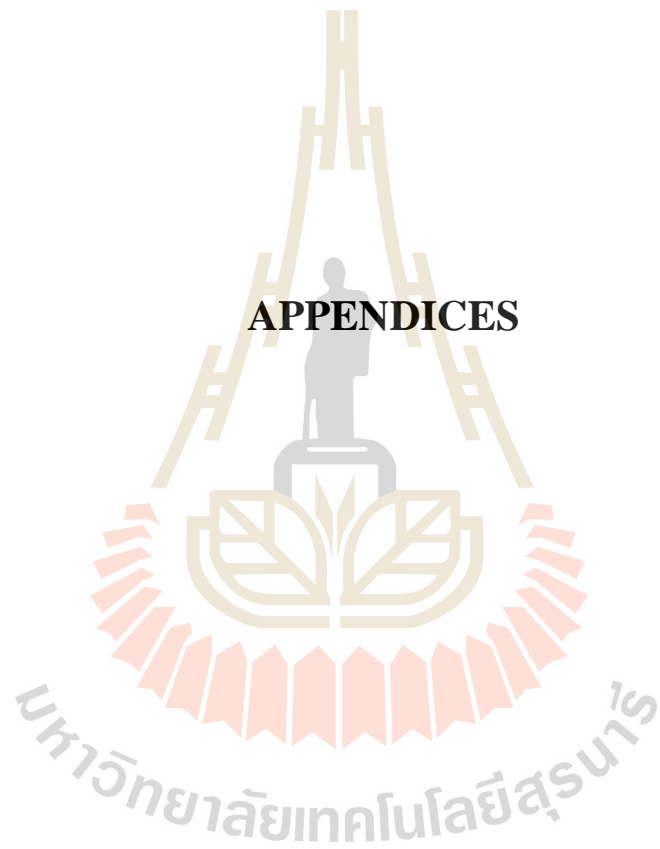
- Schicker, R., and Moon, V. (2012). Comparison of bivariate and multivariate statistical approaches in landslide susceptibility mapping at a regional scale. **Geomorphology**. (161-162): 40-57.
- Setzer, A. W., and Malingreau, J. P. (1996). AVHRR monitoring of vegetation fires in the tropics: towards a global product. In Levine, J.S., editor, **Biomass burning and global change**, Cambridge. 48-81.
- Simard, A. J. (1991). Fire severity, changing scales, and how things hang together. **International Journal of Wildland Fire**. 1 (1): 23-34.
- SPSS (2003). **SPSS Regression Models 12.0** SPSS Inc. United States of America.
- Stein, S. M., Menakis, J., Carr, M. A., Comas, S. J., Stewart, S. I, Cleveland, H. Bramwell, L., and Radeloff, V.C. (2013). Wildfire, wildlands, and people: understanding and preparing for wildfire in the wildland-urban interface- a Forests on the Edge report. **Rocky Mountain Research Station**. 36 pp.
- Stocks, B. J., Fosberg, M. A., Lynham, T. J., Mearns, L., Wotton, B. M., Yang, Q., Jin, J-Z., Lawrence, K., Hartley, G. R., Mason, J. A., and McKENNEY, D. W. (1998). **Climate Change and Forest Fire Potential in Russian and Canadian Boreal Forests**. 38: 1.
- Tshering, K. (2006). **Development of an effective forest fire management strategy for Bhutan**. M.Sc. Dissertations, University of Montana
- Vasconcelos, M. J. P., Pereira J. M. C., and Zeigler, B. P (1995). Simulation of fire growth using discrete event hierarchical modular models. EARSel. **Advance Remote Sensing**. 4 (3): 54-62.

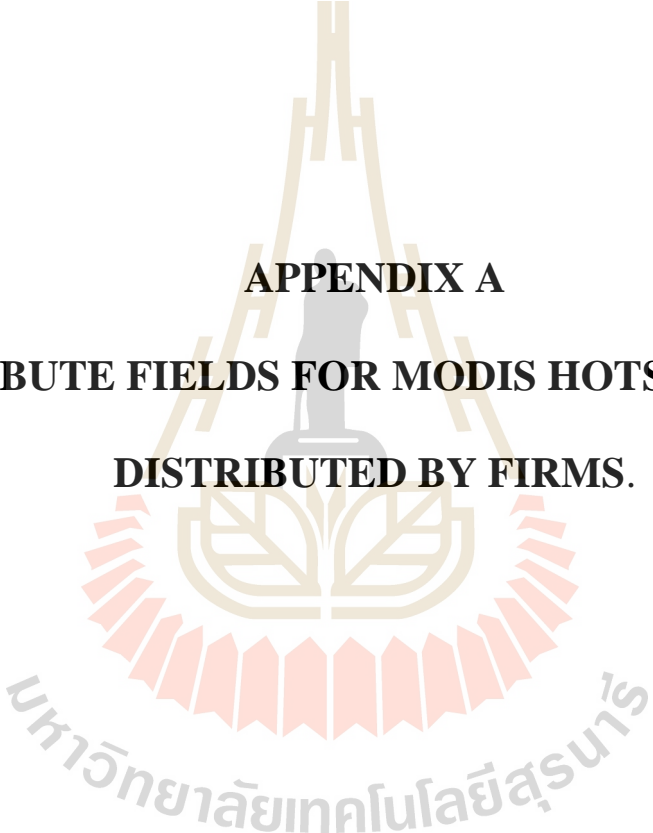
- Wan, Z., Zhang, Y., Zhang, Q., and Li, Z. L (2004). Quality assessment and validation of the MODIS global land surface temperature. **International. Journal of Remote Sensing**. 25: 261-274.
- Williamson, G. J., Cochrane, M. A., Freeborn, F. H., Holden, Z. A., Brown, T. J., Jolly, W. M., and Bowman, D. M. J. S. (2015). Climate-induced variations in global wildfire danger from 1979 to 2013. **Fire ecology**.
- Wilson, J. P., and Gallant, J. C. (2000). **Terrain analysis principles and applications**. Wiley: New York, USA.
- Wu, Z. W., He, H. S., Yang, J., and Liang, Y. (2015). Defining fire environment zones in the boreal forests of northeastern China. **Science of the Total Environment**. 106-116.
- Yalcin, A., Reis, S., Aydinoglu, A., and Yomraloiglu, T. (2011). A GIS-based comparative study of frequency ratio, analytical hierarchy process, bivariate statistics and logistic regression methods for **landslide susceptibility mapping in Trabzon**. NE Turkey. *Catena* 85(3): 274-287.
- Yeshey, L. (2015). Disaster Management, Country Report (ADRC), Visiting Researcher Program (FY2014B). **Asian Disaster Reduction Center**.
- Yesilnacar, E., and Topal, T. (2005). Landslide susceptibility mapping: A comparison of logistic regression and neural networks methods in a medium scale study, Hendek region (Turkey). **Engineering Geology**. 79 (3-4): 251-266.
- Yilmaz, I. (2009). Landslide susceptibility mapping using frequency ratio, logistic regression, artificial neural networks and their comparison: a case study from Kat landslides (Tokat -Turkey). **Computers and Geoscience**. 35: 1125-1138.

- Zhang, H., Han, X., and Dai, S. (2013). Fire Occurrence Probability Mapping of Northeast China with Binary Logistic Regression Model. **Applied earth observations and remote sensing**. 6 (1): 121-127.
- Zhang, Z. X., Zhang, H. Y., and Zhou, D. W. (2009). Using GIS spatial analysis and logistic regression to predict the probabilities of human-caused grassland fires. **Journal of Arid Environments**. 74 (2010) 386-393.
- Zhu L., and Huang, J. (2006). GIS-based logistic regression method for landslide susceptibility mapping in regional scale. **Journal of Zhejiang University SCIENCE**. A7 (12): 2007-2017.



APPENDICES





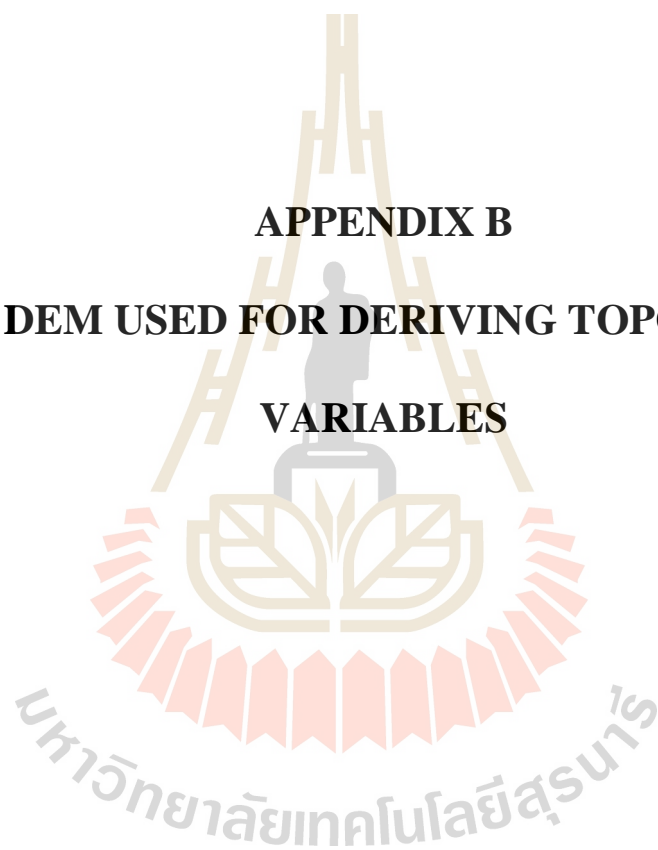
APPENDIX A
ATTRIBUTE FIELDS FOR MODIS HOTSPOT DATA
DISTRIBUTED BY FIRMS.

มหาวิทยาลัยเทคโนโลยีสุรนารี

Table A Attribute fields of MODIS hotspot data distributed by NASA firms.

Attribute	Short Description	Long Description
Latitude	Latitude	Center of 1km fire pixel but not necessarily the actual location of the fire as one or more fires can be detected within the 1km pixel.
Longitude	Longitude	Center of 1km fire pixel but not necessarily the actual location of the fire as one or more fires can be detected within the 1km pixel.
Brightness	Brightness temperature 21 (Kelvin)	Channel 21/22 brightness temperature of the fire pixel measured in Kelvin.
Scan	Along Scan pixel size	The algorithm produces 1km fire pixels but MODIS pixels get bigger toward the edge of scan. Scan and track reflect actual pixel size.
Track	Along Track pixel size	The algorithm produces 1km fire pixels but MODIS pixels get bigger toward the edge of scan. Scan and track reflect actual pixel size.
Acq_Date	Acquisition Date	Date of MODIS acquisition.
Acq_Time	Acquisition Time	Time of acquisition/overpass of the satellite (in UTC).
Satellite	Satellite	A = Aqua and T = Terra.
Confidence	Confidence (0-100%)	This value is based on a collection of intermediate algorithm quantities used in the detection process. It is intended to help users gauge the quality of individual hotspot/fire pixels. Confidence estimates range between 0 and 100% and are assigned one of the three fire classes (low-confidence fire, nominal-confidence fire, or high-confidence fire).
Version	Version (Collection and source)	Version identifies the collection (e.g. MODIS Collection 6) and source of data processing: Near Real-Time (NRT suffix added to collection) or Standard Processing (collection only). "6.0NRT" - Collection 6 NRT processing. "6.0" - Collection 6 Standard processing. Find out more on collections and on the differences between FIRMS data sourced from LANCE FIRMS and University of Maryland.
Bright_T31	Brightness temperature 31 (Kelvin)	Channel 31 brightness temperature of the fire pixel measured in Kelvin.
FRP	Fire Radiative Power	Depicts the pixel-integrated fire radiative power in MW (megawatts).
DayNight	Day / Night	D = Daytime, N = Nighttime

APPENDIX B
ALOS DEM USED FOR DERIVING TOPOGRAPHIC
VARIABLES



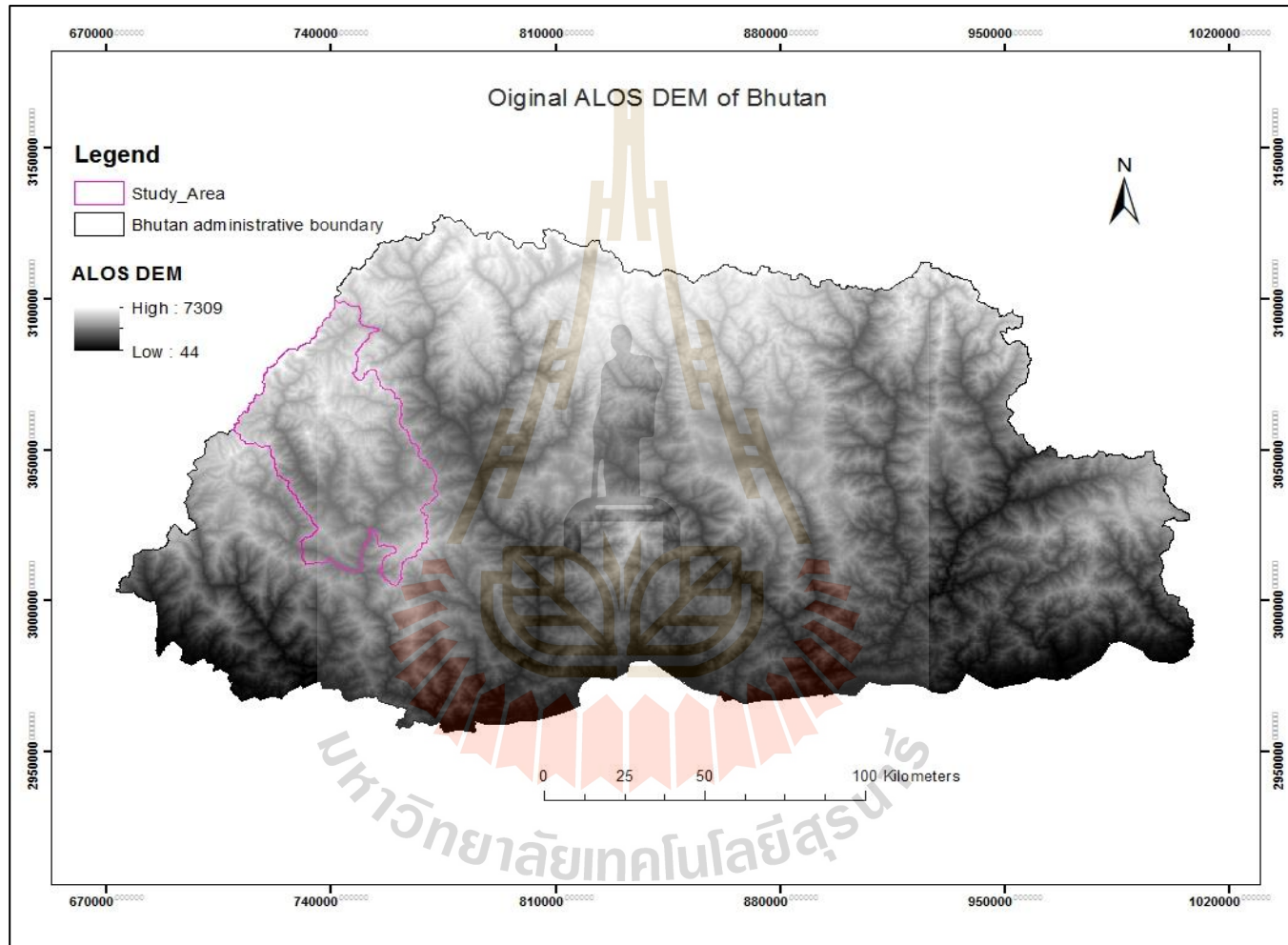


Figure B ALOS Digital elevation model of Bhutan.

APPENDIX C
METEOROLOGICAL STATIONS USED TO
INTERPOLATE WEATHER VARIABLES

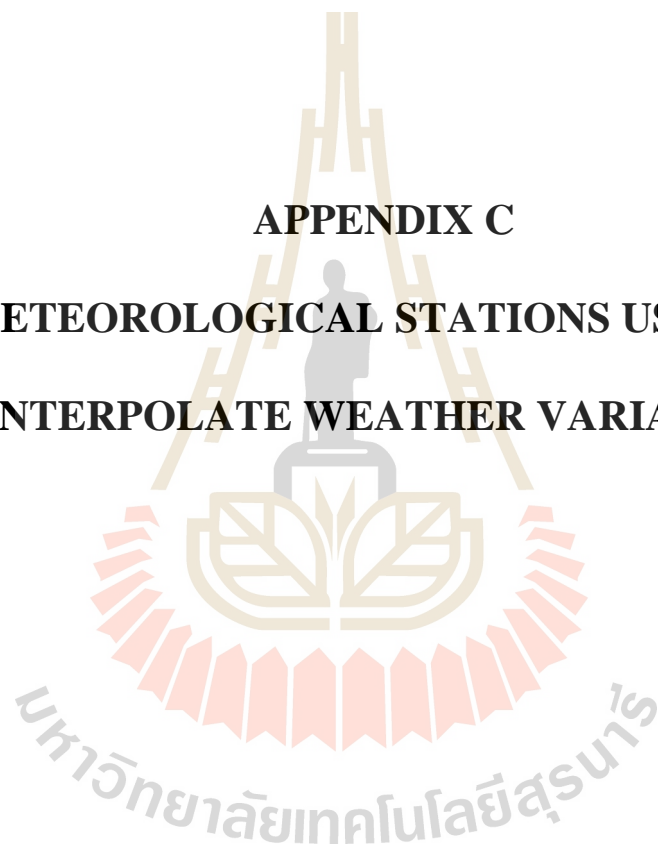
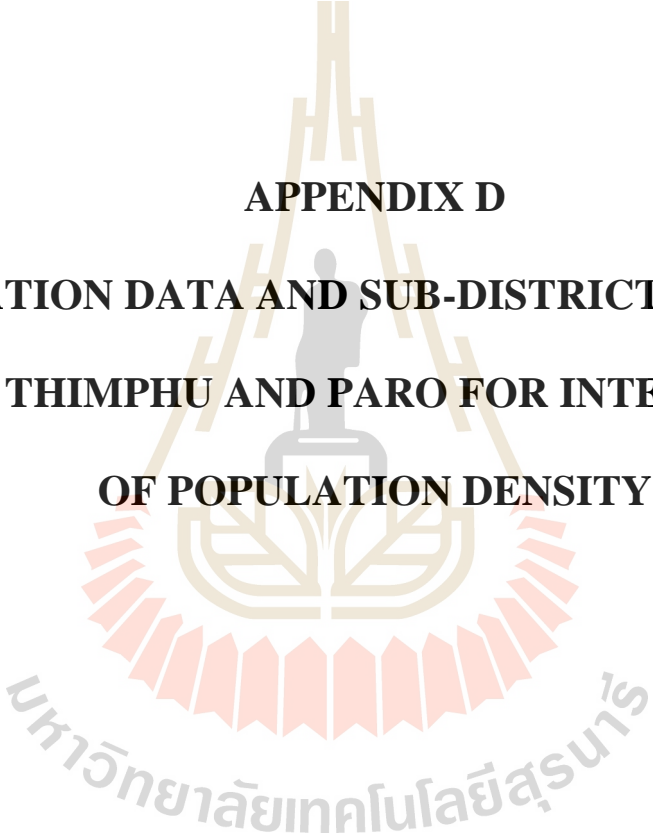


Table C Input meteorological data used in the analysis.

Station	Northing	Easting	Height	Mean annual rainfall	Mean annual temperature	Mean annual relative humidity
Simtokha	3037832.00	764447.00	2310	555.58	14.92	65.06
Paro	3031189.00	739323.00	2406	599.37	13.53	72.34
Drugyel	3043984.00	730479.00	2547	773.83	13.08	73.69
Begana	3052725.00	760887.00	2520	919.03	12.94	73.68
Gidacom	3031681.00	754681.00	2210	537.37	13.01	75.04
Betikha	3016053.00	738516.00	2660	2986.73	11.74	75.37
Gunitsawa	3056212.68	725694.65	3060	1554.49	10.75	76.71





APPENDIX D

**POPULATION DATA AND SUB-DISTRICT BOUNDARY
MAP OF THIMPHU AND PARO FOR INTERPOLATION
OF POPULATION DENSITY**

มหาวิทยาลัยเทคโนโลยีสุรนารี

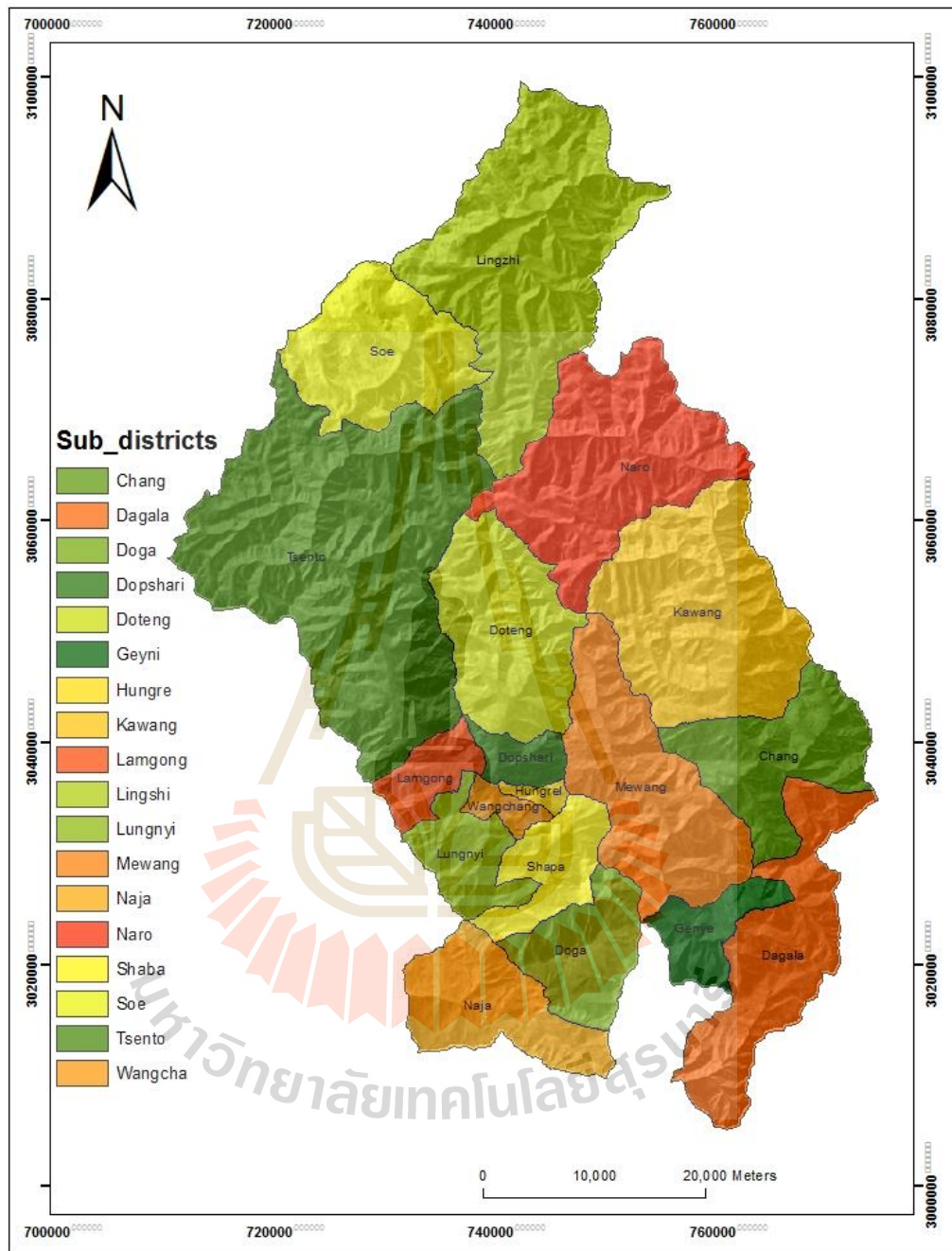
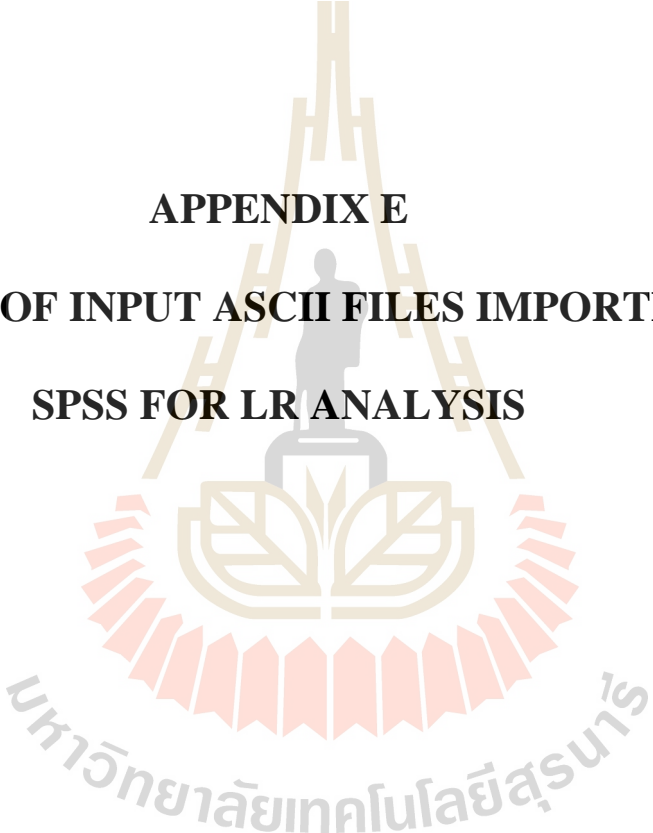


Figure D Sub-districts boundary of the two districts used for interpolation of population density.

Table D Population data of each sub-district in Thimphu and Paro districts.

No	Gewog Names	Total Population	District Names	Remarks
1	Chang	42,730	Thimphu	Population of Thromde is merged with the respective Gewogs (Sub-district)
2	Dagala	1,497		
3	Geney	918		
4	Kawang	42,174		
5	Lingzhi	495		
6	Mewang	5,916		
7	Naro	189		
8	Soe	183		
9	Dogar	1,866	Paro	Population of Thromde is merged with the respective Gewogs
10	Doteng	1,149		
11	Hungrel	1,250		
12	Lango	3,336		
13	Lungney	2,543		
14	Naja	3,007		
15	Shaba	4,319		
16	Shari	3,180		
17	Tsento	5,253		
18	Wangchang	9,357		

Source PHCB-2010, NSB.

The logo of Sakon Nakhon Rajabhat University is centered on the page. It features a stylized golden structure resembling a traditional Thai temple or stupa, with a central figure of a person standing on a pedestal. Below this is a circular emblem with a lotus flower design. At the bottom, the university's name is written in Thai script: มหาวิทยาลัยเทคโนโลยีสุรนารี.

APPENDIX E

**EXAMPLE OF INPUT ASCII FILES IMPORTED TO
SPSS FOR LR ANALYSIS**

	Hotspot	ELV	SLP	CRV	TWI	EVI	RF	LST	RH	Dist_Road	Dist_River	Dist_Sett	Dist_AgrIL	Pop_Density	ASP	LU	var
1	Hotspot	.297	.374	.610	.059	.334	.161	.605	.671	.179	.272	.607	.609	.116	.511	.695	
2	Hotspot	.281	.518	.479	.368	.470	.161	.585	.670	.181	.264	.613	.616	.116	.511	.695	
3	Hotspot	.274	.425	.429	.476	.466	.162	.585	.669	.182	.263	.617	.620	.115	1.000	.695	
4	Hotspot	.282	.483	.471	.310	.403	.167	.585	.664	.196	.217	.665	.669	.114	.762	.695	
5	Hotspot	.289	.500	.457	.370	.403	.167	.568	.663	.198	.211	.672	.676	.114	.762	.695	
6	Hotspot	.297	.502	.405	.370	.407	.168	.568	.663	.200	.206	.679	.683	.113	.762	.695	
7	Hotspot	.315	.377	.485	.374	.362	.159	.605	.672	.171	.306	.581	.582	.116	.511	.695	
8	Hotspot	.305	.353	.463	.386	.384	.160	.605	.672	.173	.299	.588	.589	.116	.511	.695	
9	Hotspot	.301	.276	.549	.072	.384	.161	.605	.671	.175	.291	.594	.596	.115	.511	.695	
10	Hotspot	.290	.265	.419	.490	.384	.161	.605	.670	.177	.284	.601	.603	.115	.511	.695	
11	Hotspot	.286	.227	.481	.497	.466	.162	.585	.670	.179	.276	.608	.610	.115	1.000	.695	
12	Hotspot	.293	.474	.525	.049	.403	.167	.585	.664	.195	.224	.663	.666	.113	.762	.695	
13	Hotspot	.302	.528	.521	.043	.403	.168	.568	.663	.197	.219	.669	.673	.113	.762	.695	
14	Hotspot	.307	.541	.427	.358	.407	.168	.568	.663	.199	.214	.676	.680	.113	.762	.695	
15	Hotspot	.316	.521	.408	.348	.407	.169	.568	.662	.201	.209	.683	.687	.113	.762	.695	
16	Hotspot	.316	.343	.501	.368	.362	.160	.605	.672	.172	.312	.578	.579	.115	.511	.695	
17	Hotspot	.304	.360	.408	.439	.384	.160	.605	.672	.172	.304	.585	.586	.115	.511	.695	
18	Hotspot	.296	.307	.389	.483	.384	.161	.605	.671	.174	.297	.592	.593	.115	1.000	.695	
19	Hotspot	.311	.497	.525	.046	.403	.168	.568	.663	.196	.227	.667	.670	.113	.381	.695	
20	Hotspot	.328	.476	.471	.337	.407	.169	.568	.662	.200	.217	.681	.684	.112	.762	.695	
21	Hotspot	.307	.413	.475	.438	.437	.162	.605	.671	.174	.303	.589	.590	.115	1.000	.695	
22	Hotspot	.304	.421	.507	.054	.437	.162	.605	.670	.176	.296	.596	.597	.114	1.000	.695	
23	Hotspot	.325	.492	.467	.310	.370	.169	.568	.662	.197	.230	.672	.675	.112	.381	.695	
24	Hotspot	.320	.240	.505	.078	.437	.161	.605	.671	.171	.317	.579	.580	.114	1.000	.695	
25	Hotspot	.328	.515	.432	.369	.370	.169	.568	.662	.196	.238	.669	.672	.112	.762	.695	
26	Hotspot	.342	.517	.480	.349	.370	.169	.568	.661	.197	.234	.676	.679	.111	.762	.695	
27	Hotspot	.303	.490	.409	.336	.344	.168	.585	.663	.191	.256	.653	.656	.112	.381	.695	
28	Hotspot	.322	.544	.525	.305	.344	.169	.568	.663	.193	.251	.660	.663	.111	.381	.695	
29	Hotspot	.348	.488	.525	.047	.322	.170	.568	.661	.196	.242	.674	.677	.111	.381	.695	
30	Hotspot	.339	.477	.472	.364	.322	.170	.600	.661	.191	.272	.652	.663	.110	.892	.695	
31	Hotspot	.338	.332	.363	.530	.322	.170	.600	.660	.193	.268	.653	.670	.109	.762	.695	
32	Hotspot	.347	.405	.433	.371	.332	.171	.600	.660	.194	.265	.653	.673	.109	.381	.695	
33	Hotspot	.391	.337	.417	.368	.308	.176	.548	.648	.194	.252	.669	.683	.105	1.000	1.000	
34	Hotspot	.382	.398	.512	.057	.415	.178	.585	.639	.197	.301	.689	.697	.102	.511	1.000	
35	Hotspot	.138	.344	.510	.063	.341	.176	.722	.809	.002	.145	.007	.000	.099	.892	.676	
36	Hotspot	.352	.555	.467	.345	.322	.170	.600	.661	.190	.281	.645	.661	.109	.892	.695	
37	Hotspot	.351	.552	.436	.304	.322	.171	.600	.660	.192	.277	.645	.666	.109	.892	1.000	

Figure B Example of input ASCII for logistic regression analysis in SPSS software.

CURRICULUM VITAE

Name: Samdrup Dorji

Date of Birth: 11th January, 1981

Place of Birth: Nakzor, Orong, Samdrup Jongkhar, Bhutan.

Education: 2005 B.Sc. (General Science), Sherubtse College, Bhutan
(Affiliated. to Delhi University, India)

2008 Post Graduate in Survey Engineering, Indian Institute of Surveying and Mapping (IISM), Hyderabad, India.

Grants and Fellowships: Thailand International Cooperation Agency (TICA) scholarship.

Position and Place of Work: Senior Survey Engineer (SSE), National Land Commission, Thimphu, Bhutan.